WATER SCIENCE SERIES

Evaluating the Use of Electrical Resistivity Sounding to Characterize Aquifers in the Beaufort Watershed, B.C.

Victoria Pereversoff, Lucinda Leonard, Mark Lake, Mike Wei, and Sylvia Barroso

December 2022

No. 2022-08

The **Water Science Series** are scientific technical reports relating to the understanding and management of B.C.'s water resources. The series communicates scientific knowledge gained through water science programs across B.C. government, as well as scientific partners working in collaboration with provincial staff. For additional information visit: http://www2.gov.bc.ca/gov/content/environment/air-land-water/water/water-science-data/water-science-series.

ISBN: 978-0-7726-8097-6

Citation:

Pereversoff, V.G., L.J. Leonard, M.I. Lake, M. Wei, and S. Barroso, 2022. Evaluating the use of electrical resistivity sounding to characterize aquifers in the Beaufort Watershed, B.C. Water Science Series, WSS2022-08. Province of British Columbia, Victoria.

Author's Affiliation:

Victoria G. Pereversoff, B.Sc.
School of Earth and Ocean Sciences
University of Victoria
Victoria, B.C.

Lucinda J. Leonard, Ph.D.
School of Earth and Ocean Sciences
University of Victoria
Victoria, B.C.

Mark I. Lake, P. Geoph. (Alberta - retired)
Beaufort Watershed Stewards
Royston, B.C.

Mike Wei, P. Eng.
School of Earth and Ocean Sciences
University of Victoria
Victoria, B.C.

Sylvia Barroso, P. Geo.
Ministry of Forests
Nanaimo, B.C.

Cover Photograph:
Mike Wei

Acknowledgements

Thanks are due to Klaus Rathfelder, Keith Nunn and Jan Bednarski for reviewing the draft report. Thanks to Beaufort Watershed Stewards (BWS) members Mike Mesford, Jackie Ainsworth, Mark and Katie Lake for hosting some of the authors, and to Mike Mesford and others for excellent assistance during long field days for the survey in July 2021. Creation of some of the maps in this report was enabled by a non-profit software licence granted by ESRI to BWS.

EXECUTIVE SUMMARY

The University of Victoria, in conjunction with the Beaufort Watershed Stewards, a volunteer group, conducted a series of resistivity surveys on the eastern flanks of the Beaufort Range, eastern Vancouver Island, B.C., in the summer of 2021. The purpose of the project was to evaluate resistivity surveying as a cost-effective aquifer mapping tool for in-filling sub-surface lithology between sparse control well points, toward a goal of generating a 3D map of important aquifers.

Resistivity soundings were carried out at nine sites, mostly along 300 m profiles, from the Bowser to Royston area. This yielded nine one-dimensional (1D) profiles of subsurface resistivity to depths of up to 83 m below the ground for comparison with logged lithologies at adjacent or nearby wells. Sites were selected on the basis of: their proximity to control wells with available information on bedrock and/or shallow aquifer units of interest; their ease of access; and the ability to set up continuous cables along relatively straight and flat 300 m long sections of roads or railways.

The subsurface resistivity structure revealed from the soundings is generally consistent with the lithology logged in the adjacent control wells. However, there are some differences in interface depths and layer properties. The differences may reflect true lithologic differences between the sounding and well location or may result from deviations in the assumption, inherent to resistivity sounding methods, of lateral homogeneity in the subsurface beneath the profile. Two dimensional (2D) electrical resistivity tomography profiles were collected alongside sounding profiles at two sites in the Fanny Bay area to test for lateral heterogeneity and/or potential sea water intrusion.

A limitation of resistivity methods is that different lithologic units may have similar resistivity characteristics and thus may not be distinguishable from one another. However, the results of this project show that gravel and sand aquifer units in the study area are characterized by relatively high resistivity values (>500 ohm-m) and are distinguishable from more conductive and less permeable, more clay-rich till and shale bedrock (<300 ohm-m).

With an understanding of the local stratigraphy and the resistivity calibration of important units encountered in the control wells in this initial project, it should be possible for future resistivity surveying to contribute to mapping of significant aquifers in areas of the Beaufort Watersheds that lack control wells. The geophysical methods utilized have additional potential applications for aquifer characterization. These include, but are not limited to, evaluating aquifer vulnerability to contamination by mapping the presence, absence and relative thickness of confining sediments, and ground truthing sea water intrusion vulnerability by mapping the depth and lateral extent of the brackish transition zone between fresh water and sea water in coastal aquifers.

CONTENTS

FIGURES

TABLES

ACRONYMS

BR	Bedrock
btoc	below top of casing
BWS	Beaufort Watershed Stewards
CST	Constant Spread Traversing
ENV	Ministry of Environment and Climate Change Strategy
ERT	Electrical Resistivity Tomography
GWELLS	Groundwater Wells and Aquifers Database
LWRS	Ministry of Land, Water and Resource Stewardship
mASL	metres above sea level
mbgl	metres below ground level
SPID	Ships Point Improvement District
VES	Vertical Electrical Sounding
WSS	Water Science Series
WTN	Well Tag Number (database number in Groundwater Wells and Aquifers database)

1. INTRODUCTION

The Beaufort Watershed Stewards (BWS) is a group of local volunteers, active since 2016, who work to promote the health and resilience of local watersheds in the Beaufort Range, and to ensure the quality and quantity of fresh water for the future (BWS, 2020). The Beaufort Range is located on the eastern slopes of Vancouver Island, between the communities of Bowser and Royston, British Columbia (Figure 1). Understanding groundwater and aquifers within the Beaufort Range watersheds is a vital part of that work, as drinking water is primarily sourced from groundwater. The BWS expressed interest in using surface geophysics as a tool to characterize the groundwater and aquifer units within the Beaufort watersheds.

Surface and borehole geophysics have been sparsely used as a tool for characterizing groundwater aquifers on Vancouver Island and the Gulf Islands. Moncur (1974) conducted surface seismic reflection and resistivity surveys (predominantly lateral profiling) on Mayne Island to approximate depth to bedrock (overburden thickness) and to infer presence of faults and fractures that may localize groundwater flow. Moncur (1974) also assessed the use of a suite of borehole geophysical tests to help identify different bedrock types and to locate fractures in select wells.

With similar objectives, Abbey (2000) used lateral electromagnetic profiling and borehole geophysics at sites on southern Vancouver Island (Shawnigan Lake Quarry) and Saturna Island. Abbey (2000) noted that adequate interpretation of geophysical survey data requires the use of a sufficiently detailed database of geological data (e.g., drill logs) in order that geophysical interpretations can be extended to areas without such ground truthing data.

Foster (2014) collected six two-dimensional (2D) electrical resistivity tomography profiles in the Cowichan watershed on southern Vancouver Island to improve constraints for hydrogeologic modelling. The profiles spanned 135-830 m in length, probing the subsurface to depths of 35-100 m below the ground. Using well log lithology to calibrate the inverted resistivity models, subsurface units could be mapped between the well control points based on strong resistivity contrasts between relatively high resistivity gravel/silt aquifers and more conductive clay-rich sediments. Constraints were insufficient to characterize a resistivity range for the Nanaimo Group bedrock which comprises sandstone, conglomerate, and shale.

As part of the Geological Survey of Canada’s regional groundwater assessment program, seismic reflection and borehole geophysics data were collected in the Parksville-Deep Bay area of eastern Vancouver Island to characterize surficial and bedrock geology. Borehole geophysical data, including apparent conductivity and magnetic susceptibility, from one bedrock and four unconsolidated sediment boreholes were used to characterize lithological changes (Crow et al., 2014; Crow, 2016). Seismic reflection data were further used to constrain the stratigraphy of unconsolidated sediments and the depth to bedrock (Bednarski, 2015).

In 2021, the BWS partnered with the School of Earth and Ocean Sciences (SEOS) at the University of Victoria to conduct a series of resistivity soundings to characterize the local surficial and bedrock aquifers. The initial project idea was based on the successful use of resistivity sounding in aquifer mapping in the United Kingdom some 40 years ago by BWS member Mark Lake (Lake, 1978). The purpose of the Beaufort Watershed project was to test the viability of electrical resistivity techniques to find important boundaries between lithological units, using control wells for ground truthing.

The study area for the pilot project is on the east coast of Vancouver Island between Bowser to the south and Courtenay to the north. Nine survey sites were chosen based upon: their ease of access, the ability for continuous cables to be set up along relatively straight and flat 300-m long stretches of road-or rail-side, the availability of subsurface information from nearby deeper drilled wells, and the occurrence of known aquifer units of interest, such as sedimentary bedrock or Quadra Sand aquifers. The general locations of these sites and adjacent control wells are shown in Figure 1, along with the locations of all the registered water wells in the region.

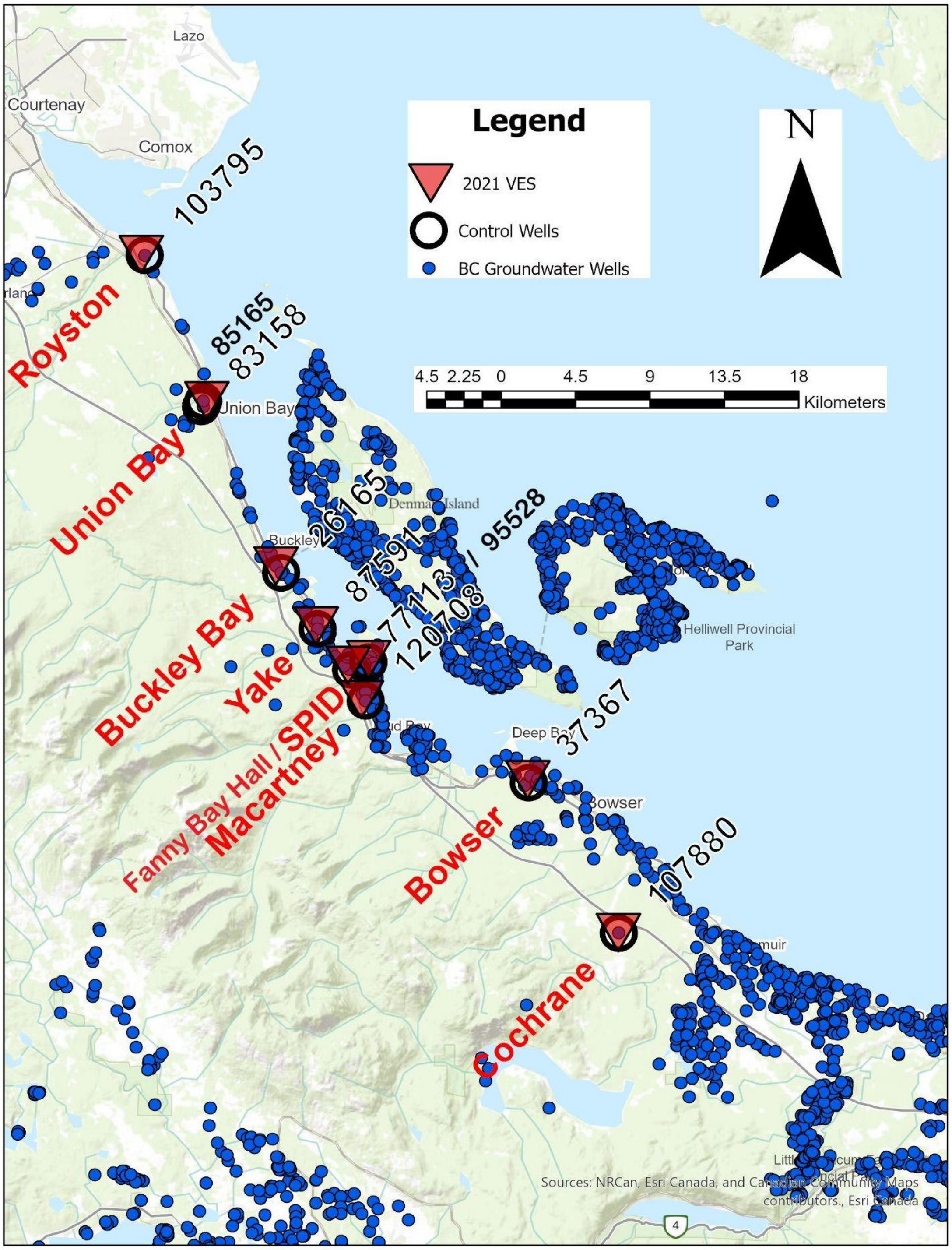

Figure 1: Generalised regional map of the Beaufort study area showing location of Vertical Electrical Soundings (VES) in red, control wells (Well Tag Number in black) and registered water wells (GWELLS, Province of B.C., 2022a).

2. LOCAL GEOLOGY AND AQUIFERS

The surficial geology of the study area consists primarily of unconsolidated sediments deposited from more than 40,000 years ago to the present (Fyles, 1960; 1963a,b). A description of the age and depositional relationships between the primary unconsolidated lithostratigraphic units is shown in Table 1, with the descriptions of surficial sediments from (Bednarski, 2015); Figure 2 is a regional map showing the spatial extent of Quaternary sediments. The mapped bedrock geology is shown in Figure 3; the bedrock stratigraphy of the region is provided in Appendix C, as mapped by Cathyl-Bickford (1992) and Cathyl-Bickford and Hoffman (1998). Figure 4 shows photos of the main unconsolidated and bedrock geological units in the study area.

Unconsolidated (sand and gravel) aquifers mapped along the central east coast of Vancouver Island are made up of sediments deposited before, during and following major periods of glaciation; sediment thickness can locally exceed 100 m (Bednarski, 2015; Fyles, 1963a).

Table 1: Description of surficial deposits in the study area (from Bednarski, 2015). Age units are denoted as "ka BP" referring to x1000 radiocarbon years before present (1950), and "ka cal BP" referring to the calibrated age x1000 years before present (1950).

Radiocarbon age		Stage/substage	Climatostratigraphy	Lithostratigraphic Unit	Environment of Deposition and Principal Materials
ka BP	ka cal BP	Holocene	Postglacial	Salish Sediments	Swamp / Organic deposits: organic matter and mud Slope deposits: Alluvial fans of poorly sorted gravels; landslide debris, colluvium Lacustrine: fine-grained sediments deposited in lakes Marine: Littoral sediments, sand, gravel and silt at the present shoreline Fluvial: deltaic and channel floodplain, stratified gravel, sand and silt
10	11.6	Late Wisconsinan		Capilano Sediments	Slope deposits: Alluvial fans of poorly sorted gravels; landslide debris, colluvium Glaciofluvial to fluvial: stratified sand and gravel, postglacial deltatic sediments and channel flood plain deposits. Glaciomarine to marine: stoney silt, sand and clay, contains marine shells and rare wood; diamictons in places.
13	15.6		Fraser Glaciation	Vashon Drift	Glaciofluvial / ice contact: poorly sorted gravels, sands and silts; stratified; Kame and kame deltas Glacial: sandy to clayey diamicton, till; in places lenses of stratified sediments
18	21.8			Quadra Sand	Glaciofluvial: stratified sand, minor gravel and silt, well-sorted, in places organic rich near base
27.1	31.1	Mid Wisconsinan	Olympia Nonglacial Interval	Cowichan Head Formation	Marine to fluvial: Pebble-gravel, peat with pebbles and wood
40	43.6				Marine: Clay, stony clay, silt, shells; basal laminations in places laminated
>50 *beyond the range of radiocarbon dating*		pre-Wisconsinan	penultimate glaciation	Dashwood drift *(including Mapleguard sediments)*	Glaciomarine: stoney silts and clay with sand lenses and shells Glacial: sandy to silty diamicton, till containing silt and gravel lenses

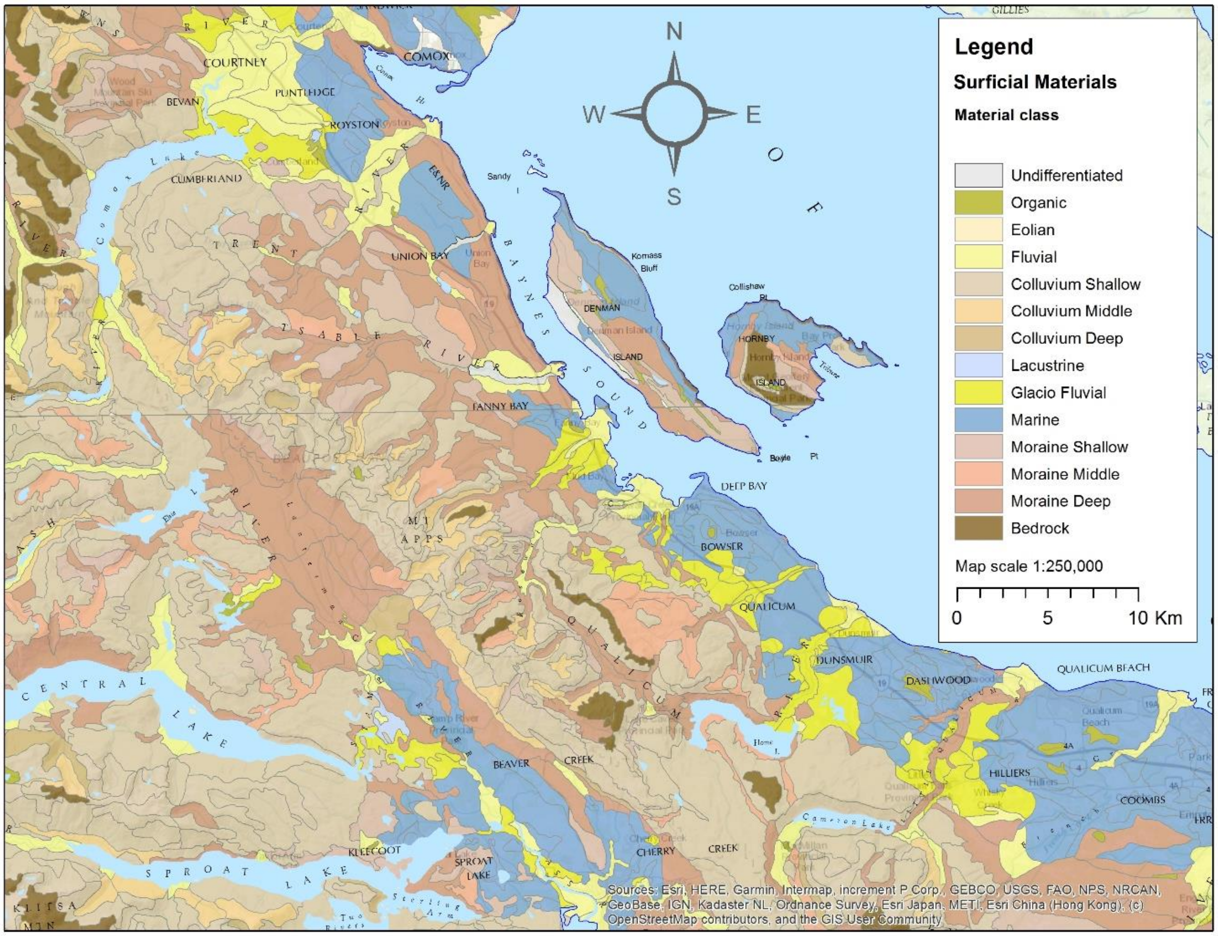

Figure 2: Surficial materials within the Beaufort study area (data from: Guthrie, 2005; Province of B.C., 2022b).

Mapped aquifers within the Beaufort study area are shown in Figure 5. Some of the most productive aquifers in the study area are comprised of younger Salish Sediments that form deltaic fan aquifers along the lower reaches of Wilfred Creek (Aquifer 419), Rosewall Creek (Aquifer 414), and Tsable River (Aquifer 415). Other deposits of older sediments associated with the Quadra sand occur at the southern edge of the study area near Bowser (Aquifer 416), as well as at the northern edge of the study area near Royston (Aquifer 951) and form important aquifers in those locales. Quadra sand deposits (example in Figure 4c) outcrop along major drainages including Qualicum River, downstream of Horne Lake and along reaches of Nile Creek inland from the coast where these major drainages have incised shallower confining sediments made up of Vashon Drift (morainal deposits containing fine grained clay and silt) mapped between Wilfred Creek and Cowie Creek (Fyles, 1963a) and between Fanny Bay and Royston (Fyles, 1960). More permeable sediments within the Vashon Drift sequence also form shallower aquifers overlying the Quadra sand, including Aquifer 417, Aquifer 661, Aquifer 663 and Aquifer 951. Additional unconsolidated aquifers may be identified in the future in areas of presently low levels of groundwater development, as additional test holes and water wells are drilled that provide subsurface information. A summary of aquifers within the entire Beaufort study area is included in Appendix B, including some aquifers that are not contained within the Beaufort watersheds in entirety, but overlap the northern and southern extents of the primary area of interest.

The bedrock geology beneath these unconsolidated sediments has been extensively mapped by Cathyl-Bickford and Hoffman (1998). Due to the eastward-dipping nature of these Upper Triassic and Upper Cretaceous deposits, the rocks sub-cropping the glacial sediments become successively younger to the east, from Triassic volcanics in the west and stepping through progressively younger members of the Nanaimo Group of sedimentary rocks (Figure 3, and Figure 4d). The Nanaimo Group is characterized by alternating coarser-grained units (dominated by sandstone and conglomerate) and finer-grained units (dominantly shale)(Hamblin, 2015). The degree of fracturing affects the hydraulic properties (i.e., hydraulic conductivity and storativity) of both the potential aquifer and aquitard units (Surrette et al., 2008; Allen et al., 2003; Mackie, 2002).

The only bedrock aquifer mapped in the region by the Province of B.C. is Aquifer 411 (AQ411) at the northern part of the study area (Figure 5). AQ411 is composed of fractured sedimentary bedrock of the Nanaimo Group. Even though no other bedrock aquifer is mapped within the study area, the Nanaimo Group underlies the entire area and even where surficial aquifers exist, wells are known to be drilled deeper into the bedrock in search of water supply.

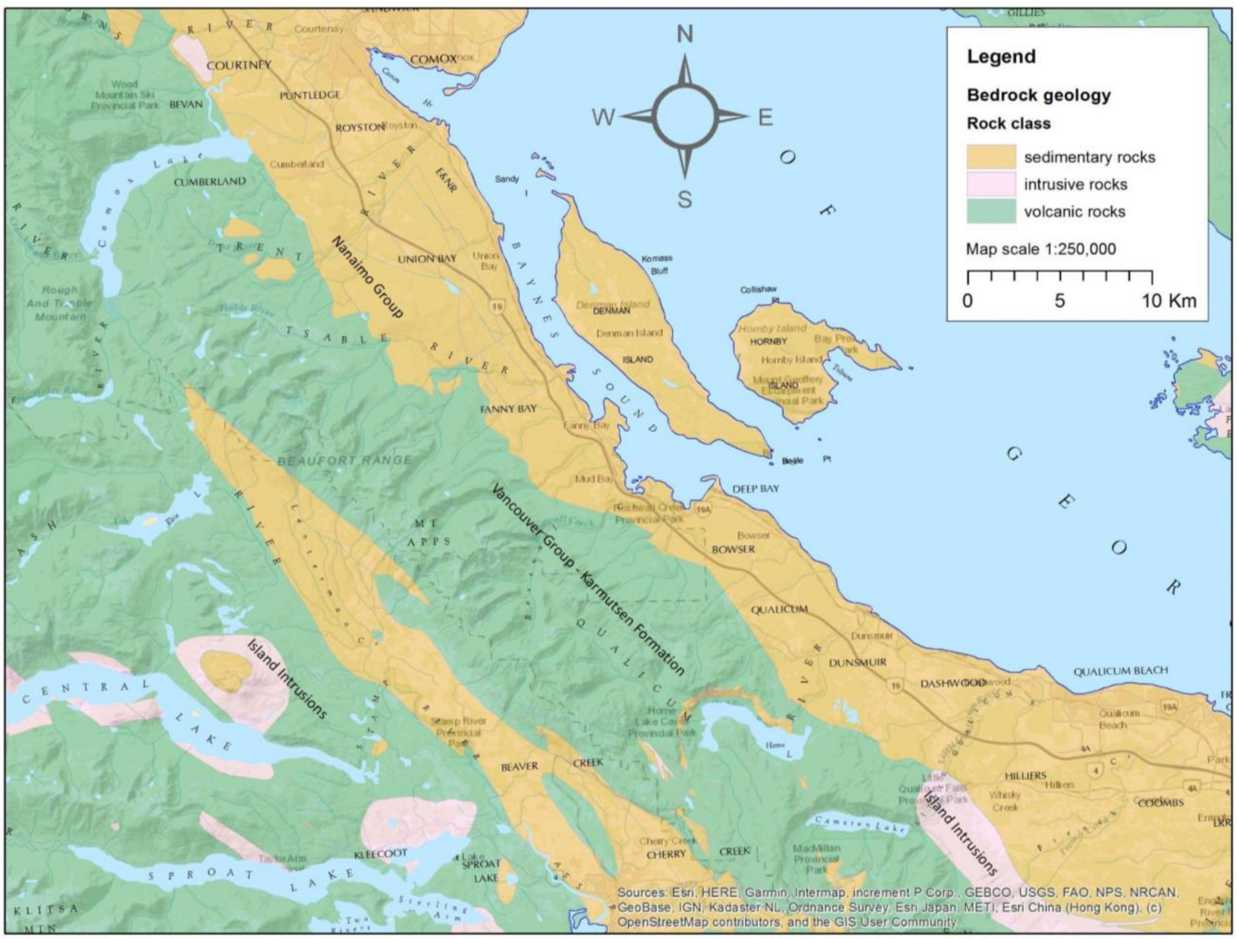

Figure 3: Bedrock geology within the Beaufort study area (data from: Cui et al., 2017; Massey et al., 1994; Province of B.C., 2022b).

At most site locations in this study (Fanny Bay Hall, Ships Point Improvement District (SPID)/Fanny Bay, Yake Road, Macartney Drive, Buckley Bay and Royston), the mapped bedrock is the Nanaimo Group Willow Point member (Trent River formation), which is made up of shale, siltstone, and minor sandstone (Cathyl-Bickford, 1992; Appendix C). At the Union Bay site, the mapped bedrock is the Tsable member of the Nanaimo Group (Trent River formation), including conglomerate, minor sandstone, and pebbly siltstone.

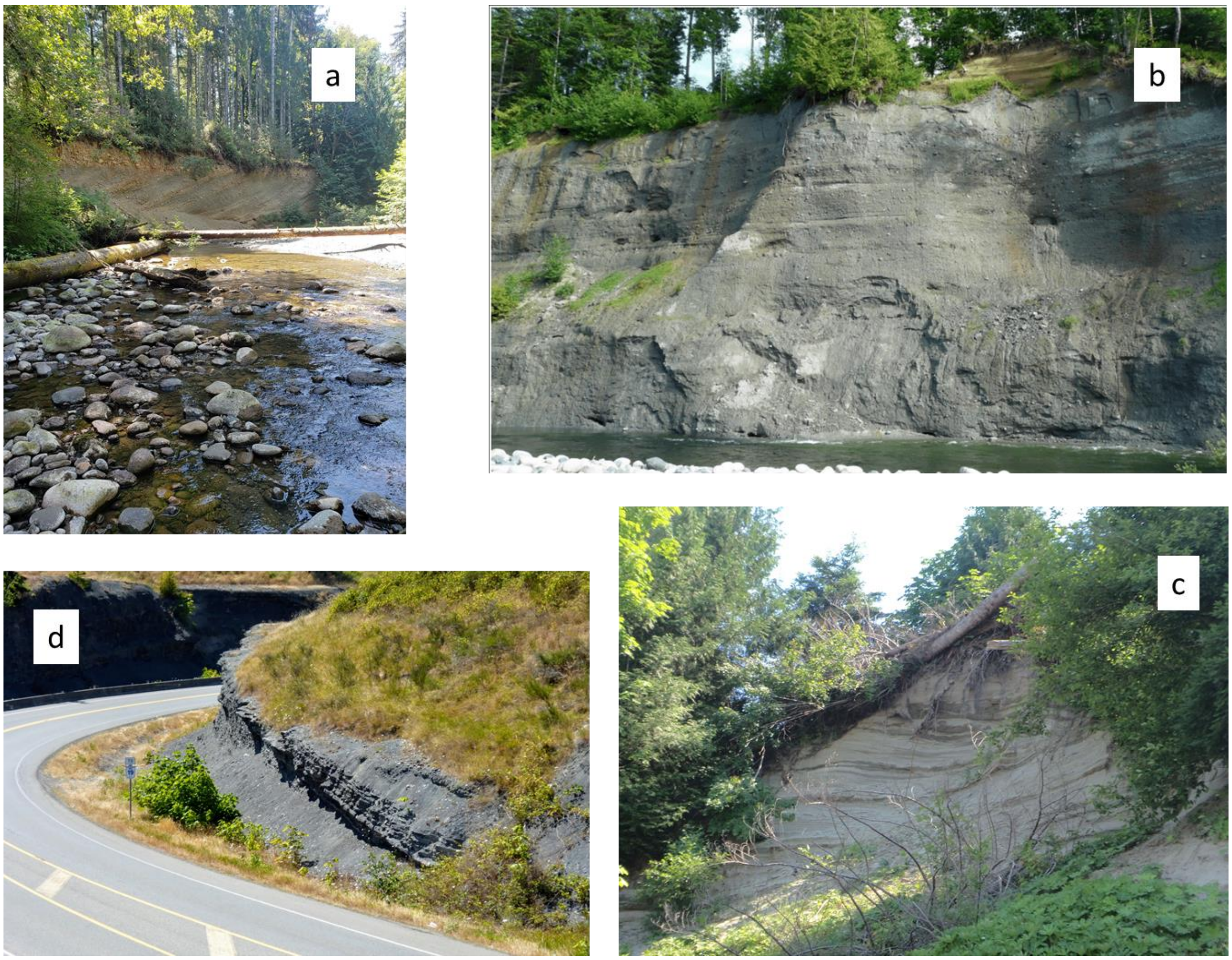

Figure 4: Photographs showing, in a clockwise direction: a) Salish Sediments within and on the banks of Wilfred Creek and Capilano Sediments (outcrop in the background), b) Vashon Till at Englishman River (from Bednarski, 2015), c) Quadra Sand near Bowser, B.C., and d) Nanaimo Group sedimentary bedrock at Buckley Bay.

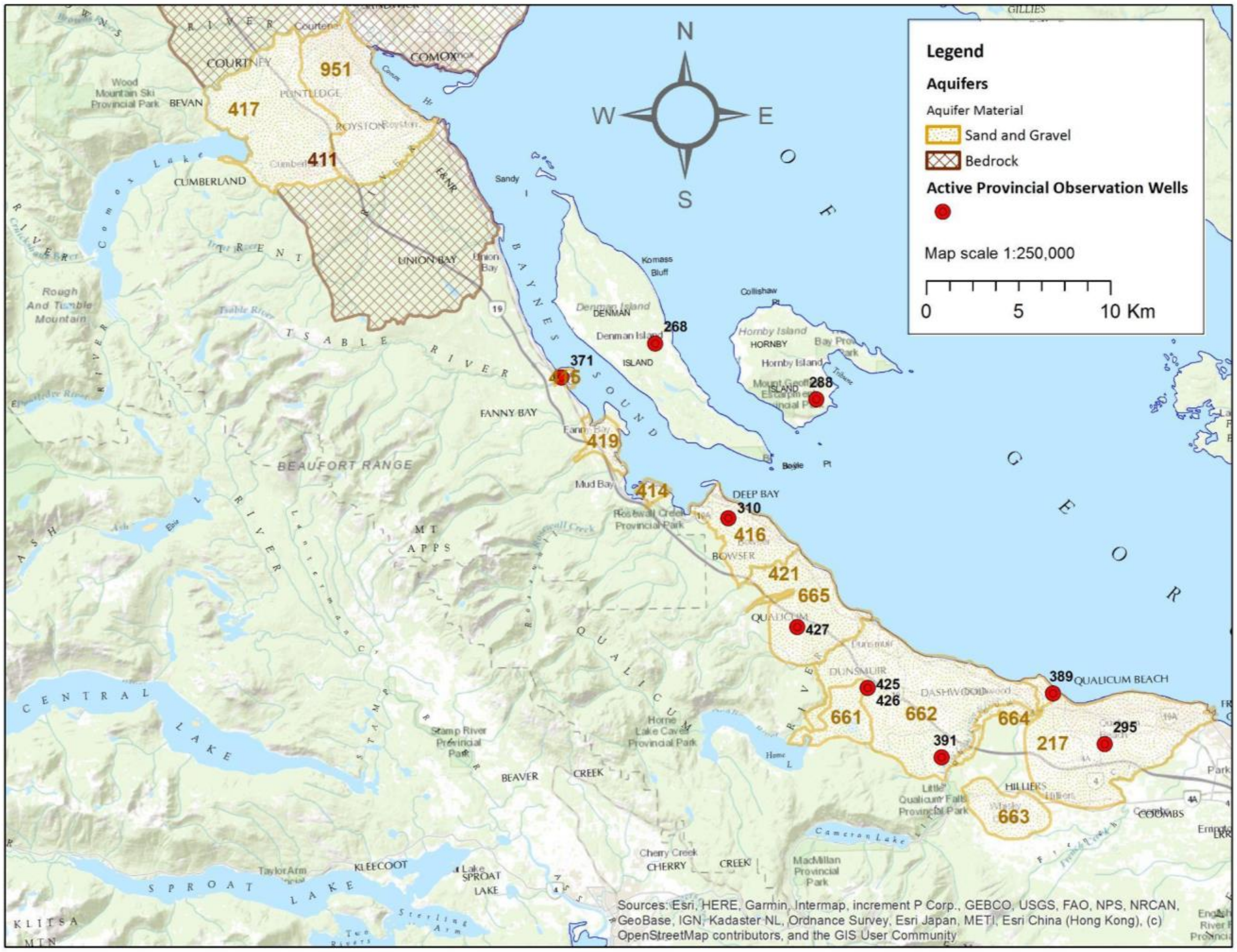

Figure 5: Mapped aquifers within the Beaufort study area (data from: Province of B.C., 2022b). Aquifer descriptions included in Appendix B.

3. <u>ELECTRICAL RESISTIVITY: THEORY AND METHODS</u>

3.1 Resistivity of Geological Materials

Electrical resistivity, the inverse of conductivity, is a measure of how well a material resists the flow of electrical current. It is material dependent; metals tend to have a resistivity near zero (high conductivity), whereas air has a value of resistivity approaching infinity (Griffiths, 2017). Rock tends to have relatively high resistivity; however, resistivity values depend on mineral composition, porosity and the salinity of the pore fluids (Burger et al., 2006). Lithology is an especially significant factor; if the rock has a higher content of metals or graphite, resistivity will be reduced by electronic conduction. For example, a graphite-rich rock will be much less resistive than a young granitic pluton with high silica content. However, if the granitic pluton is extremely weathered with cracks and larger permeable pore spaces, its resistivity values can decrease significantly because the enhanced porosity can contain groundwater which lowers resistivity. Clay-rich sediments typically have low resistivity because of the negative surface charge of clay minerals and their typically high porosity to hold fluids. Clay-rich shale bedrock may have resistivity values overlapping those of unconsolidated clay sediments.

The porosity and water content of the rock and sediments also plays an important role. If the rock/sediment is porous, but unsaturated, it will most likely have high resistivity due to the high air content. If the rock/sediment is porous and saturated, the resistivity will decrease. Depending on the pore fluid chemistry, the resistivity could decrease even more. For example, salt water has a resistivity below 1 ohm-m and fresh water has a resistivity varying from around 4 ohm-m up to 100 ohm-m depending on the concentration of dissolved ions (Palacky, 1988). Typical ranges of resistivity (and conductivity) values of rock and sediment types are shown in Figure 6.

As a result of the factors described above, resistivity alone tends not to be diagnostic of a particular rock or sediment type. However, the goal of this project is to determine if resistivity surveying can help distinguish between contrasting lithological units, such as the boundary between fluid-filled coarse gravel and shale bedrock. In saturated unconsolidated units, resistivity contrasts could highlight differences in groundwater chemistry, such as zones of higher salinity in a coastal environment. Based on the mapped bedrock and surficial geology in the study area, resistivities in the typical range of shales and clays to gravel and sandstone could be expected (10 - 10,000 ohm-m).

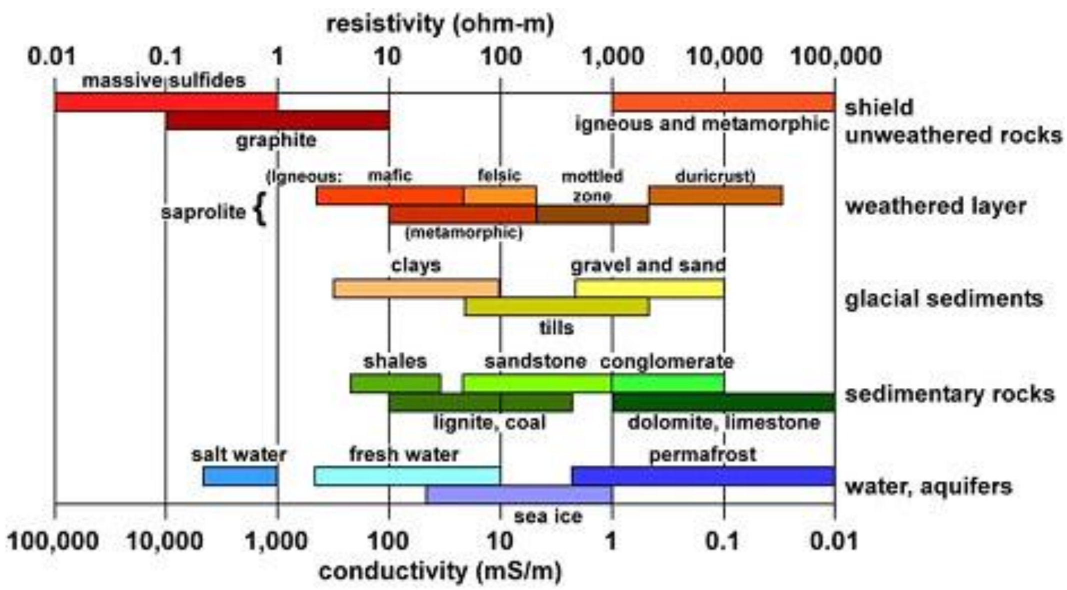

Figure 6: Resistivity of common rock and sediment types and fluids (Palacky, 1988).

3.2 Resistivity Survey Methods

The resistivity in the subsurface can be estimated by applying a voltage or current through a pair of electrodes inserted partway into the ground (typically to ~25 cm depth) and measuring the potential difference via a separate pair of electrodes. The measured potential difference is proportional to the resistivity, averaged over the sampled subsurface; it also depends on the input current and on the electrode array geometry. The current and potential electrode pairs can be placed in different configurations or arrays depending on the survey objectives.

There are three different types of resistivity surveys:

1) Vertical Electrical Sounding (VES) is used to determine the one-dimensional (1D) resistivity structure of the subsurface. The length of the 4-electrode array is gradually increased in order to sample progressively deeper into the subsurface. This is typically done using one of two electrode configurations: the Wenner array or the Schlumberger array (described in the

following sections), as these arrays provide the best vertical resolution. VES surveys were carried out at all sites in this study.

2) Constant Spread Traversing (CST) is used to determine lateral changes in the subsurface, e.g., to locate vertical fault zones. A fixed-length 4-electrode array is moved stepwise along a profile. CST surveying was not conducted in our study.
3) Electrical Resistivity Tomography (ERT) combines VES and CST surveying to investigate both vertical and lateral variations in the subsurface, resulting in a 2D profile. Many electrodes are used, connected by cable, and programmed so that a subset of four electrodes is used in each measurement. The program works through different subsets of electrodes to effectively carry out both CST and VES surveying during the automatic data collection. The dipole-dipole array, described in Section 3.3.2, is typically used in ERT surveys, as it has good lateral resolution. ERT surveys were carried out at two sites in this study.

3.2.1 Wenner Array

The Wenner array (Zohdy et al., 1974) is shown in Figure 7, where the current electrodes (A and B) and the potential electrodes (M and N) are placed an equal distance 'a' apart around a central point, the location beneath which the 1D resistivity structure will be interpreted. The battery sends a known current between electrodes A and B and the potential difference (ΔV) is measured between electrodes M and N. In VES surveying, the first measurement uses a minimum value of 'a' to sample the shallowest subsurface. For subsequent measurements, the distance 'a' is increased to increase the depth of the sounding and all four electrodes are moved to a new position, remaining centred on the same point. The calculation of apparent resistivity (ρ_a) for a particular measurement using the Wenner array is shown in Figure 7 where ΔV is the measured potential difference between electrodes M and N, I is the current from the battery, and 'a' is the spacing between adjacent electrodes.

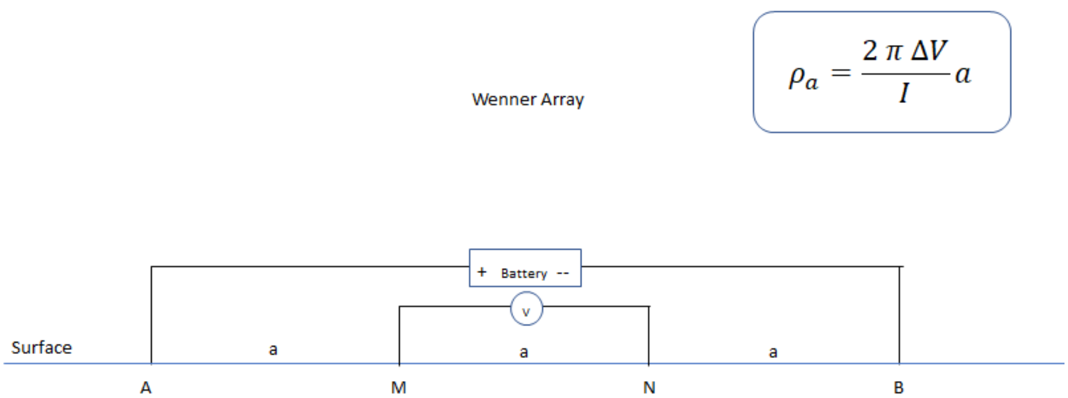

Figure 7: Electrode configuration for the Wenner array with the equation for apparent resistivity (ρ_a), based on the input current (I), the electrode spacing 'a', and the measured potential difference (ΔV) between electrodes M and N.

3.2.2 Schlumberger Array

The Schlumberger array (Zohdy et al., 1974) involves the same order of electrodes around a central point, where the outer current electrodes (A and B) are connected to the battery with a known voltage and the inner electrodes (M and N) measure the resulting potential difference. However, the spacing between electrodes does not remain equal; generally only the outer electrodes are moved further apart for subsequent measurements during a VES survey. As the current electrode spacing is increased, the current travels deeper and the measured potential difference is a result of sampling a greater depth range in the subsurface. Figure 8 shows the Schlumberger array, and the apparent resistivity equation, where the distance between the inner potential electrodes (M or N) and the centre of the array is ‘l’ and the distance between electrode A and centre is ‘L’, which is the same as the distance between the centre and electrode B.

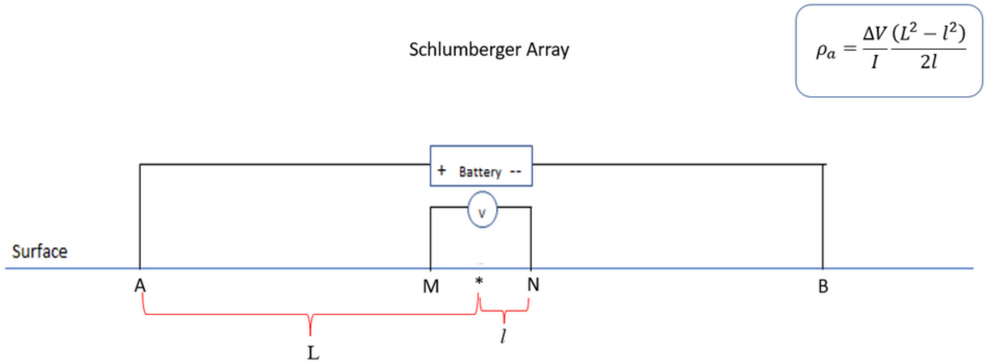

Figure 8: Electrode configuration for the Schlumberger array with the equation for apparent resistivity (ρ_a), based on the input current (I), spacings ‘L’ and ‘l’, and the measured potential difference (ΔV). The asterisk (*) indicates the centre of the array.

The Schlumberger array offers a more efficient method for sounding because it is possible to do multiple soundings by only moving the outer electrodes (increasing ‘L’) while maintaining the position of the inner electrodes. Once the outer electrodes are too far apart (when ‘L’ is greater than 10’l’), ‘l’ is increased. The Schlumberger array can sound deeper with the same length of spread as the Wenner array, while providing higher vertical resolution with greater efficiency.

3.2.3 Dipole-Dipole Array

Resistivity surveying can also be carried out with the dipole-dipole array (Zohdy et al., 1974), where the current electrode pair is separated from the potential electrode pair (Figure 9). The dipole-dipole array has spacing ‘a’ within each pair of electrodes. It differs from the Wenner and Schlumberger arrays because the electrodes M and N are not within the spread of electrodes A and B. The spacing between the A-B electrode pair and the M-N electrode pair must be an integer multiple (n) of ‘a’.

The dipole-dipole array has lower vertical resolution than the Wenner and Schlumberger arrays, but higher lateral resolution, making it a good choice for interpreting the 2-dimensional structure of the subsurface using ERT. During an ERT survey, the collection of data is controlled by software which selects four of the electrodes, arranged in a dipole-dipole array, for each individual measurement. It starts with spacing ‘a’ and traverses along the profile at this spacing. After the length of the survey has been traversed, a greater depth is sampled by increasing the spacing ‘a’ and the length of the survey is traversed again. This continues until the ‘a’ and ‘n’ spacings can no longer be increased.

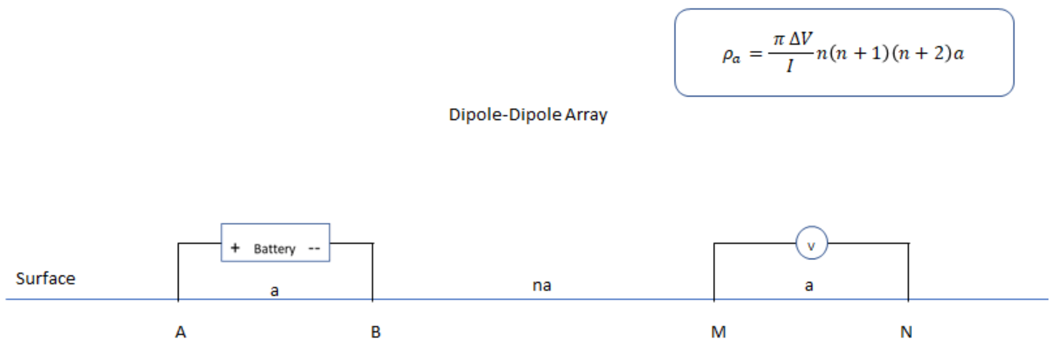

Figure 9: Electrode configuration for the dipole-dipole array with the equation for apparent resistivity (ρ_a), based on the input current (I), spacings 'a' and 'na', where 'n' is an integer multiple (n = 1, 2, 3,..), and the measured potential difference (ΔV).

3.3 Data Analysis

3.3.1 Analysis of VES Data

VES provides a vertical 1D profile of subsurface resistivity. As the electrodes are moved further apart, the sampling depth range is increased. Typically, with vertical profiling, it is possible to sound to a depth of between 15% and 25% of the full final array length (Advanced Geosciences, Inc., 2014). Interpretation of sounding data assumes that the layers below the surface are relatively horizontal and laterally continuous. This assumption is necessary because the initial resistivity calculation using the input current and the measured potential difference provides the apparent resistivity. Apparent resistivity (ρ_a) is the weighted average of resistivity that the current experiences on its journey through the subsurface.

For the first measurement, when the electrodes are close together, ρ_a is typically equal to the resistivity of the shallowest layer (ρ_1). For example, as indicated in Figure 10, if the outer electrodes were at S and T with the green line as the current flow path between them, the apparent resistivity would equal the resistivity of layer one because that is the only layer sampled by this path. The deeper the current travels, the more layers it can travel through. As shown in Figure 10, the current between electrodes A and B (the red line) travels through three layers with three different resistivities (ρ_1, ρ_2, ρ_3). Thus, the apparent resistivity (ρ_a) calculated from this array does not equal ρ_3 but reflects a combination of the resistivities of all layers the current travelled through.

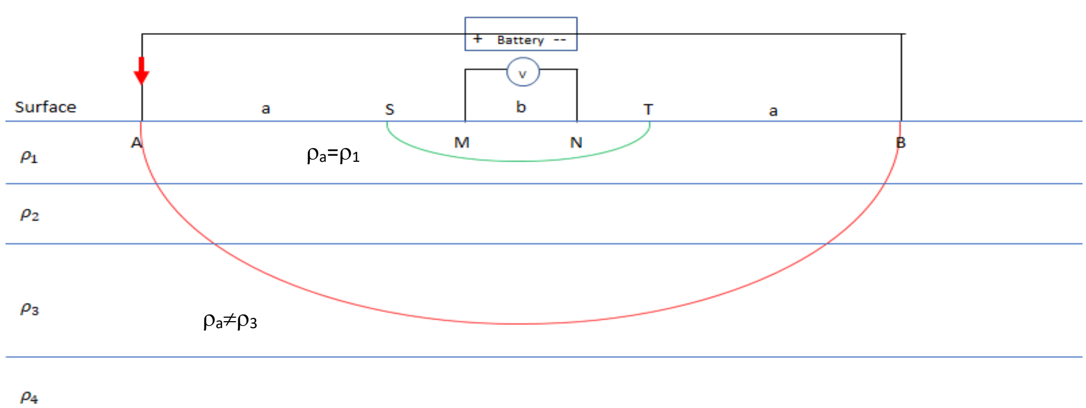

Figure 10: Simplified diagram of a Schlumberger array. Red line shows the current flow path between the current electrodes A and B. Green line shows the shallower path for a shorter array with current electrodes placed at S and T.

True layer resistivities and interface depths (a layered resistivity model) can be approximated using the master curve approach or by using inverse modelling software. The master curve approach is typically used during the sounding survey and may guide data collection. During fieldwork, ρ_a values are displayed on the resistivity instrument following each measurement. ρ_a values are plotted against electrode spacing on log-log graph paper. For a Wenner array, this spacing is 'a'; for a Schlumberger array, distance AB/2 is plotted (e.g., Figure 11).

A data curve that shows an increase in apparent resistivity with increased spacing implies a downward change from a lower- to a higher-resistivity layer, and vice versa. The size of the resistivity contrast controls the steepness of the curve, and the depth of the interface between the contrasting layers controls the spacing at which this change occurs. Sounding of a multi-layer subsurface will result in multiple curve segments on the apparent resistivity versus spacing plot.

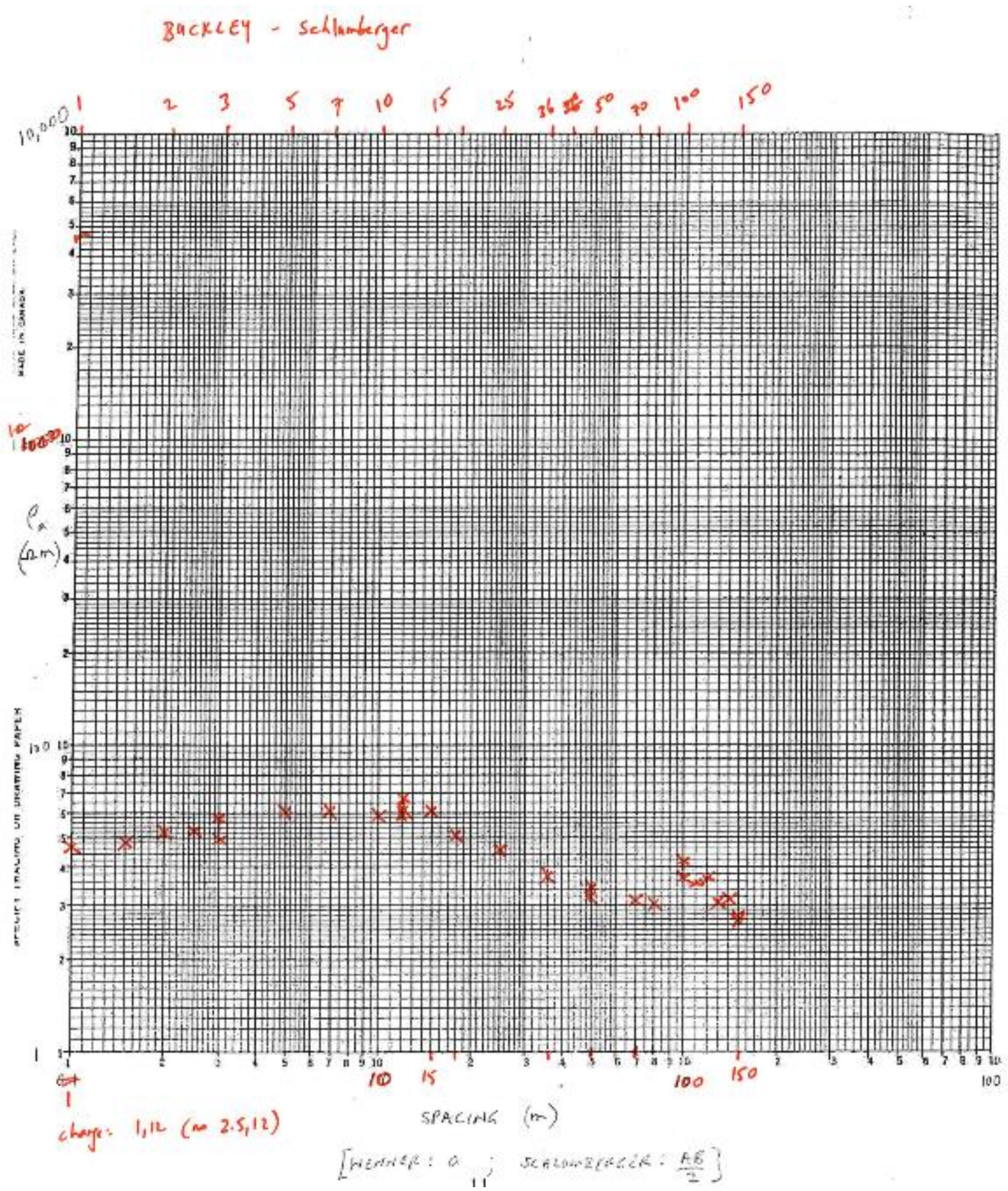

Figure 11: Data from the Buckley Bay 1D sounding, plotted in the field for preliminary interpretation.

Sets of 2-layer theoretical "Master Curves" have been developed to encompass the full range of possible positive and negative resistivity contrasts across an interface, with reflection coefficient '*k*' (Equation 1) ranging from +1 to -1 (e.g., Zohdy et al., 1974). A transparent master curve overlay, at the same scale as the log-log graph paper, is placed over a curved segment of the plotted data. The overlay is moved up/down and right/left, keeping the axes of the two sheets parallel, until a best fit is found between the data curve segment and one of the master curves. In this position, the true resistivity of the shallower layer ("ρ_1") can be read off the y-axis, the depth of the interface between the two contrasting layers is read off the x-axis, and the true resistivity of the deeper layer ("ρ_2") can be calculated using the '*k*' value of the best-fit master curve, using the equation below:

$$\rho_2 = \left(\frac{1+k}{1-k}\right)\rho_1$$

(Equation 1)

The process is repeated with subsequent curved segments of the data, to yield an approximate 1D resistivity model of the subsurface.

Inverse modelling can be carried out to provide a more detailed and accurate 1D resistivity model following the VES survey, using software such as Res1D (freeware, available at: geotomosoft.com/downloads.php) or EarthImager 1D (Advanced Geosciences, Inc., 2009) as used in this study. After loading the data file, the program constructs a starting model that is based on the recorded data and a fixed number of layers (this can be specified by the user). Automatic inversion will retain the number of layers and modify the layer resistivities and thicknesses over a number of iterations. Each successive iteration is used to model a set of predicted data for comparison with the observed data points, with the best-fit model having the lowest root mean square (RMS) error, as defined below:

$$RMS(\%) = \sqrt{\frac{\sum_{i=1}^{N}\left(\frac{d_i^{pred}-d_i^{obs}}{d_i^{obs}}\right)^2}{N}} \text{x}100\%$$

(Equation 2)

where N is the total number of measurements, d^{pred} is the modeled set of predicted data and d^{obs} is the set of measured data. The inversion can be set to stop either after a fixed number of iterations or once a set RMS value is reached. The preferred layered resistivity model is typically one that has a relatively low RMS value that is also geologically reasonable.

3.3.2 Analysis of ERT Data

As with VES surveys, an ERT survey collects apparent resistivity and electrode spacing information. The apparent resistivity data points collected with small spacings are representative of the shallow subsurface, and those collected with larger spacings sample a greater depth range. The ERT apparent resistivity dataset is represented on a 2D pseudo-section, "pseudo" because the resistivity values are weighted averages shown at median subsurface positions based on the electrode geometry for each measurement. The ERT data must be inverted for the true 2D subsurface resistivity profile. With many points making up a pseudo-section, data analysis must use inversion software such as Res2DINV (from Geotomo Software) or EarthImager 2D (Advanced Geosciences Inc., 2009) as used in this study. The automatic least-squares inversion follows a similar process to the 1D inversion modelling, but it uses the pseudo-section as a starting model and inverts for the 2D structure instead of 1D.

3.4 Resistivity Survey Sites and Data Collection

Resistivity surveys were carried out at nine locations in total as indicated in Figure 1. At all locations a VES was done using a Schlumberger array; at Fanny Bay Hall, a VES using a Wenner array was also done, for comparison. Additionally, at the Fanny Bay Hall and SPID/Fanny Bay sites, a 2D survey using ERT was done. Table 2 summarizes the surveys at each site. A straight, horizontal line of 300 m was needed for the best results, so the majority of the soundings were done on the side of roads or along the side of the E&N railbed with the centre of the spread located as close as possible to the control well. Offset distances are detailed in Appendix A. The data were acquired using an Advanced Geosciences Inc. MiniSting resistivity meter (details at https://www.agiusa.com/ministing, last accessed June 2022), powered by a 12-V battery, and connected by cables to stainless steel electrodes.

Table 2: Summary of the nine survey sites; for more details of each site, see Appendix A and Appendix E.

Site (Well Tag Number (WTN) for control well(s))	VES - Wenner 1D	VES - Schlumberger 1D	ERT Dipole-Dipole 2D	Note
Fanny Bay Hall (WTN 77113)	✓	✓	✓	Exploring which 1D array to use and application of 2D section. Decided to go with the more efficient Schlumberger array.
SPID/Fanny Bay (WTN 95528)		✓	✓	Application of 2D section to map occurrence of saltwater in the aquifer.
Bowser (WTN 37367)		✓		
E & N Railway near Yake Road (WTN 87591)		✓		
Cochrane Road (WTN 107880)		✓		
E & N Railway near Macartney Drive (WTN 120708)		✓		
Buckley Bay (WTN 26165)		✓		
E & N Railway at Union Bay ENV(WTN 83158 and 85165)		✓		
Royston (WTN 103795)		✓		

The spacing of electrodes used for the Schlumberger array was the same at almost all the soundings (spacing tabulated in Appendix D). Each apparent resistivity measurement was plotted on a log-log graph (as shown in Figure 11) and the results were monitored. If better resolution was needed to characterize a sharp change in resistivity, the electrode spacing was adjusted or additional measurements were made. The electrode spacing was also adjusted at the Cochrane and Bowser sites due to obstructions that prevented the placement of electrodes (e.g., large rocks or hard-packed surfaces). The location for the centre of the spread was determined considering a few factors. The centre needed to be as close to the control well as possible, while also being a convenient and safe place to set up the battery and MiniSting equipment. A straight line was set up by rolling out a measuring tape on either side of the centre point.

To maximize efficiency, the 28 available electrodes were hammered to a depth of approximately 25 cm at predetermined spacings (see Appendix D) up to 50 m from the centre. The first measurement involved the smallest spacing, with all electrodes close to the centre, moving outwards to increase the spacing through the survey. After the data were collected with the outer electrodes at 50 m, all the electrodes (except for the ones needed as the inner electrodes for the next set of measurements) were removed and hammered in at greater distances, up to 150 m from centre on each side. Each time electrodes were placed, 0.5 litres of salt water (from the ocean) were poured at the base of each electrode to reduce contact resistance. The outer electrode spacing was maintained at no less than 3 times, increasing to 10 times the inner electrode spacing, and each time the inner electrode spacing was expanded, the outer electrode spacing was retained for an extra measurement to improve the later inversion results. GPS coordinates were collected at the centre and end points of each spread (Appendix E) and at a few positions along the line, if not straight, to record the location of the sounding. Figure 12 shows the centre of the spread at the Cochrane site; the potential electrodes can be seen, connected to the MiniSting, as well as the cables connecting to the current electrodes (out of view in the photo).

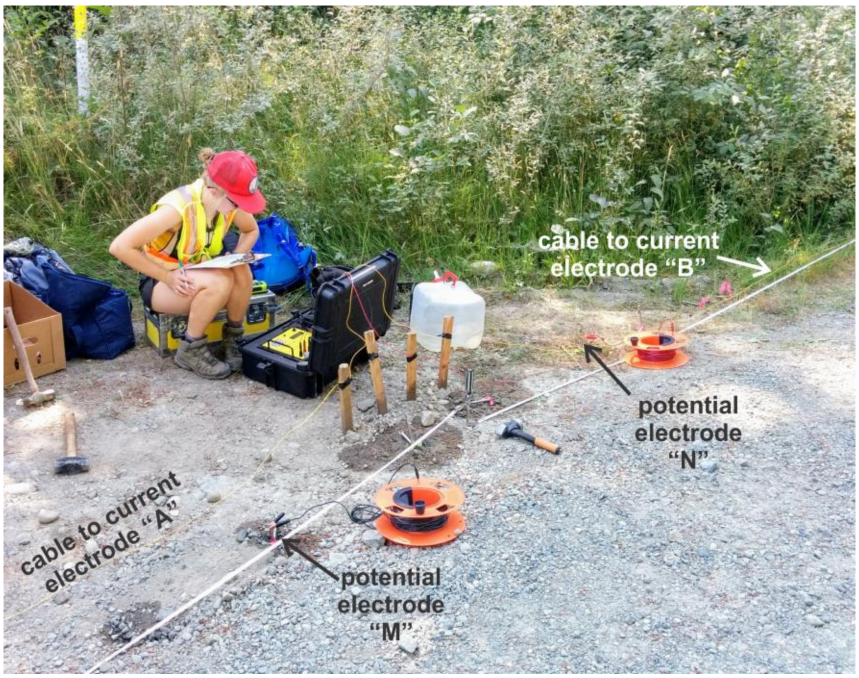

Figure 12: Centre of the VES spread at the Cochrane site. The MiniSting instrument is connected by red and black cables to the inner, potential electrodes, and by yellow cables to the outer, current electrodes (out of view in the photo). The cables are wound and taped around wooden stakes near the instrument, to avoid damage to the connectors as cables are unwound. Wet patches in the ground reflect the application of salt water at the base of electrodes to reduce contact resistance.

The ERT surveys were less labour intensive. The electrodes were hammered in 3 m increments along an 81 m line to a depth of approximately 25 cm, saltwater was once again poured at the base of each electrode before the electrodes were connected by cable to the resistivity system, and the resistivity line was kept free of potential obstructions (e.g., dogs or people). A contact resistance test was completed to assess variations in contact resistance, and to check that all electrodes were properly connected to the cable. More salt water was added to reduce contact resistance as required. Data were collected automatically, using the pre-set dipole-dipole ERT program and the SWIFT Mode software integral to the MiniSting instrument. Data were stored in the instrument and were downloaded to a laptop computer immediately following completion of the survey. The survey centre position was recorded with a handheld GPS.

4. RESULTS AND INTERPRETATIONS

The following subsections present the results from each sounding site as well as the interpretation of each model, with reference to the adjacent control wells. The order of the subsections is based on the order in which the sites were surveyed in July 2021. The data for each control well and site including the coordinates, elevation, depth drilled, and surface geology can be found organized in a table in Appendix A. Note that the colour scale for the resistivity model figures varies from site to site. Relatively resistive layers are shown in warm colours and relatively conductive layers in cool colours, but for each model the colour scale is optimized to best illustrate the contrasts between layers, i.e., the same shade of blue may represent very different resistivity values from one site to another.

4.1 Fanny Bay Hall (WTN 77113)

At the Fanny Bay Hall site, Salish Sediments are mapped at the location of the well and the resistivity profiles (Fyles, 1963a). The control well (WTN 77113) is located approximately 120 m southeast of the centre of the spread (Figure 13). At this site, a variety of surveys were carried out to test the equipment and to determine which array to use for the rest of the 1D soundings. Soundings using both the Wenner and Schlumberger arrays were completed in the northwest to southeast direction (the yellow line in Figure 13). After this comparison, the Schlumberger array was used for the remaining soundings, as use of this array is significantly more efficient with no compromise to data quality. An orthogonal Schlumberger sounding (NE-SW orientation) was also completed, to test for lateral variations. Finally, a 2D ERT profile was also collected in the NE-SW direction (the red line in Figure 13). Applying all the survey methods in the same location allowed a comparison of the advantages and shortcomings of each approach.

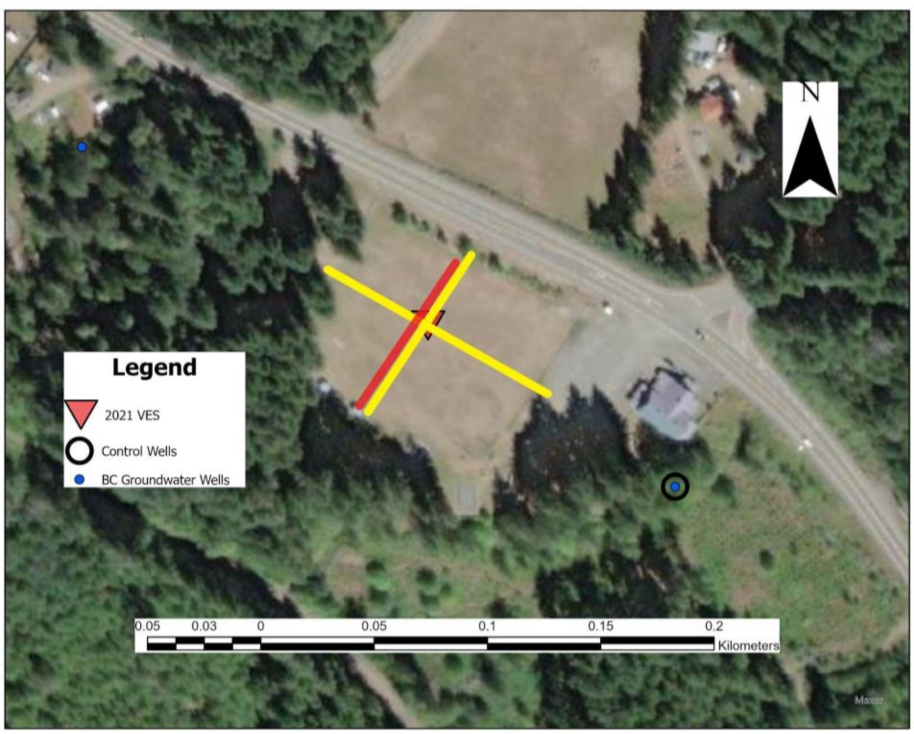

Figure 13: Locations of the resistivity profiles and the control well (WTN 77113; open circle) near Fanny Bay Hall. Yellow lines show the 1D sounding profiles; the red line marks the 2D ERT survey.

4.1.1 Wenner (NW-SE) 1D array

Figure 14 shows the final (10 layer) resistivity model and the observed and predicted apparent resistivity values for the Wenner (NW-SE) array at Fanny Bay Hall. An initial default 12-layer model was produced - this showed a large decrease in resistivity at a depth of around 16 m and a general trend of decreasing resistivity with depth. The number of layers was decreased to 6 for a subsequent inversion, but multiple layers near the surface had large differences in resistivity and the model lost detail at greater depth. After comparing the model with the Schlumberger array results and the 2D model, it appears that 10 layers is the minimum number of layers to maintain a reasonable amount of detail in the resistivity model (Figure 14).

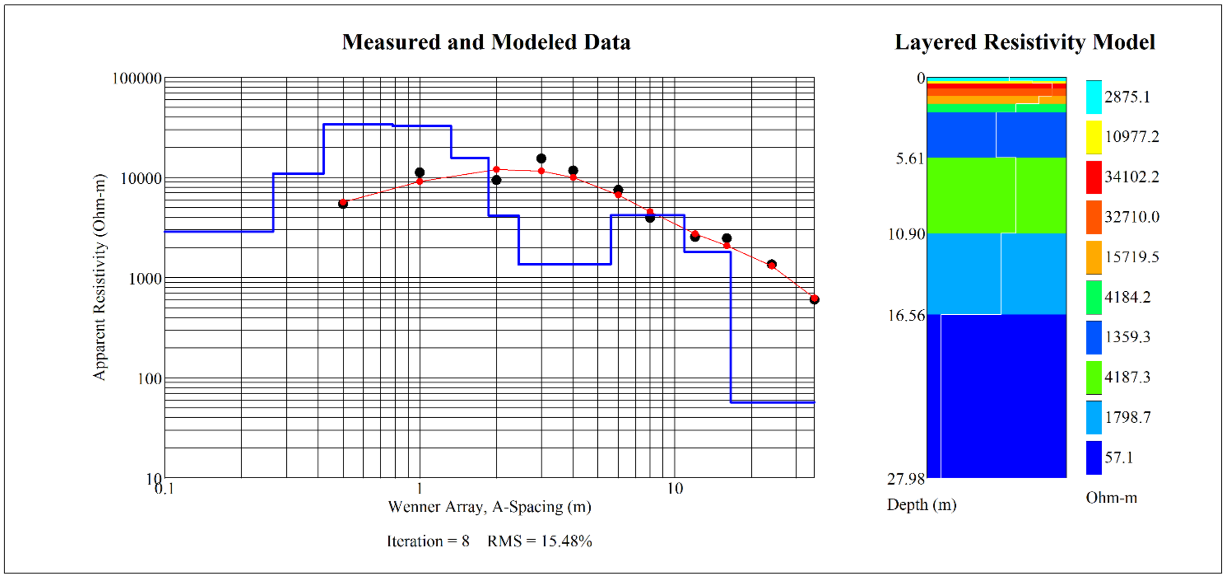

Figure 14: Final Fanny Bay Hall Wenner (NW-SE) 1D array resistivity data and 10-layer model. Left: measured (black circles) and best-fit modelled (red circles) apparent resistivity plotted against electrode spacing a (as shown in Figure 7). Blue line shows the resistivity model layer thicknesses and resistivity values. Right: layered resistivity model showing RMS value calculated from the variance of the best fit (red line) and original data.

4.1.2 Schlumberger (NW-SE) 1D array

Figure 15 shows the final (9 layer) resistivity model and the observed and predicted apparent resistivity values for the Schlumberger (NW-SE) array at Fanny Bay Hall. A similar inversion process as for the Wenner array data was followed; detail was lost from approximately 4 m to 29 m when fewer than 9 layers were used. The boundaries in the Schlumberger (NW-SE) and Wenner (NW-SE) models are consistently within 1 m of each other, though the layer resistivity values vary. The deepest layer in both models begins at approximately 16.5 m, but the layer resistivity is 57 ohm-m for the Wenner array and 266 ohm-m for the Schlumberger array. Notably, a comparison of the initial 12-layer model inversions (Figure 16) reveals a similar trend for both the Wenner and Schlumberger arrays, with a strong negative resistivity contrast at ~2-3 m depth, a positive resistivity contrast at ~4.5-5 m depth, and negative resistivity contrasts at ~12 m and at ~16 m.

Both arrays gave broadly similar results, but the Schlumberger array sampled to a slightly greater depth for the same array length. Given that surveying with the Schlumberger array is significantly less labour intensive than with the Wenner array, it was decided to employ the Schlumberger array for the remainder of the sites.

4.1.3 Schlumberger 1D array NE-SW

To assess heterogeneity in the subsurface, a Schlumberger array was also conducted along the NE-SW direction, perpendicular to the NW-SE profile. As seen in Figure 16, the initial 12-layer model shows a generally similar trend to the NW-SE Schlumberger model, but the change to the low-resistivity deepest layer occurs at a significantly shallower depth, implying that the interface is not laterally homogeneous. Figure 17 shows the final (7 layer) resistivity model and the observed and predicted apparent resistivity values curve for the Schlumberger (NE-SW) array at Fanny Bay Hall, with the number of layers being reduced to 7, in order to group several layers near the surface that were very close in resistivity.

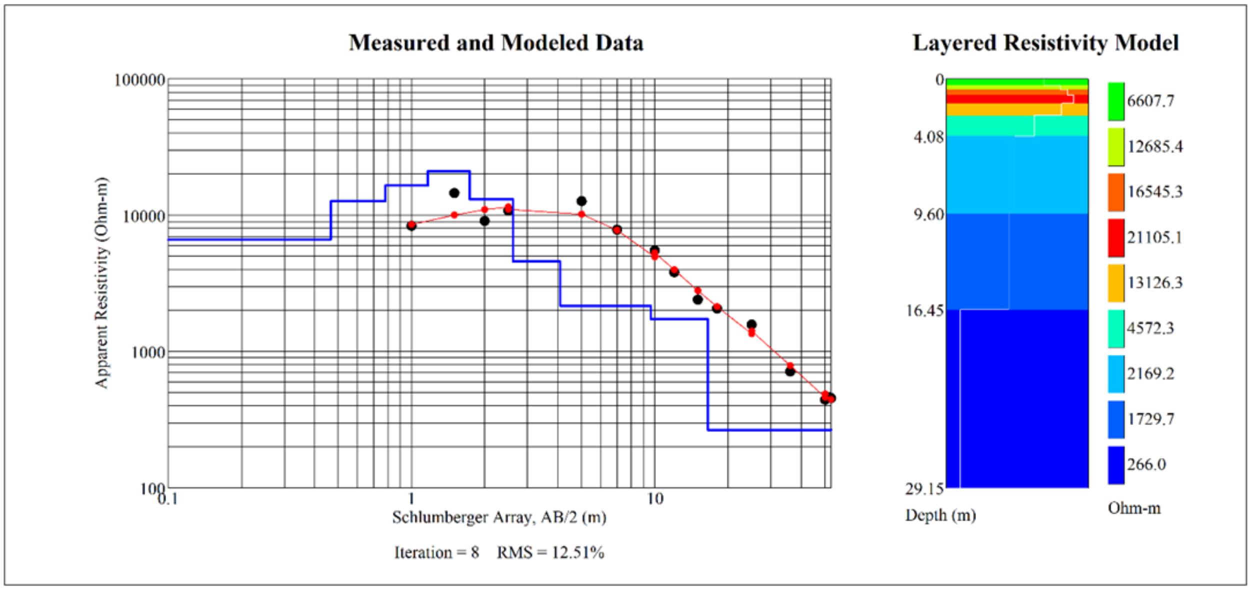

Figure 15: Fanny Bay Hall Schlumberger (NW-SE) 1D array resistivity data and the 9-layer model. Left: measured (black circles) and best-fit modelled (red circles) apparent resistivity plotted against electrode spacing. Blue line shows the resistivity model layer thicknesses and resistivity values. Right: layered resistivity model showing RMS value calculated from the variance of the best fit (red line) and original data.

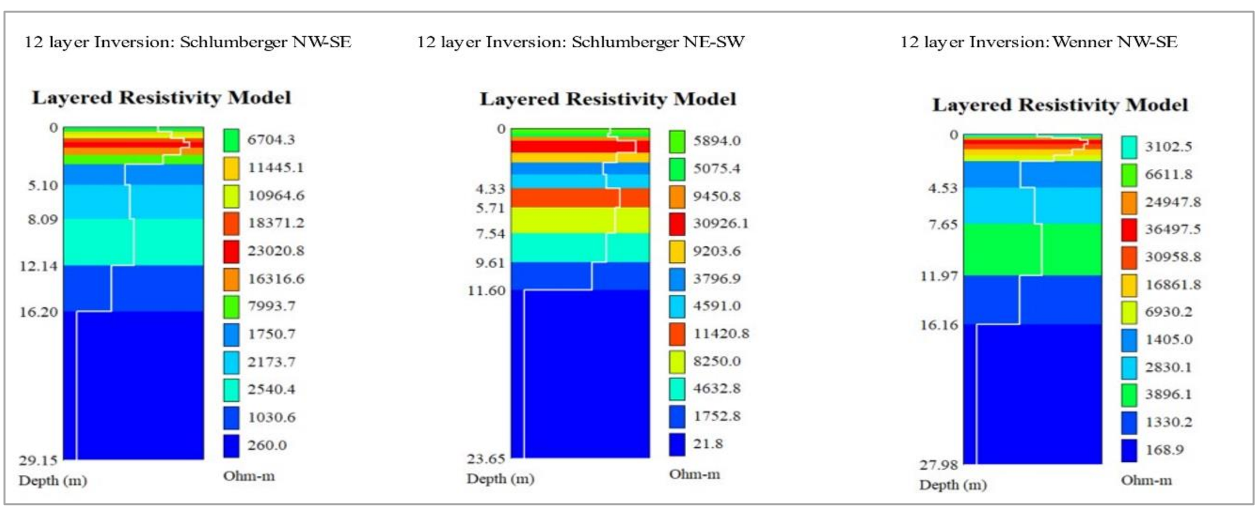

Figure 16: Comparison of the initial 1D 12-layer model inversions at Fanny Bay Hall.

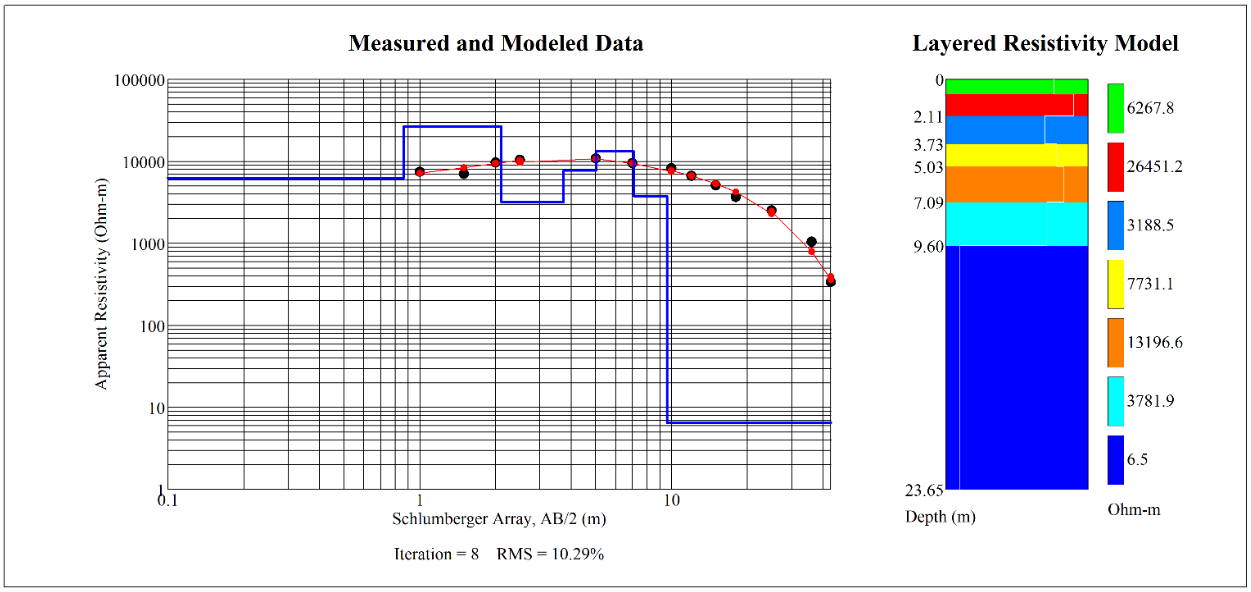

Figure 17: Final Fanny Bay Hall Schlumberger (NE-SW) 1D array resistivity data and 7 layer model. Left: measured (black circles) and best-fit modelled (red circles) apparent resistivity plotted against electrode spacing. Blue line shows the resistivity model layer thicknesses and resistivity values. Right: layered resistivity model showing RMS value calculated from the variance of the best fit (red line) and original data.

4.1.4 Dipole-Dipole 2D (NE-SW)

Collection of an ERT profile provided an additional opportunity to assess lateral variability in the subsurface at the Fanny Ball Hall site. Figure 18 shows the 2D resistivity model based on data collected using a dipole-dipole array and the 28-electrode system. The inversion process involved removing a few data points that were not within 15% of the mean value. The final root mean square (RMS) error of the model is 5.8%.

4.1.5 Interpretation

All final 1D resistivity models from the Fanny Bay Hall site are shown in Figure 19, with the well log lithology for comparison. There is some variation between the models in the upper layers, but a similar pattern appears with a high resistivity close to the surface and a decrease in resistivity in the lower layers. The upper layers most likely have a high resistivity due to the VES being on a very dry field in mid-summer with no irrigation. The well log does not show any large lithological changes from 6 to 16 m depth, but the resistivity models all show a large decrease in resistivity at around 7 to 10 m. The section from 6 to 16 m is logged as water-bearing coarse gravel. The interface characterized by the decrease in resistivity in each section is potentially the water table. At the time of drilling (December 1998), the static water level was at 6 m below the top of the collar casing. It is possible that the water table was lower at the time of our measurements due to seasonal fluctuations. However, the difference may also be unrelated to the pore saturation and instead result from a small lithological change within the coarse gravel. Interpreting the bottom layer in each section as the grey till from the well log seems reasonable because it is the deepest layer, and its upper surface corresponds reasonably well with the till in the well lithology, although it is considerably shallower in the NE-SW array model. The till appears to have a resistivity range of 6 to 266 ohm-m, and extends to at least 28 m, the greatest depth sampled by the soundings. The bedrock has been attributed to a depth of greater than 28 m (< 23 mASL elevation).

After reviewing the 2D survey results, the variation in the 1D models seems reasonable. The variation between the Wenner and the Schlumberger arrays as well as variation between the orthogonal Schlumberger array surveys can be explained by the lateral variations shown in the 2D section (Figure 18). Since there is only one cross section in the NE-SW direction, it is not possible to tell if the undulations of the deepest interface are continuous in the NW-SE direction, but its depth appears to range from approximately 9 m to greater than 17 m, which is consistent with the 1D models' range for the depth to the top of the deepest layer. Figure 20 shows a possible interpretation of the 2D resistivity model. In both the 1D and 2D models, the aquifer appears to be quite thin, ranging from a thickness of about 2 m to 8 m thick. From the well record, the aquifer thickness is closer to 10 m thick.

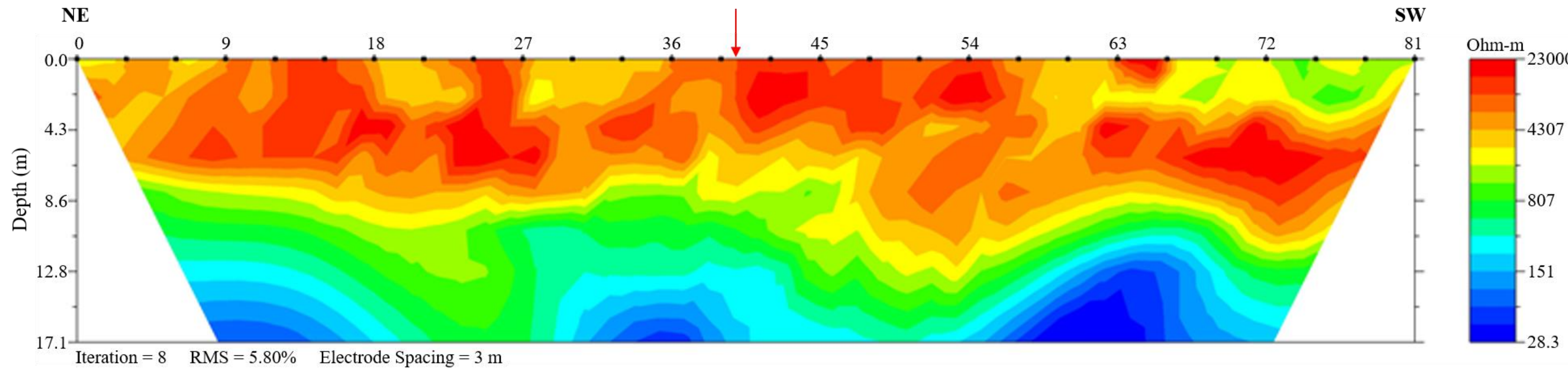

Figure 18: 2D (NE-SW) resistivity model at Fanny Bay Hall. The red arrow indicates the location of the centre for all 1D soundings.

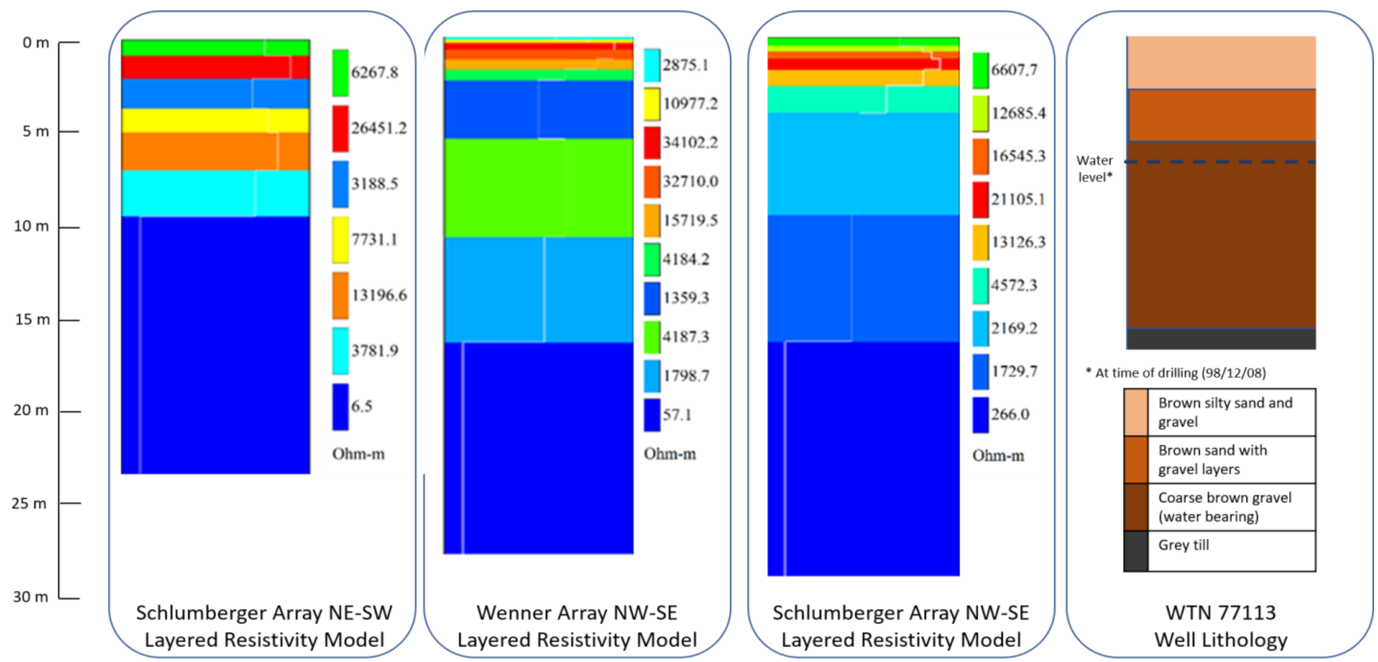

Figure 19: Lithology from well log (WTN 77113 at right) scaled to all the 1D resistivity models from the Fanny Bay Community Hall survey. Lithology based on well construction record, static water level recorded at time of well construction.

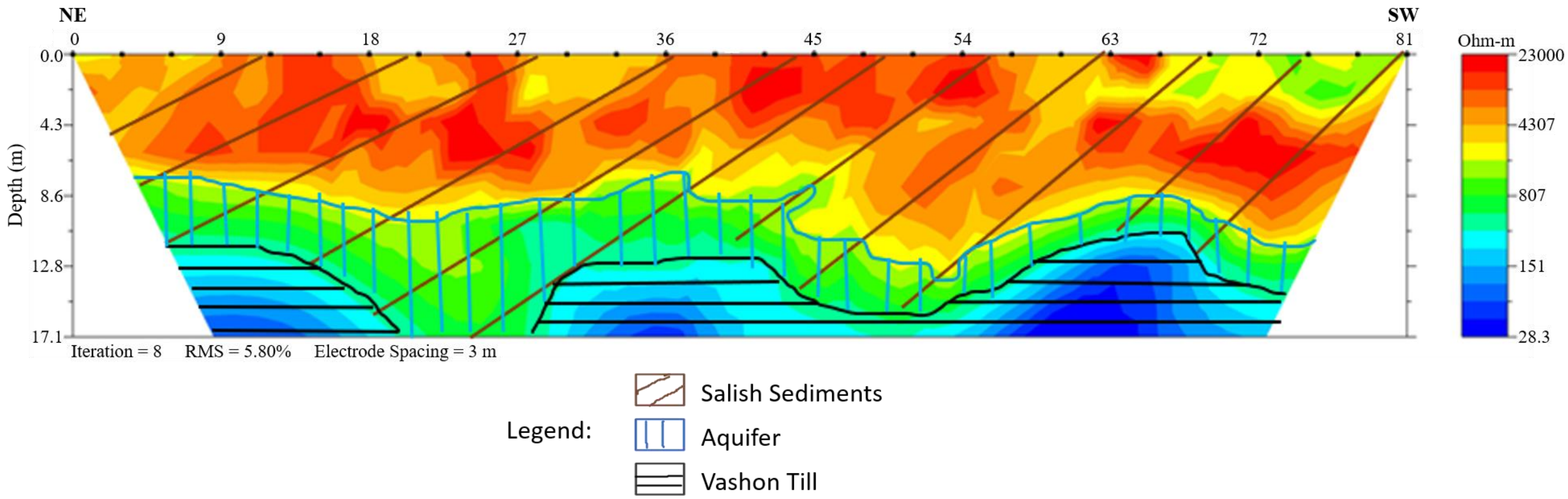

Figure 20: Schematic lithological interpretation of the 2D resistivity model at Fanny Bay Hall.

4.2 Ships Point Improvement District/Fanny Bay (WTN 95528)

Similar to the Fanny Bay Hall site, the well and the centre of the spread for the Ships Point Improvement District (SPID)/Fanny Bay site are both co-located with surficial Salish Sediments (Fyles, 1963). The well is located approximately 20 m northwest of the centre of the spread (Figure 21). The static water level was only 0.6 m below the top of the casing at the time of drilling (November 2001).

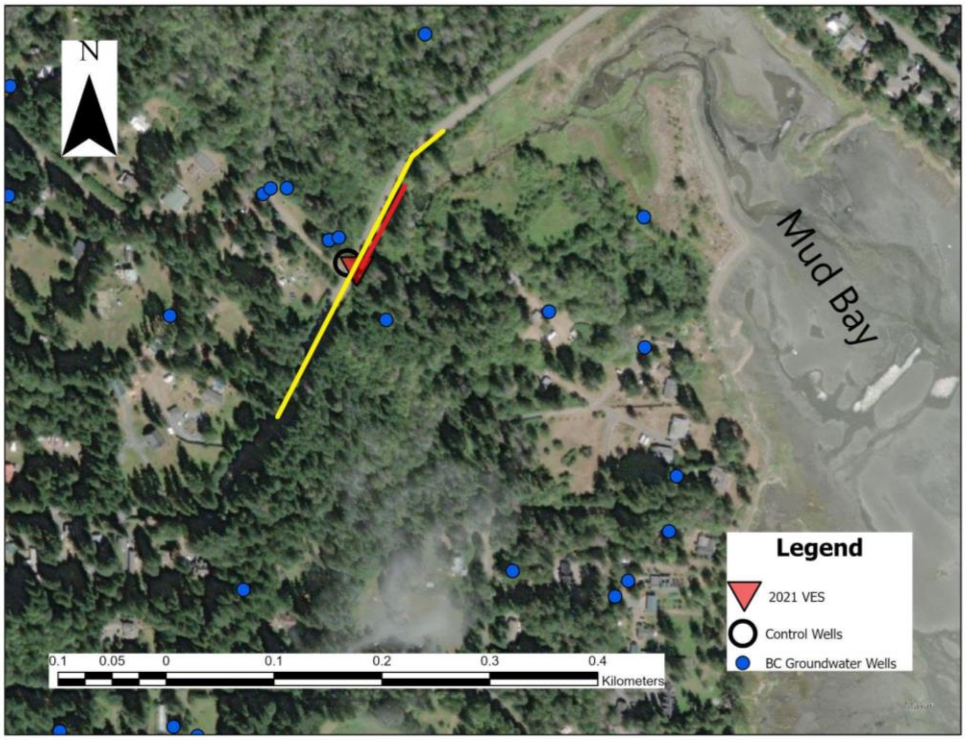

Figure 21: Locations of resistivity profiles and the well (WTN 95528; open circle) at SPID/Fanny Bay. Yellow line shows the 1D sounding profile; red line marks the 2D ERT survey.

4.2.1 Schlumberger 1D array

Figure 22 shows the final layered resistivity model and the observed and predicted apparent resistivity curve for the Schlumberger array at SPID/Fanny Bay. The 8-layer model was chosen because of its balance between detail and clarity. The data point at the largest electrode spacing shows an increase in apparent resistivity that is not reflected in the model; adjustments to the inversion settings did not make a difference.

4.2.2 Dipole-Dipole 2D

After the 1D data were acquired, a 2D dipole-dipole profile was also surveyed at SPID/Fanny Bay, in the same fashion as at the Fanny Bay Hall site; the resulting ERT profile is shown in Figure 23. The southwest end of the profile was located at the centre of the VES, and the profile extended 81 m to the northeast along Ships Point Road (red line on Figure 21).

4.2.3 Interpretation

The 1D resistivity model for SPID/Fanny Bay follows the lithology from the well log reasonably well (Figure 24). The high resistivity at the surface is likely due to the centre of the spread being located on a dry gravel road shoulder. The water table is quite shallow at this location (0.6 m depth at the time of drilling, and approximately 2.0 m at time of the sounding, according to SPID records for WTN 93741, which is roughly 100 m northwest of the control well) and could be reflected by the first or second boundary where there is a reduction in resistivity. The transition from light brown gravel to dark brown gravel at 10 m depth appears to be reflected in the resistivity model, with an increase in resistivity at ~9 m (from 572 to 821 ohm-m). The large decrease in resistivity (from 821 to 186 ohm-m) at 20 m depth is possibly the bottom of the aquifer. The well log states the presence of fine grey sand with wood, but this layer could be till, because the resistivity of 186 ohm-m falls within the range seen at Fanny Bay Hall. Fanny Bay Hall is located less than 1 km to the west of this location and is also located where Salish Sediments are mapped at the surface (Fyles, 1963a), overlying till (stratigraphically, this is most likely Vashon Till). The sounding at SPID/Fanny Bay sampled the subsurface to a greater depth than the well. The deepest boundary in the resistivity model is at 30 m depth (-29 mASL), where the resistivity decreases from 186 to 51 ohm-m. This interface is ~6 m below the maximum drilled depth for the control well. This deepest layer is within the resistivity range of the till sampled at Fanny Bay Hall; it could also reflect bedrock, or there is a possibility of the presence of saltwater at depth. The bedrock in the area is mudstone of the Willow Point member (Cathyl-Bickford and Hoffman, 1998) and it is possible that the layer starting at 30 m depth is this bedrock. It is less likely to be till because, according to the resistivity model, this unit has a thickness of at least 50 m and Vashon Till has a maximum thickness of 60 m (Bednarski, 2015). It is difficult to say whether saltwater incursion at depth is a factor without more information.

Over the ~17 m depth range where the models overlap, the resistivity values in the 2D model are on average lower than the 1D Schlumberger sounding (Figure 23). This is most likely due to moisture level; the shoulder of the road was dry starting at the southwest end of the 1D sounding, including the whole central part of the profile which would result in higher resistivity for the shallow layers in the 1D model. The northeast end of the sounding profile and most of the 2D profile was more vegetated, with more surface moisture (lower resistivity).

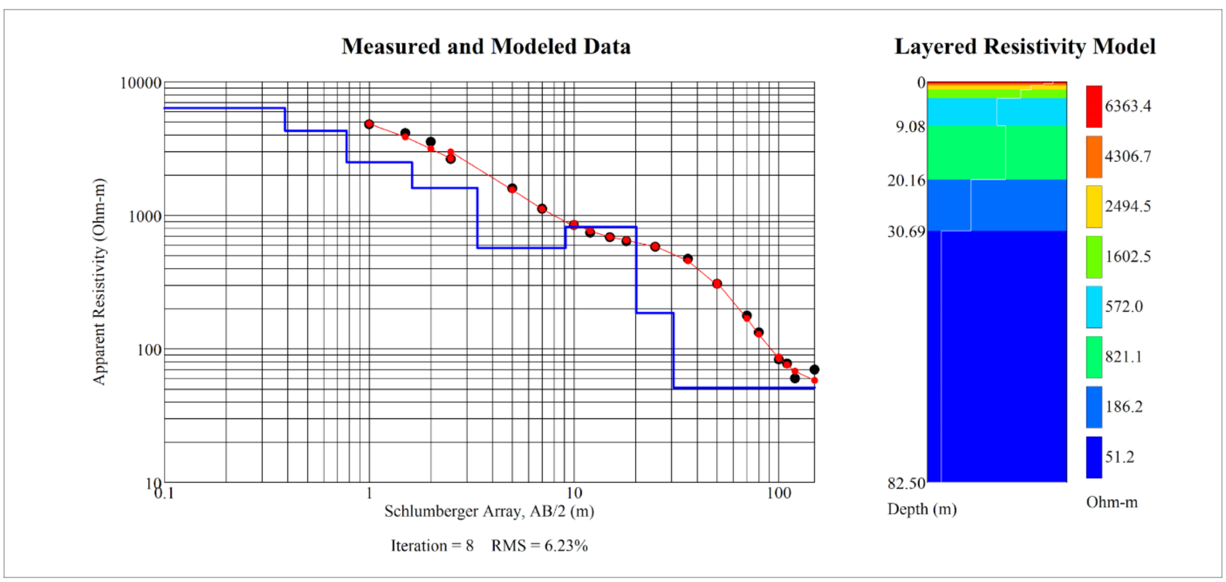

Figure 22: SPID/Fanny Bay Schlumberger 1D array resistivity data and model. Left: measured (black circles) and best-fit modelled (red circles) apparent resistivity plotted against electrode spacing. Blue line shows the resistivity model layer thicknesses and resistivity values. Right: layered resistivity model showing RMS value calculated from the variance of the best fit (red line) and original data.

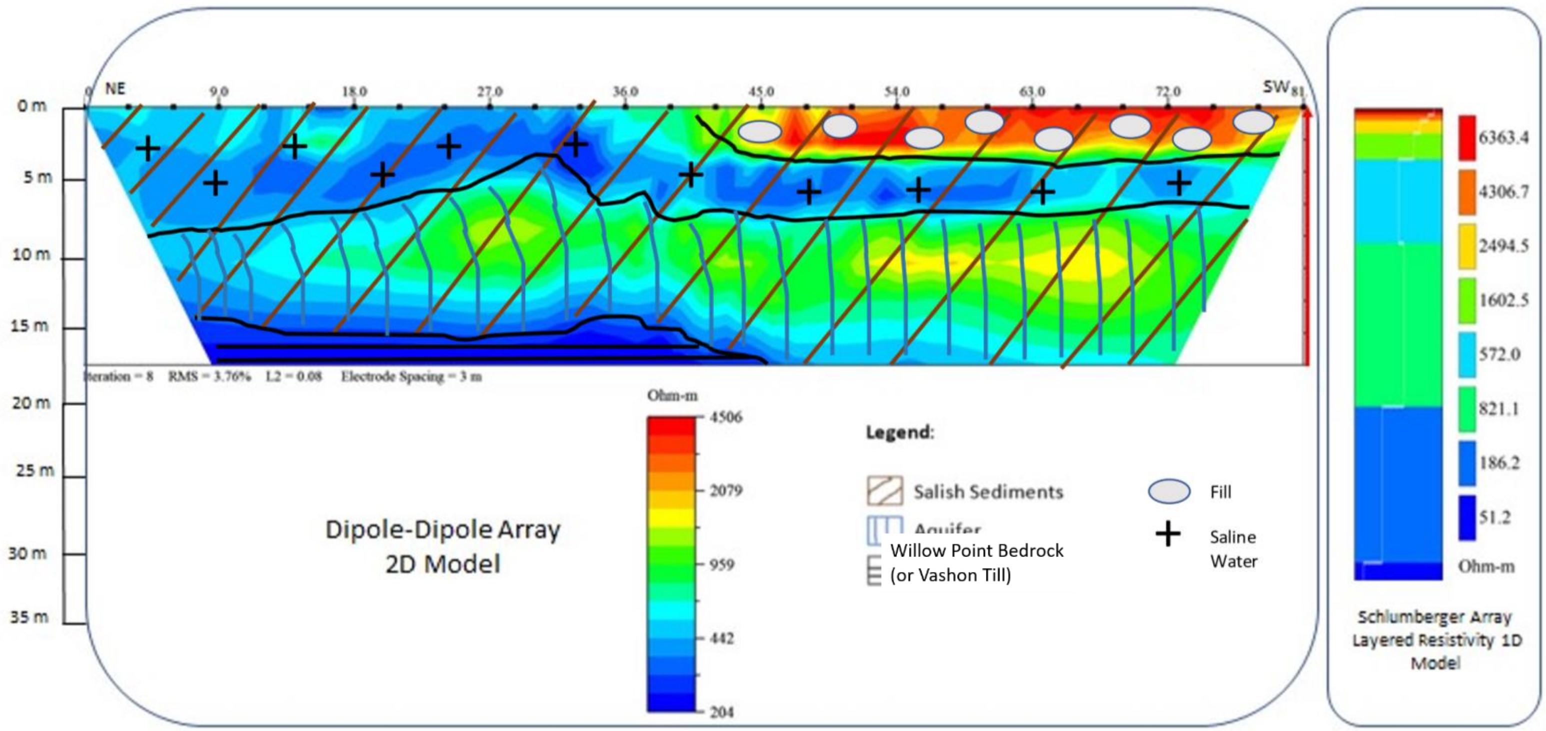

Figure 23: Scaled comparison of the 1D layered resistivity model and the 2D resistivity model at SPID/Fanny Bay. The red arrow indicates the centre of the 1D spread. Overlain on the 2D model is a schematic lithological interpretation.

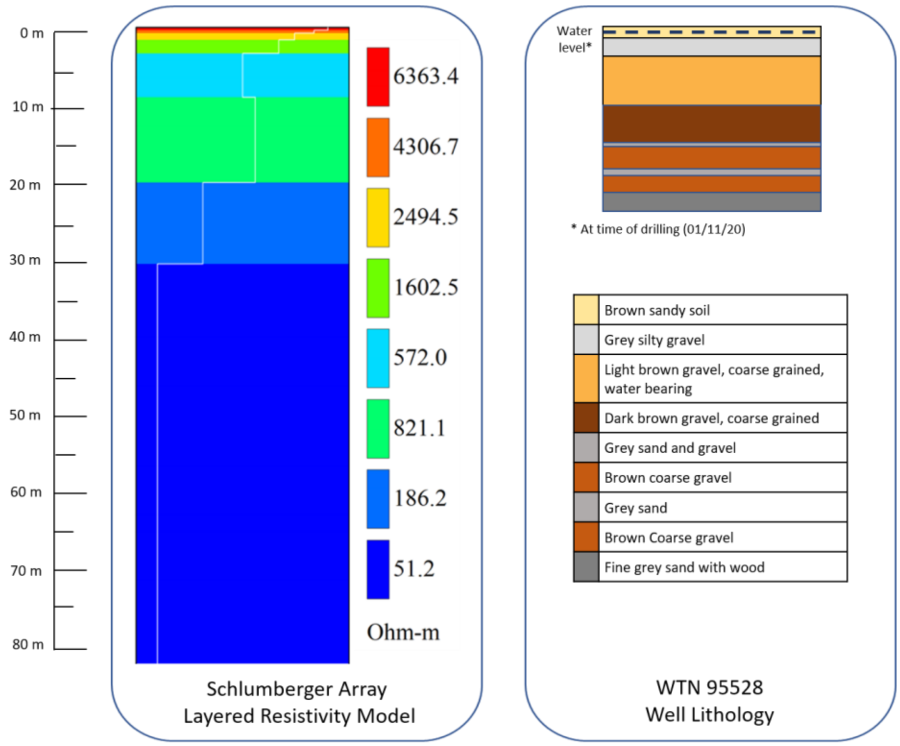

Figure 24: Scaled comparison of the control well lithology and the 1D layered resistivity model at SPID/Fanny Bay.

The high resistivity (red) in the upper ~3 m of the southwestern half of the 2D profile could be explained by the gravel shoulder of the road where the centre of the 1D survey was located. Towards the northeast, the ground changes from compacted gravel to a ditch with thick brush. Throughout the 2D section, there is a trend of decreasing resistivity from the southwest to the northeast (Figure 23). There are a few different factors to consider when interpreting this trend. The tidal flat of Mud Bay lies to the east (Figure 21) and the high tide line appears to be close to the NE end of the resistivity line (approximately 100 m). Additionally, the ground elevation in the area is about 1 m above sea level. There is a creek (Bob's Spring) that runs parallel to the survey profile, ~30 m to the SE. The high level of moisture in the ground from both the creek and the tidal flats would be a significant factor in decreasing the resistivity in the NE, especially if the water is brackish from tidal influences, which seems likely given the low elevation and coastal proximity. The water table is high. Assuming that the lithological layers are relatively horizontal and laterally continuous, it is possible that at the northeast end of the profile, there is coarse gravel and sand from 2 to 20 m depth and that the changes in resistivity are largely affected by variations in the salinity of the water in the subsurface. In the northeastern half of the profile, there is a low resistivity layer (~200-250 ohm-m) that appears to be rising to the northeast at ~14 m depth (-13 mASL); this could be either bedrock or till. It is more likely to be bedrock, based on the interpretation of bedrock at 30 m depth (-29 mASL) from the VES, which is centred at the SW end of the 2D profile. The apparent NE shallowing of bedrock is consistent with geological mapping at Ships Point, which indicates a reversal of the regional trend of bedrock elevation from eastward-deepening to eastward-shallowing. Bedrock elevation is mapped to be as shallow as 1 mASL at the north end of the Ships Point peninsula (WTN 12964).

Another interesting feature in this model is the high resistivity at the surface, followed by a substantial decrease in resistivity at around 4.3 m depth and then an increase in resistivity at around 9 m depth.

Although this could be due to lithology variations, there is a possible tidal influence; Bob's Spring may host saltwater at high tide that could infiltrate into the shallow aquifer underneath and decrease the resistivity at this site. The SPID/Fanny Bay 2D profile should be repeated in future, to determine if there is any temporal variability in the interface between fresh water and sea water.

4.3 Bowser (WTN 37367)

The Bowser sounding was centred about 10 m from the control well along an access road. The surface geology in this area consists of marine veneer deposits from the Capilano Sediments over the Quadra sand (Fyles, 1963).

4.3.1 Schlumberger 1D array

The final 1D resistivity model at Bowser (Figure 25) indicates very high resistivity at the surface, most likely due to dry conditions on the shoulder of the road. The initial 12-layer model had a few interfaces at depth, including one at 30 m and one at 40 m, but their resistivity contrasts were small relative to the changes at ~20 m and ~50 m, and they followed the same trend. There were quite a few higher resistivity layers near the surface, and by decreasing the number of layers to seven for the final model, the multiple similar layers at the surface were combined, while maintaining the deeper prominent boundaries.

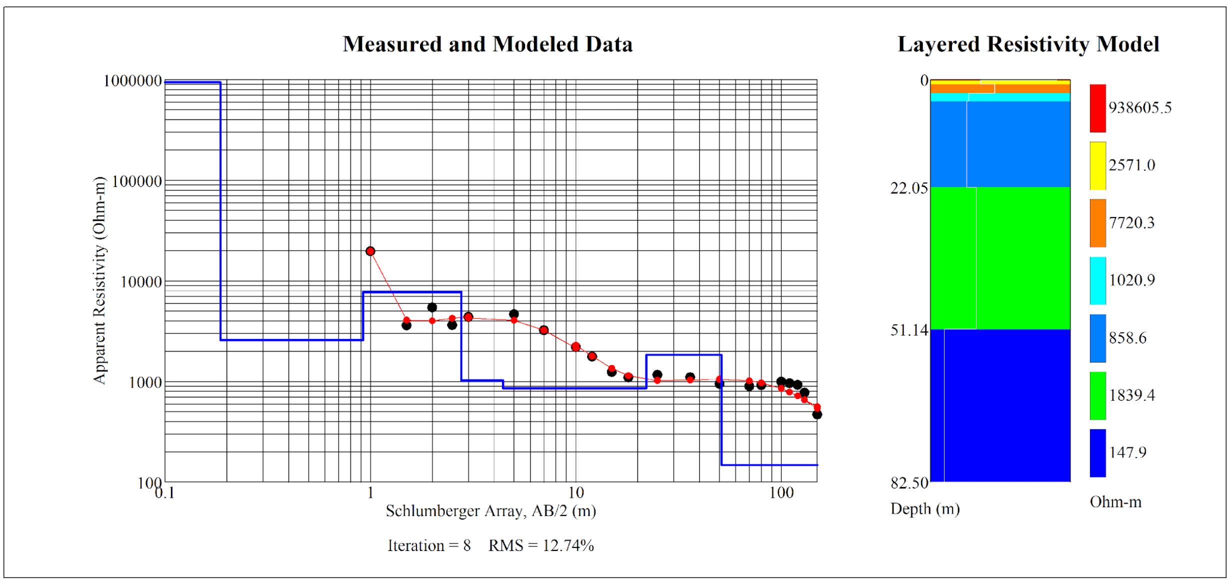

Figure 25: Layered resistivity model and curve for Bowser Schlumberger 1D array resistivity data and model. Left: measured (black circles) and best-fit modelled (red circles) apparent resistivity plotted against electrode spacing. Blue line shows the resistivity model layer thicknesses and resistivity values. Right: layered resistivity model showing RMS value calculated from the variance of the best fit (red line) and original data.

4.3.2 Interpretation

The centre of the spread at Bowser was quite close to the control well (WTN 37367) and at the same elevation, but the southwest end of the spread was 5 m higher than the northeast end. The Bowser well was documented in the well log as penetrating a Quadra sand aquifer. The section from approximately 5 m to 17 m depth appears to be the potential aquifer sediments, from both the well log and the resistivity model, although it extends deeper in the resistivity model (Figure 26). The well log indicates the presence of sand and gravel from approximately 2 m to 17 m depth, and the resistivity model shows a layer with a relatively low resistivity (compared to its neighbours) of 859 ohm-m from 5 m to just below 20 m. At the time of drilling, the water depth was recorded at 9 m, which further confirms the aquifer location.

There is a significant increase in resistivity from 859 ohm-m to 1,839 ohm-m at around 22 m depth, extending to 51 m in the layered resistivity model. The deepest layer in the well log, which overlaps the depth of this resistivity contrast, is clay. It is very unlikely that the ~1,840 ohm-m layer is clay, as this is far above the typical resistivity range for clays (< 100 ohm-m; Figure 6), and surficial clay sampled at the Buckley Bay site (Section 4.7) had resistivity of less than 100 ohm-m. Stratigraphically, it is possible that the layer is part of the Cowichan Head formation from a non-glacial interval. This formation consists of clayey silt and sand as well as an upper member of estuarine and fluvial sandy silt and gravel (Bednarski, 2015). The resistivity value of 1,839 ohm-m appears consistent with fluvial sediments from Cowichan Head that could form an aquifer (like at Fanny Bay Hall or Cochrane). Although it cannot be discounted that the well log details at least 6 m of blue clay (extending to the base of the well at 25 m depth, 51 mASL), a 30 m thickness of clay seems unlikely. For the purposes of mapping from the VES, the high resistivity (1839 ohm-m) layer extending from 22 to 51 m depth (53.6 to 24.6 mASL), was interpreted as Cowichan Head sediments.

The deepest layer in the resistivity model, extending from 51 m to the 83 m depth base of the model has a low resistivity (148 ohm-m). More geological correlation work needs to be done to determine what this layer, starting at 25 mASL, equates to; it may be Nanaimo Group bedrock. A review of the 2011 Geological Survey of Canada (GSC) seismic reflection data (Line 01b CMP 100 offsets the control well by 400 m to the SW) shows a strong reflector at 20 mASL, but this has not been interpreted as bedrock (Benoit et al., 2015). In this study, bedrock has been attributed an elevation of lower than -4 mASL (the deepest penetration of the VES).

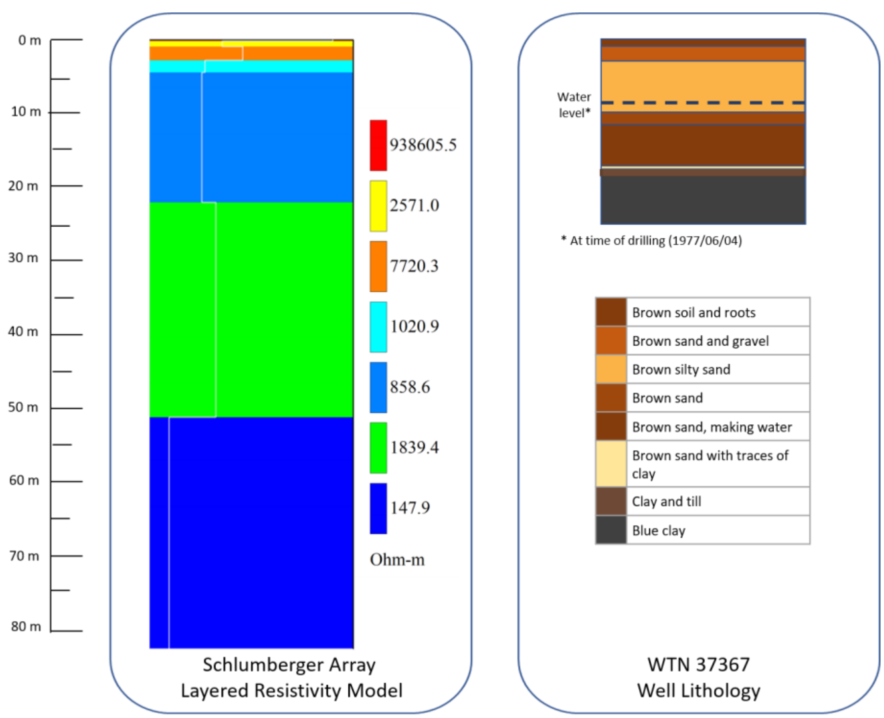

Figure 26: Scaled comparison of the control well lithology and the 1D layered resistivity model at Bowser.

4.4 Yake Road (WTN 87591)

The control well for the Yake Road sounding (WTN 87591) was located 50 m east of the centre of the spread and was 2 m lower in elevation. The mapped surface geology at this location includes marine veneer deposits from the Capilano Sediments over top of Vashon Till (Fyles, 1960). The mapped bedrock at this location is the Willow Point Member (Cathyl-Bickford and Hoffman, 1998).

4.4.1 Schlumberger 1D array

The final 1D resistivity model at Yake Road is shown in Figure 27. The initial 12-layer model was similar to the 9-layer final model near the surface, and both models have their deepest interface at around 35 m depth above a layer with a resistivity of ~27 ohm-m. The final model combines a few intervening layers with small resistivity differences (within 5-10 ohm-m).

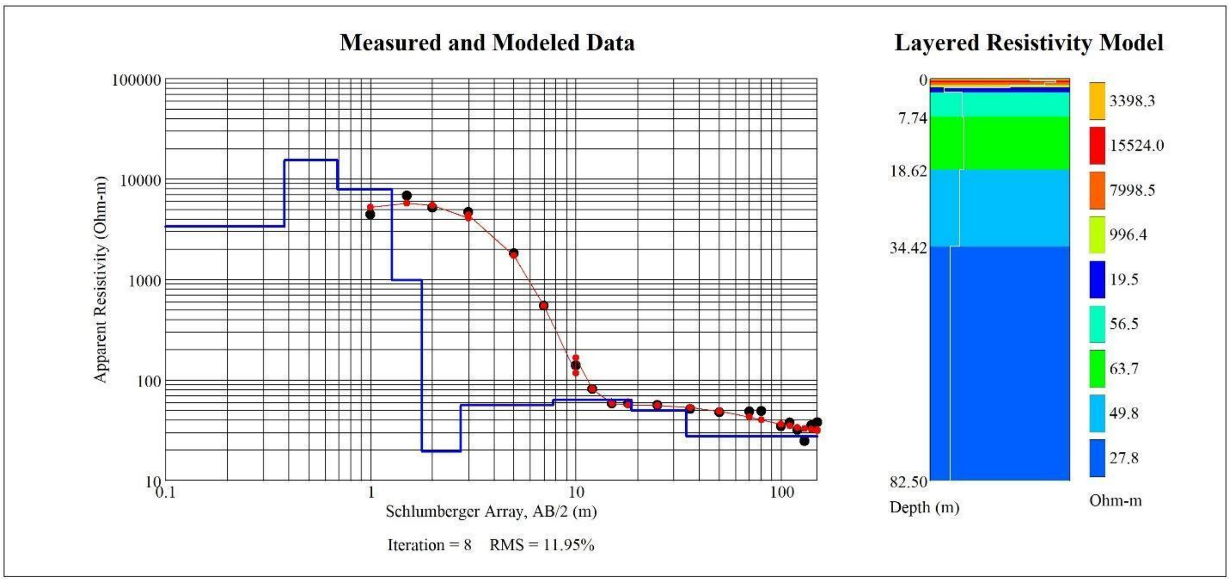

Figure 27: Yake Road layered resistivity model and curve for the Schlumberger 1D array resistivity data and model. Left: measured (black circles) and best-fit modelled (red circles) apparent resistivity plotted against electrode spacing. Blue line shows the resistivity model layer thicknesses and resistivity values. Right: layered resistivity model showing RMS value calculated from the variance of the best fit (red line) and original data.

4.4.2 Interpretation

The Yake Road sounding was located on the west side of the E&N railbed. The well log (WTN 87591) states that at the time of drilling, the well was dry. As expected, the 1D resistivity model shows that resistivity was quite high at the surface (Figure 28). The uppermost few metres are affected by the railroad gravel bed, and they may not be true to the natural shallow subsurface nearby or at the nearest well. The units that could be interpreted as till in the resistivity model lie between ~2 m and 35 m depth, with resistivity between ~50 and 65 ohm-m. The layer below 35 m depth has a resistivity of around 28 ohm-m and is modelled to be at least 45 m thick, which is a strong indication that it is the Willow Point Member bedrock, although a 35 m depth (-17.3 mASL) is significantly shallower than the 54 m (-38 mASL) bedrock depth at the control well, where a much thicker unit of till was documented than is seen in the resistivity model. One possible factor contributing to this discrepancy in the interpretation is the similarity of resistivity values between till and shale found at other sites. An interface between these layers may be more difficult to distinguish, especially if the interface is uneven. Another, and more likely possibility, is that the bedrock interface is vertically offset due to faulting (down to the NE) between the well and the sounding profile.

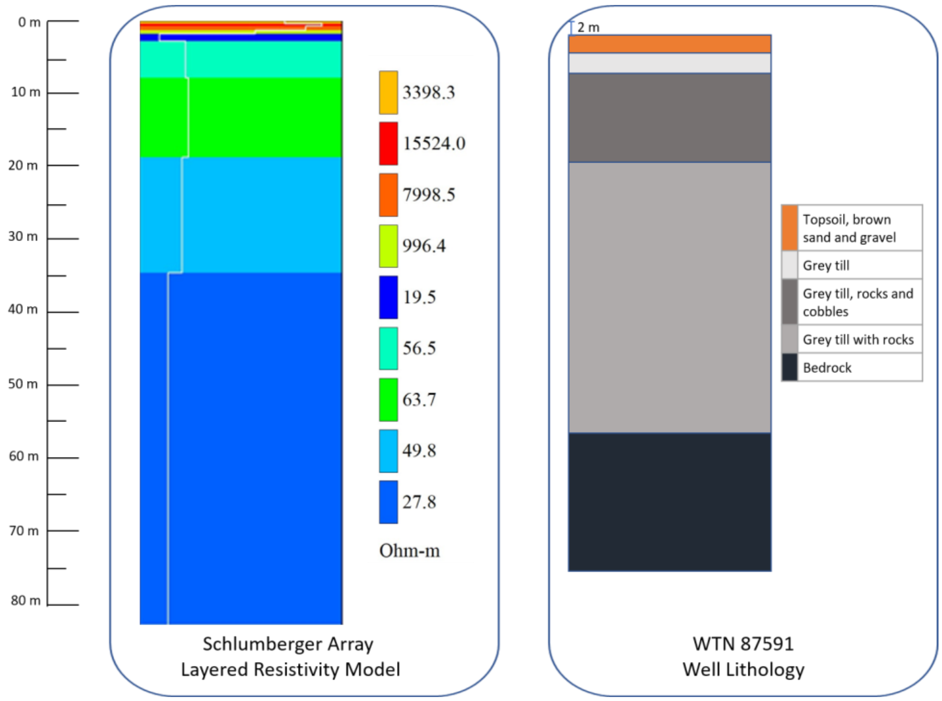

Figure 28: Yake Road scaled comparison of the control well (WTN 87591) lithology and the 1D layered resistivity model. The well lithology is vertically offset by 2 m to account for the ground elevation difference.

4.5 Cochrane Road (WTN 107880)

The control well (WTN 107880) for the Cochrane Road sounding is located about 10 m northeast of the centre of the spread. This site is Observation Well 427 (see Figure 5) in which groundwater levels are monitored as part of the Provincial Ground Water Observation Well Network. The mapped surface geology at this location includes up to ~1.5 m of marine veneer deposits from the Capilano Sediments overlying Vashon Till (Fyles, 1960). The well was drilled 129 m deep and did not hit bedrock. The deepest sand layer in this well log consists of Quadra sand (Bednarski, 2015).

4.5.1 Schlumberger 1D array

The final 1D resistivity model for the Cochrane Road site is shown in Figure 29. The model has a relatively good fit to the data, with an RMS of ~6%. The initial 12-layer model had 3 layers within 50 ohm-m of 1,100 ohm-m from 16 to 56 m depth. These variations seemed close enough to be combined into one layer because they are part of the same unit in the well log (fine to medium sand).

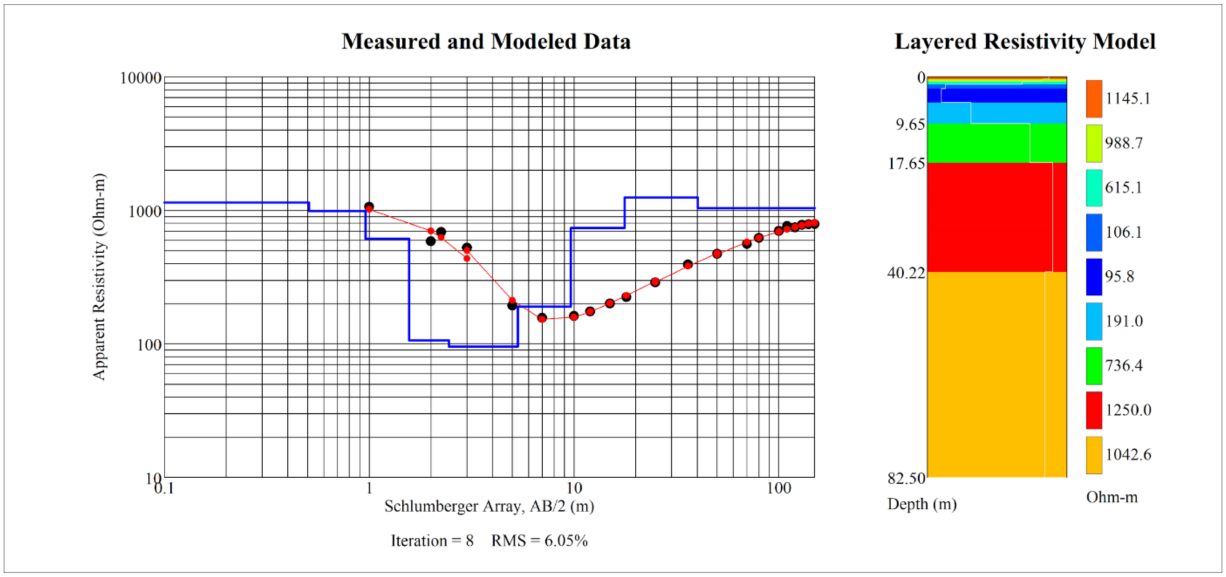

Figure 29: Cochrane Road Schlumberger 1D array resistivity data and model. Left: measured (black circles) and best-fit modelled (red circles) apparent resistivity plotted against electrode spacing. Blue line shows the resistivity model layer thicknesses and resistivity values. Right: layered resistivity model showing RMS value calculated from the variance of the best fit (red line) and original data.

4.5.2 Interpretation

At the time of drilling, the water level in the Cochrane Road well (WTN 107880) measured around 40 m depth (Figure 30). However, according to well monitoring data (Province of B.C., 2021), the water level was at a depth of ~58 m below ground at the time of the resistivity survey. The 1D resistivity model shows lower resistivity in the shallow subsurface than at other surveyed locations. This is likely due to the presence of diamicton close to the surface. There is an abrupt drop in resistivity at around 2 m depth which coincides with the silty diamicton in the well log. This layer with a value of ~106 ohm-m is most likely the Vashon Till. The layer that most likely correlates with the Quadra sand in the well log begins at a depth of 10 m with a resistivity of ~736 ohm-m. Below ~20 m, resistivity values of 1,250 ohm-m and 1,043 ohm-m are also consistent with the Quadra sand, likely reflecting slight lithological or fluid changes. The base of the aquifer is at around 90 m depth (21 mASL), where the control well intersects more diamicton.

For the purposes of geological mapping, the bottom of the well was treated as minimum depth to bedrock, at around 129 m below surface (-18 mASL). For the purposes of the VES interpretation the minimum depth to bedrock was the deepest penetration of the VES at 83 m (30 mASL).

This control well has a full set of downhole geophysical logs available, which could be used for further aquifer characterisation (Crow, 2014). In addition, the GSC acquired a 2D seismic reflection line very close to this control well (Benoit et al., 2015). A review of these seismic reflection data (Line 02a CMP900 offsets the control well by less than 50 m to the south) shows two strong reflectors, one at 25 mASL and another at around -20 mASL. The first is probably the base of the Quadra aquifer and the second could be bedrock, just below the deepest penetration of the control well.

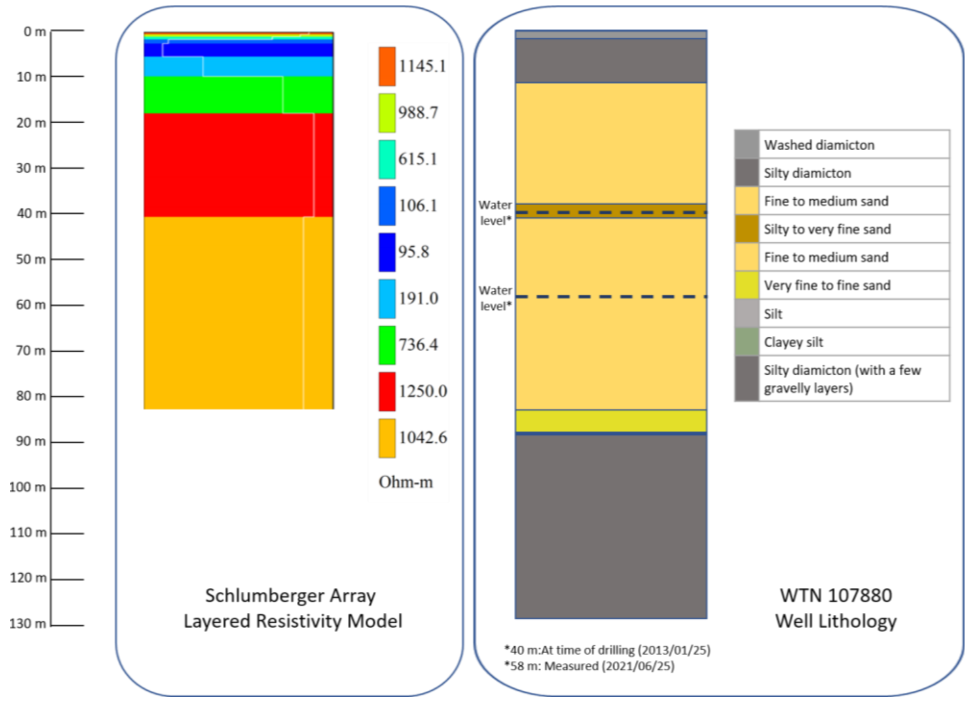

Figure 30: Cochrane Road scaled comparison of the control well lithology and the 1D layered resistivity model.

4.6 Macartney Drive (WTN 120708)

The control well at Macartney Drive (WTN 120708) is located almost 200 m to the east of the centre of the 1D resistivity spread, and is 5 m lower in ground elevation. The surface geology in this area consists of terraced fluvial (deltaic) deposits from the Capilano Sediments (Fyles, 1963a). The bedrock is projected to be the Willow Point member (Cathyl-Bickford and Hoffman, 1998).

4.6.1 Schlumberger 1D array

The sounding at Macartney Drive was done on the west side of the E&N railway. The surrounding area on the west side was quite wet (swampy) and it appeared that a lot of fill had been used to build the railway higher. The fill comprised large cobbles with diameters ranging from 5 to 10 cm, or loosely packed soil. Both these media led to high contact resistance at the electrodes; as a result, it was only possible to send 2 mA through the electrodes at most positions in the array (see Appendix F for the initial Macartney Drive data). This fill may have contributed to the high error values and negative resistivity values associated with some data points. The final resistivity model shown in Figure 31 is a result of removing data points that had a negative resistivity value, as well as data points that had an uncertainty higher than 10%. When the data were left unedited, the model had an RMS of 61.59%. Most of the data points with negative resistivity values and high errors were measured when the distance between electrodes was greatest. As a result, this sounding was unable to reach as deep as at the other sites.

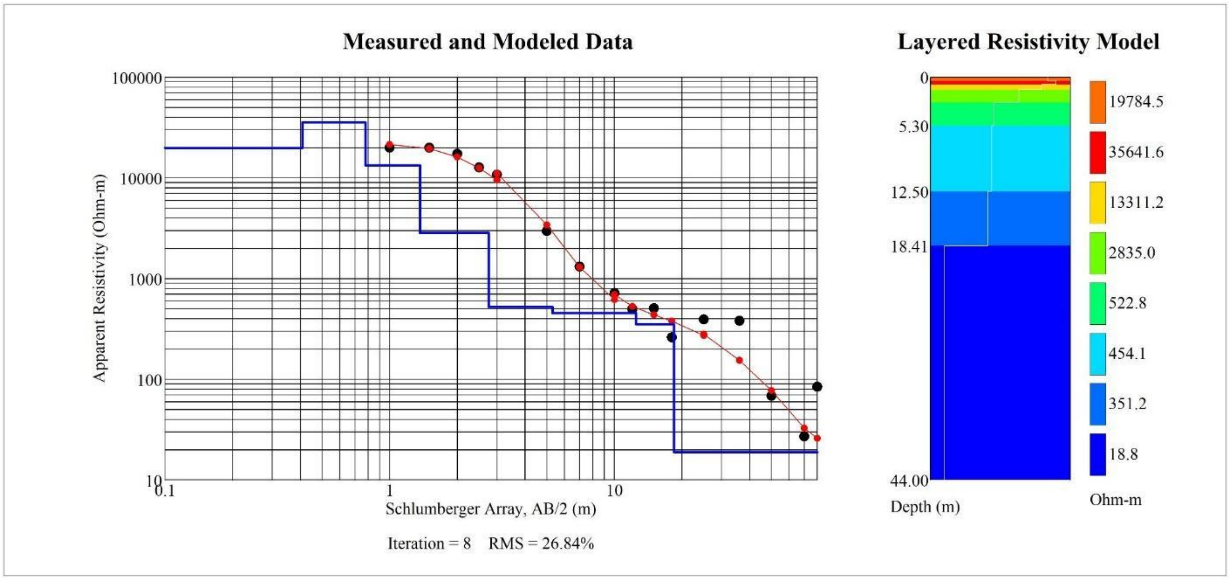

Figure 31: Macartney Drive Schlumberger 1D array resistivity data and model. Left: measured (black circles) and best-fit modelled (red circles) apparent resistivity plotted against electrode spacing. Blue line shows the resistivity model layer thicknesses and resistivity values. Right: layered resistivity model showing RMS value calculated from the variance of the best fit (red line) and original data.

4.6.2 Interpretation

The resistivity model for the Macartney Road site is shown with the lithology from the control well in Figure 32. As discussed above, the near-surface geology beneath the sounding is most likely fill under the railway bed. The layer starting at 5 m with a resistivity of 454 ohm-m may be the start of the wet till noted in the well log at a similar elevation. The mapped surface geology in this area is Capilano Sediments, which consist of deltaic deposits (gravel and sand).

In the resistivity model, the Capilano Sediments may be marked by units between 2.5 m and 18 m depth, with resistivities in the range of 350 to 520 ohm-m. The layer beginning at 18 m (0 mASL) with a value of 19 ohm-m is most likely the Willow Point member bedrock (shale). The boundary between the sediments and the bedrock in the well lithology is about 7 m lower (-7 mASL) than the interpreted matching boundary in the resistivity model. This is not unreasonable considering the 170-m distance between the spread centre and the control well. There may be a down-to-the-NE normal fault between the VES and the control well, as interpreted at the Yake VES. A lesson from this sounding location is that if VES surveys are completed near railbed locations in future, the presence of aggregate fill should be anticipated.

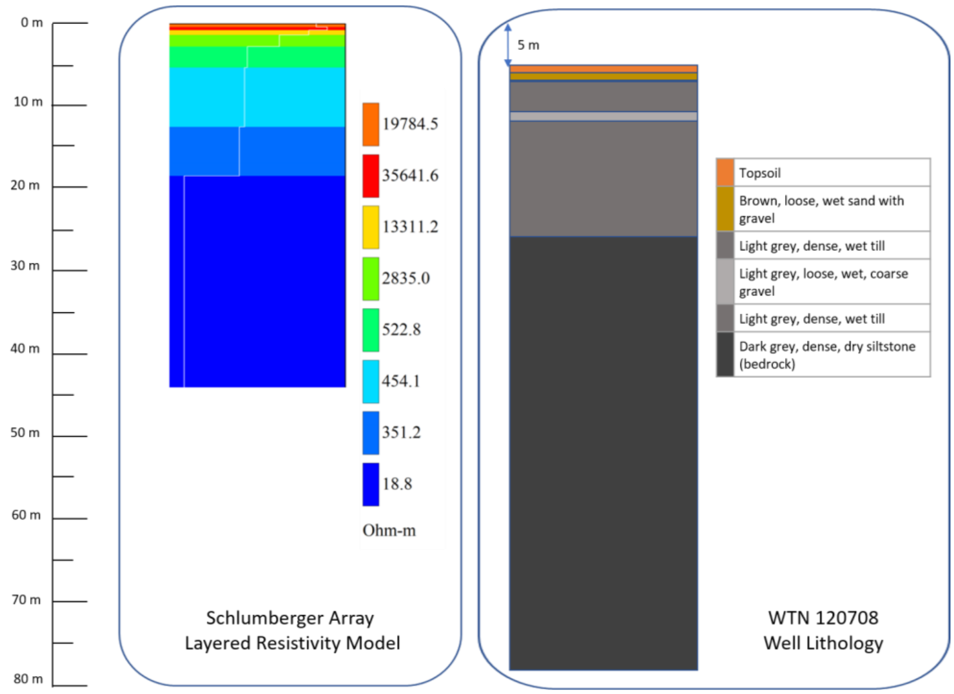

Figure 32: Scaled comparison of the control well lithology and the 1D layered resistivity model at Macartney Drive. The well is vertically offset 5 m lower in ground elevation.

4.7 Buckley Bay (WTN 26165)

The Buckley Bay sounding was completed beside the E&N Railway. The control well (WTN 26165) is located about 250 m to the southeast of the centre of the sounding, and at a 6 m lower ground elevation. The mapped surface sediments are marine veneer Capilano sediments over Vashon Drift (Fyles, 1963a). However, the Willow Point member bedrock is very near the surface here (Cathyl-Bickford and Hoffman, 1998), as is evident from nearby roadcuts (Figure 4d).

4.7.1 Schlumberger 1D array

The final 1D resistivity model for the Buckley Bay site is shown in Figure 33. The model has a good fit to the data, likely because of low contact resistance in surficial clay-rich sediment, enabling the maximum current of 200 mA to be sent through the electrodes for much of the sounding. This sounding was quite different from the other locations in this study because the modelled resistivity range is very small, from 17.1 to 83.4 ohm-m (Figure 33). This created more of a challenge to determine an appropriate number of layers in the model. A 9-layer model was chosen because it had a lower RMS (6.85%) than a model with more layers.

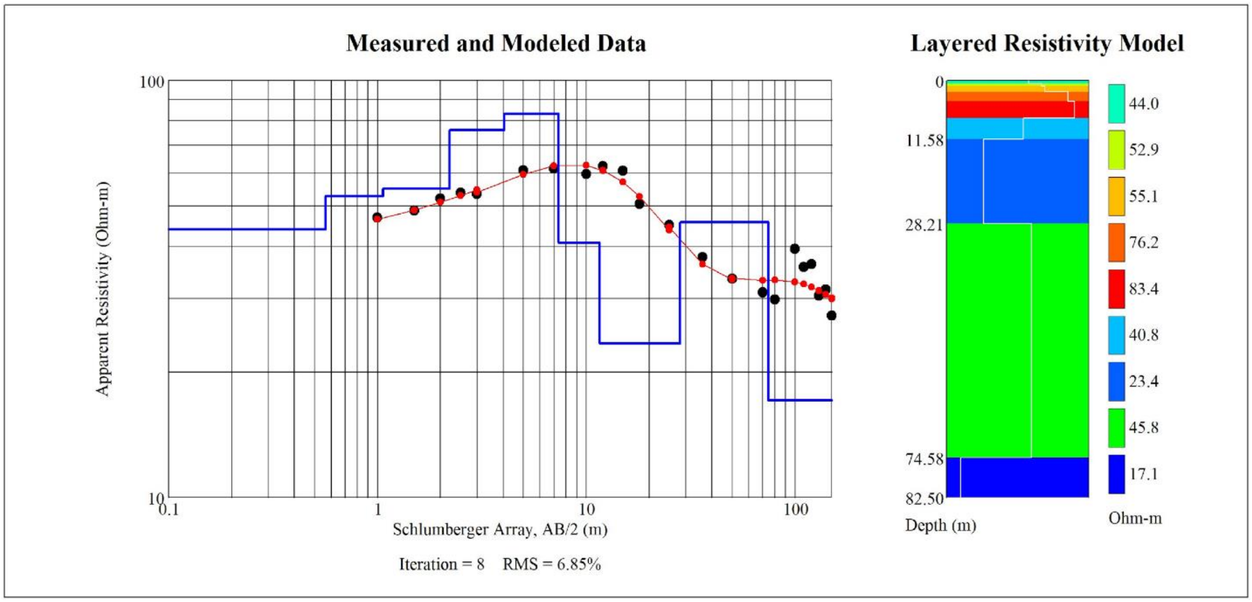

Figure 33: Buckley Bay Schlumberger 1D array resistivity data and model. Left: measured (black circles) and best-fit modelled (red circles) apparent resistivity plotted against electrode spacing. Blue line shows the resistivity model layer thicknesses and resistivity values. Right: layered resistivity model showing RMS value calculated from the variance of the best fit (red line) and original data.

4.7.2 Interpretation

The Buckley Bay resistivity model is shown beside the control well lithology for comparison in Figure 34. Ground truthing was provided by the well lithology and a bedrock outcrop at the road that is about 200 m south of the centre of the spread. The outcrop is shale from the Willow Point member (Cathyl-Bickford and Hoffman, 1998). Some strike and dip measurements were taken at the outcrop, enabling calculation of the projected depth of the shale to be about 5 m below the surface at the sounding site (assuming no differential erosion and that the bedrock is laterally continuous). The bedrock in the offsetting well is at 17 m below surface (-8 mASL) and consists of shale (probably Willow Point). The interpreted bedrock (23 ohm-m) at the VES is at 12 m depth (9 mASL), some 7 m lower than calculated at the VES from the outcrop projection. The bedrock elevation difference between the VES and the control well is 17 m, again down to the east. Although there is little variation in resistivity values in the VES model, there are significant changes below the ~12 m interpreted bedrock depth: at 28 m depth (from 23 to 46 ohm-m) and at 75 m (46 to 17 ohm-m). The resistivity increase at 28 m could be a lithological change in the bedrock from predominantly shale to hard grey shaley sandstone, as reported in the driller’s log. The lower negative resistivity contrast could be another lithological change or could be simply due to noisy data, as seen in the larger electrode spacings (Figure 33).

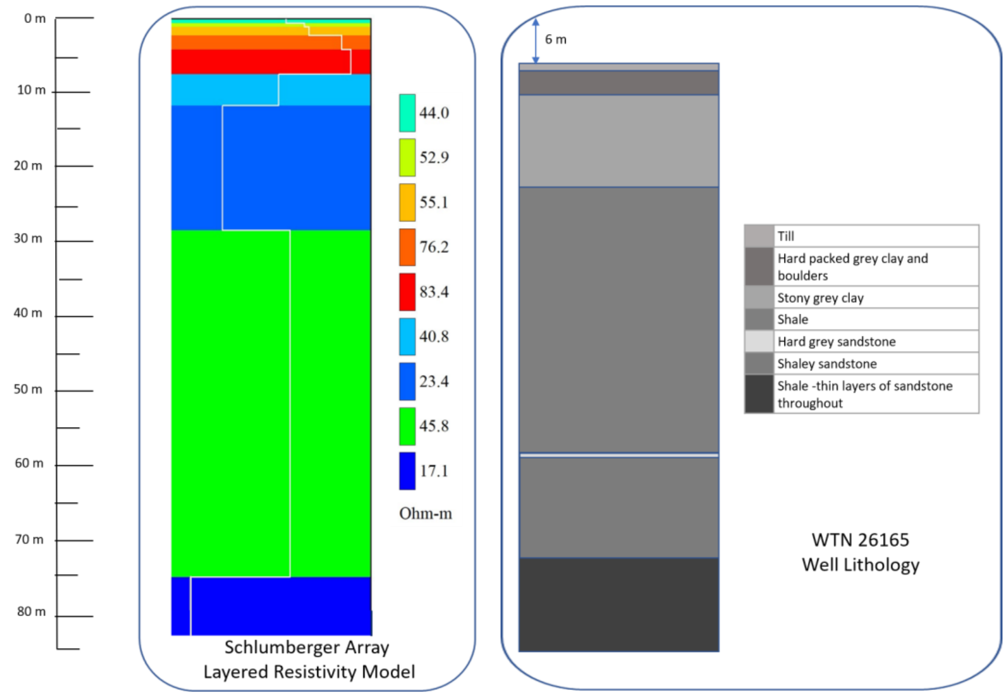

Figure 34: Scaled comparison of the control well lithology and the 1D layered resistivity model at Buckley Bay. The well is vertically offset 6 m lower in ground elevation.

4.8 Union Bay (WTN 83158 and WTN 85165)

The sounding at Union Bay used two wells for control. A test well drilled for the Ministry of Environment (ENV) (WTN 83158) is located approximately 260 m southwest of the centre of the spread with a ground elevation of 37 m above sea level. A private well (WTN 85165) is located approximately 170 m northwest of the centre of the spread with a ground elevation of 26 m above sea level. The centre of the sounding was 20 m above sea level and the spread was situated on the west side of the E&N railway. The mapped surface geology in the area varies slightly between the wells and the centre of the spread. All locations are in Capilano Sediments, but the ENV well and the centre of the spread are in marine veneer Capilano over Vashon Till, and the private well intersects the deltaic deposits seen at Macartney (Fyles, 1960). The mapped bedrock is the Tsable member which comprises conglomerate, sandstone, and pebbly siltstone (Cathyl-Bickford and Hoffman, 1998).

4.8.1 Schlumberger 1D array

The final 1D resistivity model for the Union Bay site is shown in Figure 35. The model shows very high resistivity in the shallow subsurface with a significant reduction in resistivity starting at around 2 m depth. Below 2 m, the resistivity variations are within a relatively small range: 25-200 ohm-m. The deeper well log (WTN 83158; Figure 36) indicates variations of till and siltstone, which may have similar resistivities but are separate units, so the final model comprises 9 layers in order to maintain these small variations.

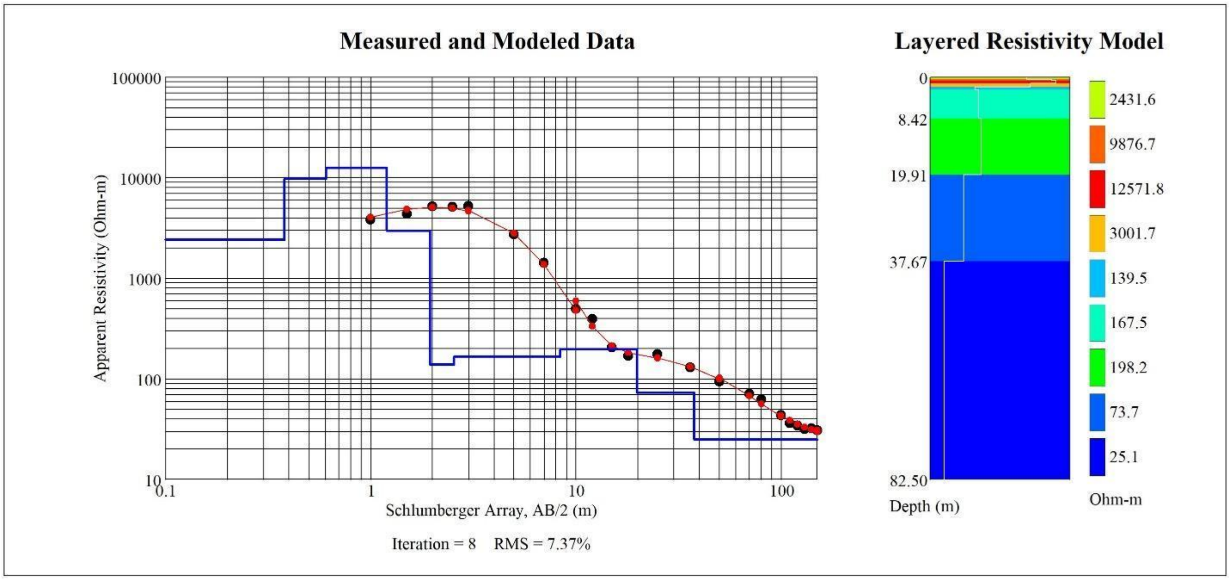

Figure 35: Union Bay Schlumberger 1D array resistivity data and model. Left: measured (black circles) and best-fit modelled (red circles) apparent resistivity plotted against electrode spacing. Blue line shows the resistivity model layer thicknesses and resistivity values. Right: layered resistivity model showing RMS value calculated from the variance of the best fit (red line) and original data.

4.8.2 Interpretation

The Union Bay resistivity model is shown beside the logs for the two control wells in Figure 36. Like most of the other locations, the resistivity was high at the surface, likely due to the dry material that makes up the railway bed. Both well logs reveal significant layers of till with intermittent thin layers of sand and silt. The presence of till is reflected in the resistivity model starting at approximately 2 m below the top of the resistivity model, or 20 m depth in Figure 36. At this point, the resistivity drops from ~3,000 ohm-m to 140 ohm-m. 140 ohm-m is well within the range documented for till at other locations in this study. From 2 to 20 m depth (20-38 m in Figure 36), there are small resistivity variations that most likely reflect changes in the composition of the till. The resistivity drops from 198 to 74 ohm-m at 20 m below surface at the VES (0 mASL). This could still be a variation within the till, or it could be the start of the soft siltstone bedrock at 36 m depth (2 mASL) in the ENV well. There is another drop to 25 ohm-m at approximately 38 m depth (-18 mASL) in the VES. This interface is interpreted here as the soft siltstone bedrock, at 20 m lower elevation than at the ENV well. It is interesting to note that at the ENV well salty water was noted at 48 m below surface (approximately -11 mASL). This could be complicating the interpretation of bedrock in this area. It is unlikely that the sounding reached the boundary between the logged siltstone and conglomerate, because conglomerate would be expected to have a higher resistivity (depending on its composition and pore fluid).

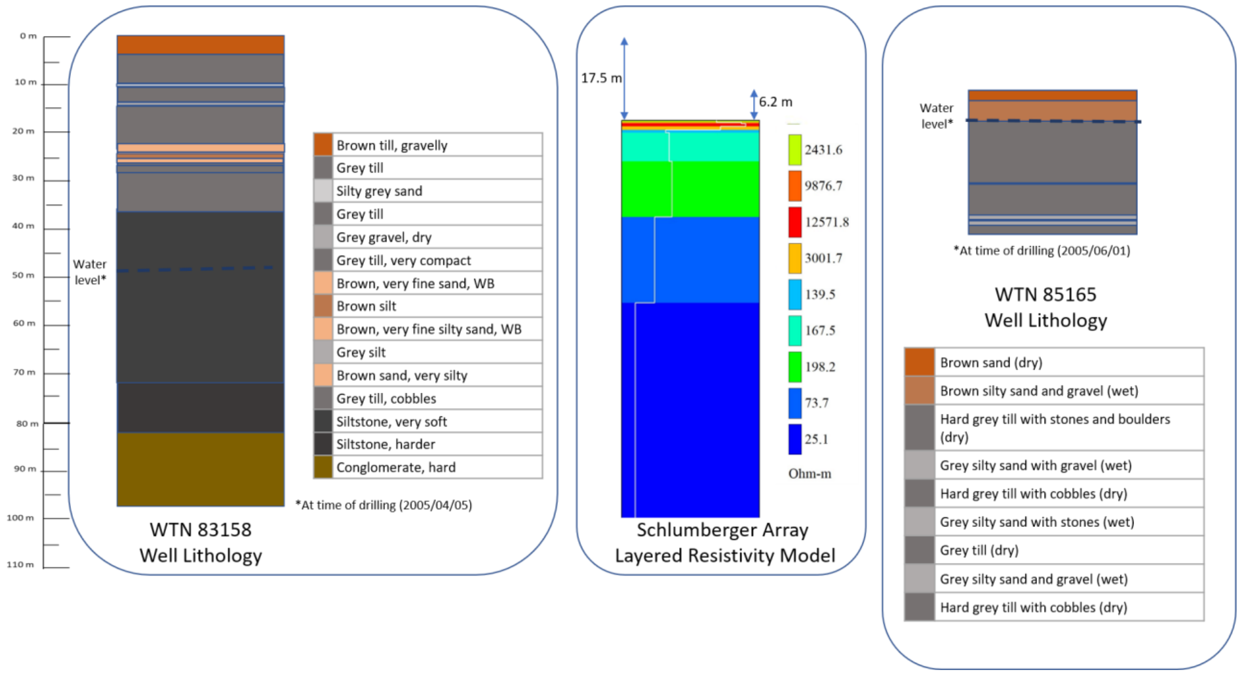

Figure 36: Scaled comparison of the lithology of the control wells and the 1D layered resistivity model at Union Bay. WTN 83158 is vertically offset 17.5 m higher in ground elevation and WTN 85165 is vertically offset 6.2 m higher than the centre of the sounding.

4.9 Royston (WTN 103795)

At Royston, the control well (WTN 103795) is located approximately 150 m northeast of the centre of the resistivity spread and is 1 m lower in elevation. The ground elevation of the centre of the spread was 7 m above sea level. The surface geology in the area is Salish Sediments (Fyles, 1960) and the bedrock is from the Willow Point member (Cathyl-Bickford and Hoffman, 1998). The sounding was done on the north shoulder of a driveway.

4.9.1 Schlumberger 1D array

The final 1D resistivity model for the Royston site shows a good fit to the data, with a relatively low RMS value (Figure 37). The initial 12-layer model was reduced to 8 layers in order to combine similar near-surface layers while maintaining variations at greater depth.

4.9.2 Interpretation

The lithology for the control well is shown beside the 1D resistivity model for the Royston site in Figure 38. The near-surface resistivity was found to be lower than most of the other locations (the top layer had a resistivity of 1,779 ohm-m). One layer at approximately 2 m depth has a modelled resistivity of 3,520 ohm-m, significantly higher than the surrounding layers. This could be due to anthropogenic factors since the road is quite high relative to the adjacent ground, or attributable to a layer of dry gravel or sand. The water table was calculated to be at ~6 m depth (1 m ASL) from a well measurement taken nearby at the time of the survey.

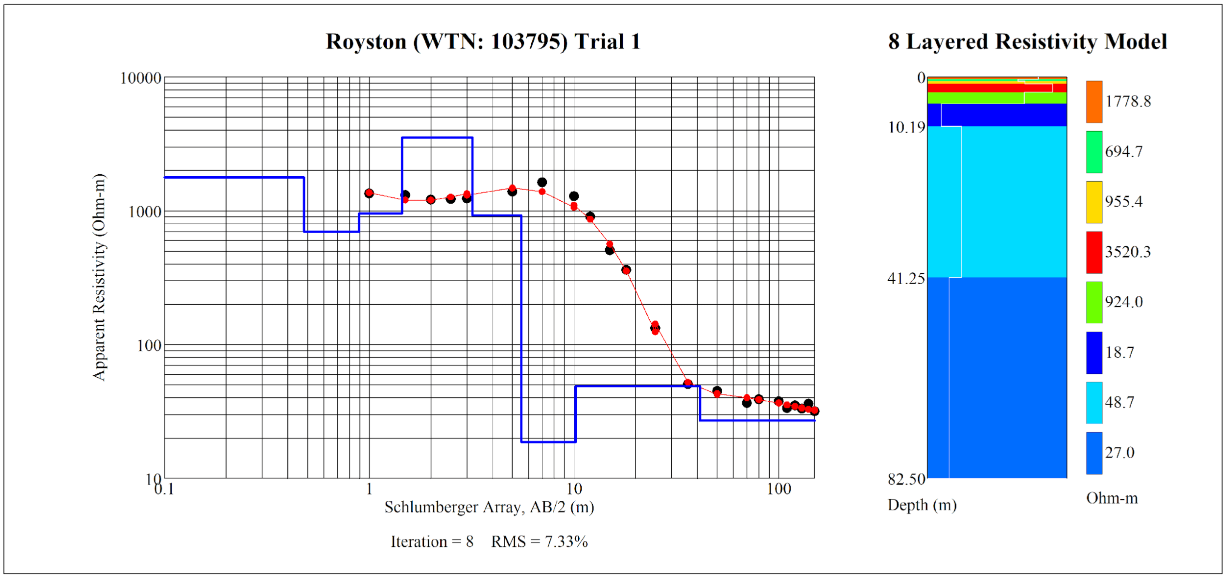

Figure 37: Royston Schlumberger 1D array resistivity data and model. Left: measured (black circles) and best-fit modelled (red circles) apparent resistivity plotted against electrode spacing. Blue line shows the resistivity model layer thicknesses and resistivity values. Right: layered resistivity model showing RMS value calculated from the variance of the best fit (red line) and original data.

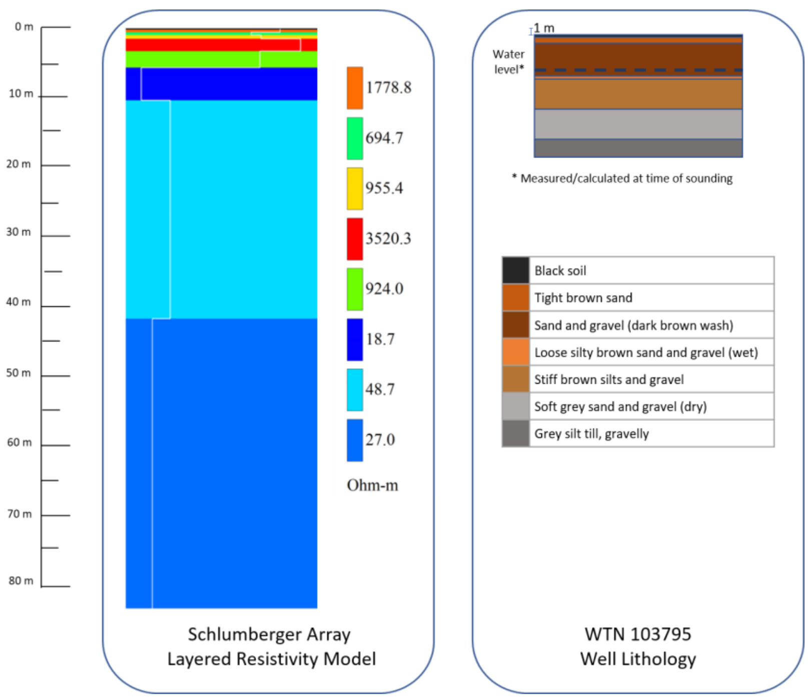

Figure 38: Scaled comparison of the control well lithology and the 1D layered resistivity model at Royston. The control well is 1 m lower in ground elevation than the centre of the VES.

The 924 ohm-m layer starting at approximately 4 m depth (3 m ASL) could be the start of the gravel or water-bearing sand logged at the well. The 19 ohm-m layer at ~5 m depth in the VES (2 mASL) could be the water level in the aquifer. This has a similar elevation to wet silty brown sand and gravel in the control well. The rise in resistivity up to 49 ohm-m at approximately 10 m could represent the top of till, although this interface is a few metres higher in elevation than in the control well. There is a drop in resistivity to 27 ohm-m at approximately 42 m depth (-35 mASL) that could be attributed to the top of the Willow Point Member bedrock. The control well was not drilled to this depth, but the resistivity is reasonable for shale bedrock. Bearing in mind that the eastern end of the VES is only 50 m from the high-water mark on Gartley Beach, there may be influences of saline water that are not accounted for here.

4.10 Bedrock Elevation

The resistivity sounding results and control well data have enabled the creation of a preliminary bedrock surface elevation map (Figure 39 and Figure 40). Mapping the elevation of the bedrock surface throughout the region is important, as it constrains the potential extent of aquifers in the overlying unconsolidated sediments. The maps show the bedrock surface elevation interpreted from the VES (in red) and the control wells (in black). A "<" symbol indicates the bedrock surface occurs at a lower elevation than the base of the control well or resistivity model. These maps show all control wells available to us in the area, including the following wells that have not been offset by a VES, listed from north to south:

- Van West WTN 110114: bedrock elevation of <43 mASL
- Tsable WTN 83159: bedrock elevation <-5 mASL
- Holiday Road WTN 96053: bedrock elevation -11 mASL
- Ships Point WTN 12964: bedrock elevation 1 mASL
- Stelling Road WTN 77157: bedrock elevation -43 mASL
- Qualicum Village WTN 12733: bedrock elevation - 61 mASL. Note that the location of this 1950 well was not confirmed in the field (accuracy of location claimed as only 100 m on GWELLS database).

There is a considerable amount of geologically defined elevation variation on the bedrock, varying from -7 mASL at the Macartney control well to -38 mASL at the Yake control well. The -61 mASL of the Qualicum Village control well should be regarded as unreliable, due to poor location confidence. In parallel to the geologically defined bedrock elevation, the interpreted VES bedrock elevation shows a similar eastward decrease in elevation in the central part of the study area, from as shallow as 9 mASL at Buckley Bay to -29 mASL at SPID.

Figure 40 shows a more detailed map of the Fanny Bay and Ships Point areas, enabling us to see how the VES sounding results correlate with the offsetting control wells. Table 3 summarises the VES results across all 9 VES sites. As a result of a number of factors, it is difficult to make a direct comparison between the VES results and the control well bedrock elevation. For instance, because of the large distance between the control wells and the VES locations at Union Bay, Buckley Bay, and Macartney, it is impossible to draw a direct comparison, as general regional dip or structural displacement make the difference significant. At Yake, even though the VES is within 50 m of the control well and the depth to bedrock is 54 m below ground, the difference between the control well depth and the VES depth is 21 m (38% of depth to control well bedrock). As the VES data quality is good, this difference is attributed to a normal, down-to-the-east bedrock fault.

Mapping the elevation of the bedrock is the first critical step in the shallow aquifer characterisation in this area. The depth to bedrock defines the lower boundary for the unconsolidated deposit aquifers above. Fractured bedrock can also be an aquifer itself, such as Aquifer 411 in the north of the study area. (Figure 5; Appendix B)

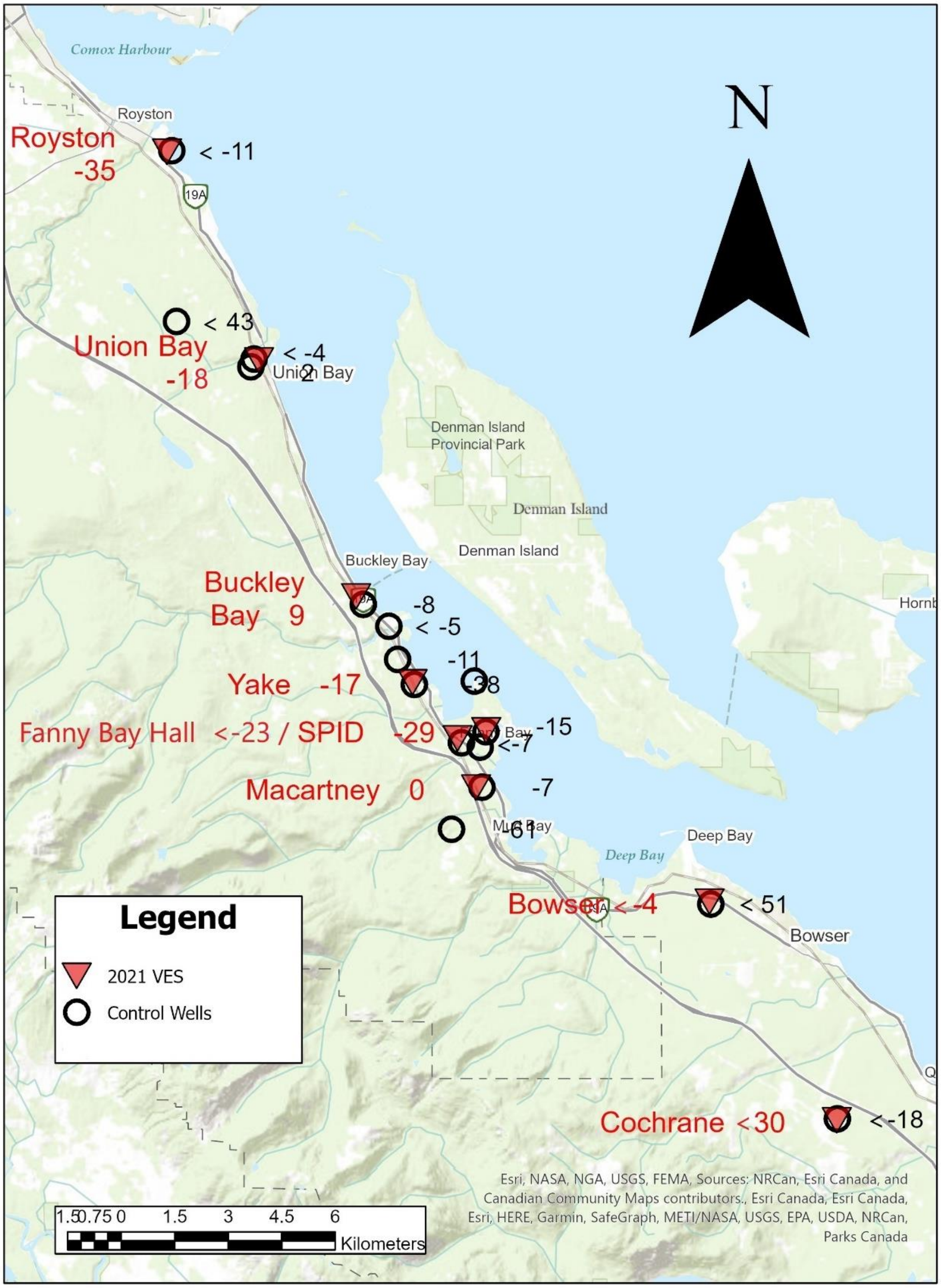

Figure 39: Comparison of bedrock surface elevation (in metres above sea level, mASL) determined from VES (red text, '<' symbol indicates that bedrock was not interpreted on the VES) and nearby control wells (black text, '<' symbol indicates that the control well did not penetrate bedrock, which must be at lower elevation than the base of the well).

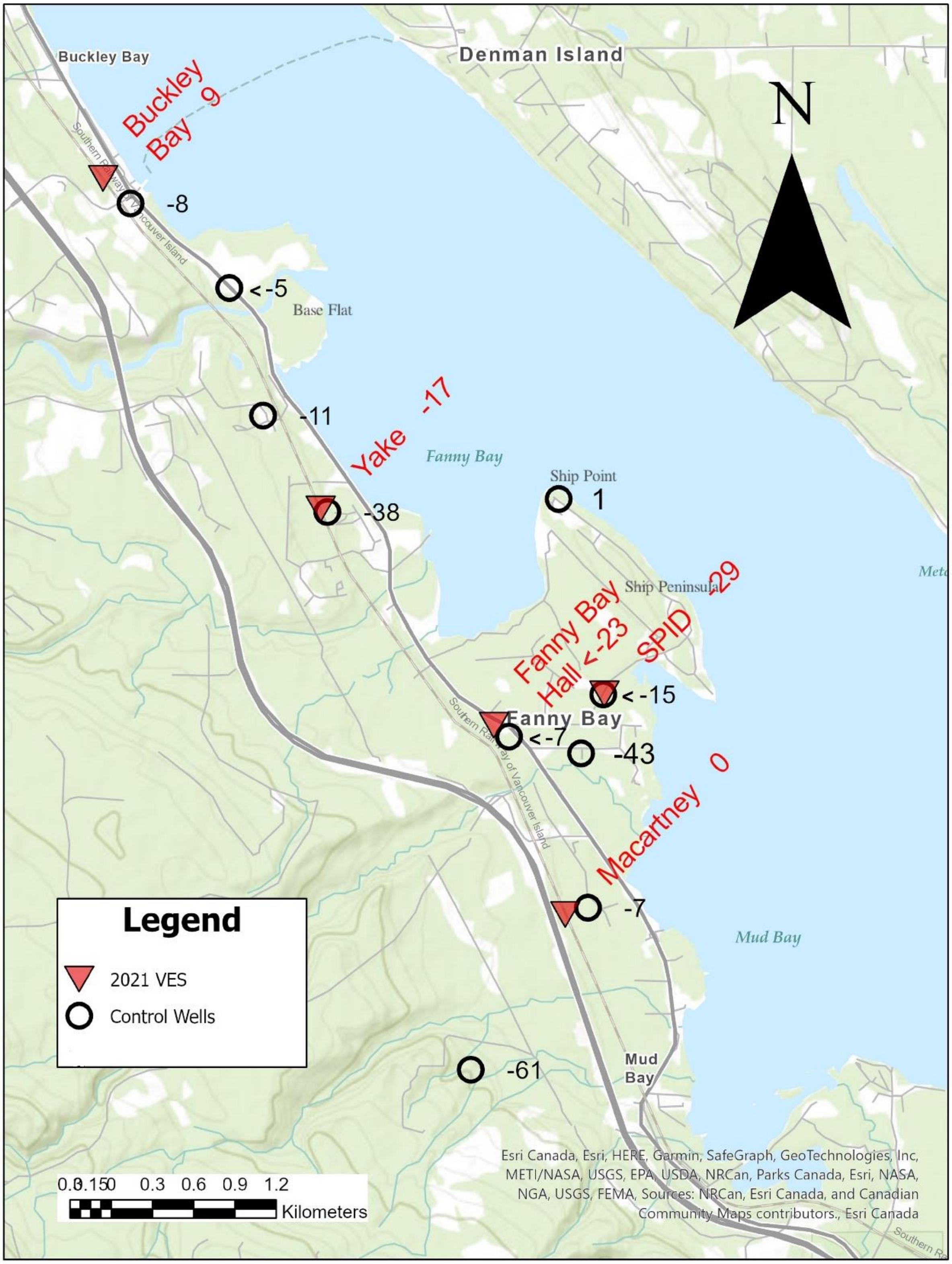

Figure 40: Fanny Bay Area bedrock elevation map (mASL). Elevation from VES shown in red ("< " indicates VES did not show bedrock), elevation from control wells shown in black ("<" indicates well did not penetrate bedrock).

Table 3: Comparison of bedrock elevation interpreted from VES surveys versus control wells.

VES Name	VES Bedrock Elevation (mASL)	Offset Distance (m)	Control WTN	Control Bedrock Elevation (mASL)	VES / Bedrock Elevation Difference (relative to control well, m)	Comments
Royston	-35	140	103795	< -11	-	No bedrock (BR) in control well
Union Bay Kens	-16	170	85165	<-4	-	No BR in control well
Union Bay ENV	-18	260	83158	2	-20	Possibility of saline water response. BR drops down to east. Possible fault between control well and VES.
Buckley Bay	9	250	26165	-8	+17	BR drops down to east from VES to control well
Yake	-17	50	87591	-38	+21	Possible BR fault, down to NE between control well and VES.
Fanny Bay Hall (FBH)	<-23	130	77113	< -7	-	No BR in control well
SPID	-29	25	95528	< -15	-	No BR in control well. BR from VES drops down to east from FBH to SPID
Macartney	0	170	120708	-7	+7	BR drops down to east from VES to control well
Bowser	< -4	10	37367	< 51	-	No BR in VES or control well. 2011 2D seismic tie
Cochrane	< 30	10	107880	< -18	-	No BR in VES or control well. 2011 2D seismic tie

The existing geological mapping in the area (Cathyl-Bickford and Hoffman, 1998) shows that the region is cut by a series of NW to SE trending normal faults. A down-to-the-NE fault that cuts Cowie and Wilfred Creek could be associated with some of the larger apparent displacements seen on Figure 40.

The spatial distribution and the sparse nature of the bedrock elevation control points in these maps make it difficult to generate a contour map. However the map generated (Figure 41) does highlight the trends previously noted: decreasing elevation to the NE and the possibility of normal down-to-the-NE faults generating steep elevation gradients. A reversal in the structure centred over Ships Point Peninsula reflects the existing mapping (Cathyl-Bickford and Hoffman, 1998) that shows an up-to-the-NE inferred extensional fault bordering the southwest edge of the peninsula. The lowest bedrock elevation documented in the Ships Point area is -43 mASL at the Stelling Road well (WTN 77157). This low point could have formed the locus of deposition of AQ419. This well is less than 150 m from the current position of Wilfred Creek. The low bedrock elevation at the Qualicum Village control well (-61 mASL) indicates a potential down-to-the-south fault with an approximate east-west trend. The poor confidence in the coordinates of this well makes any meaningful interpretation of this fault problematic.

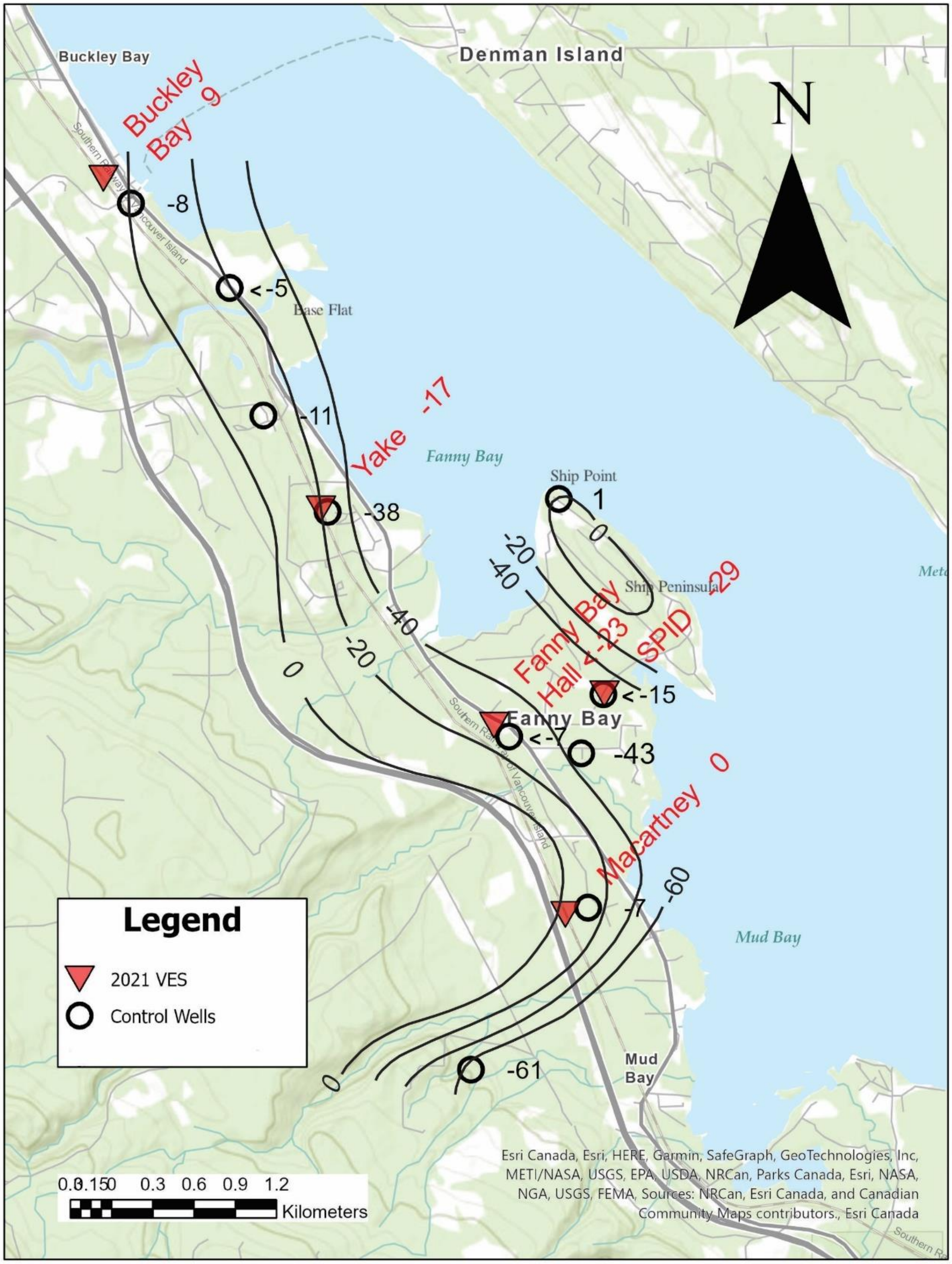

Figure 41: Fanny Bay Area bedrock elevation contour map (mASL). Elevation from VES shown in red ("< " indicates VES did not show bedrock), elevation from control wells shown in black ("<" indicates well did not penetrate bedrock).

5. CONCLUSIONS

Based on the analysis of resistivity soundings at nine sites on eastern Vancouver Island, the subsurface resistivity is generally consistent with the lithology logged in the adjacent control wells. However, there are some variations in layer depth and properties between the control wells and the final resistivity models. Some challenges and causes of uncertainty include:

- the potential for lateral variations in geology both along the sounding lines and between the lines and the control wells;
- uncertainties associated with the description of location, lithology, and static water level in the driller's well logs;
- the non-uniqueness of the resistivity interpretations; and
- at the sites at SPID/Fanny Bay and Union Bay, the inconclusive evidence of sea water impact on the resistivity.

For the Vertical Electrical Soundings, it was assumed that the subsurface had relatively few lateral variations. At most locations it was not possible to completely verify this assumption, but the surveying at Fanny Bay Hall indicated that the subsurface units have lateral continuity, at least along the length of the survey lines. Although there were variations in resistivity values and depths in the different 1D soundings at Fanny Bay Hall, it was still possible to clearly distinguish subsurface geologic boundaries and approximate depths. The potential for variation in geology between a sounding and the control well was mitigated by placing the centre of the sounding as close to the well as possible; however, this was sometimes not possible because of access problems. This could be a contributing factor in the conflicting interpretation of the depths of layer interfaces between the model and the well lithology found at some of the sites.

The amount of detail in the lithology from the well records depends on the driller who recorded it, the method of drilling, and whether cores or cuttings are being described. The coordinates of the well in the database are often dependent on the sketches of the well's location, which affect its accuracy. This did not have a serious impact because it was possible to verify the location of most of the wells visually or via the hand-drawn sketches included in the well records. The water table is variable; although most wells have a recorded static water level, this can vary depending on when (both year and season) the measurement was taken. Therefore, it was difficult to interpret any resistivity changes in the models that may have been water-related unless the well was actively monitored. However, it seemed that the largest resistivity changes (below the first couple of metres depth) were a result of lithology differences such as from sand to till, not variations in water saturation.

The resistivity models are non-unique, so it is important to have some knowledge of both the surface geology and bedrock geology. This forces the model interpretation to be more geologically realistic. With the well lithology, the surficial materials map and the bedrock geology map, it was possible to decide which model made the most geological sense. There was only one location (SPID/Fanny Bay) where a decrease in resistivity was interpreted as being due to the possible presence of salt/brackish water near the ocean shore. This interpretation was guided by the 2D survey model. However, this was difficult to verify because of the lack of water quality data from wells adjacent to the shoreline.

From the interpretations made at each site, combined with information from surface and bedrock geology mapping, the resistivity ranges of the main lithological units encountered in the study area are summarized in Table 4 and Figure 42.

The Salish Sediments have a wide range in resistivity; however, the variability may depend on water saturation. It was assumed that the extremely high surface resistivity values at most sites were not characteristic of the Salish Sediments, because the surface materials may have been impacted by anthropogenic processes (e.g., fill, compaction along railway beds and road shoulders) and extremely dry conditions at the time of the survey.

Table 4: Resistivity values determined for the primary lithologic units of interest in the study area.

Unit of interest	**Median resistivity value (ohm-m)**	**Approx. range (ohm-m)**	**No. of values, No. of sites**
Salish Sediments	1,730	440-7,730	17, 3
Capilano Sediments	454	350-525	3, 1
Vashon Till	96	5-265	15, 6
Quadra Sand	951	735-1,250	4, 2
Willow Point Member	28	15-85	9, 5

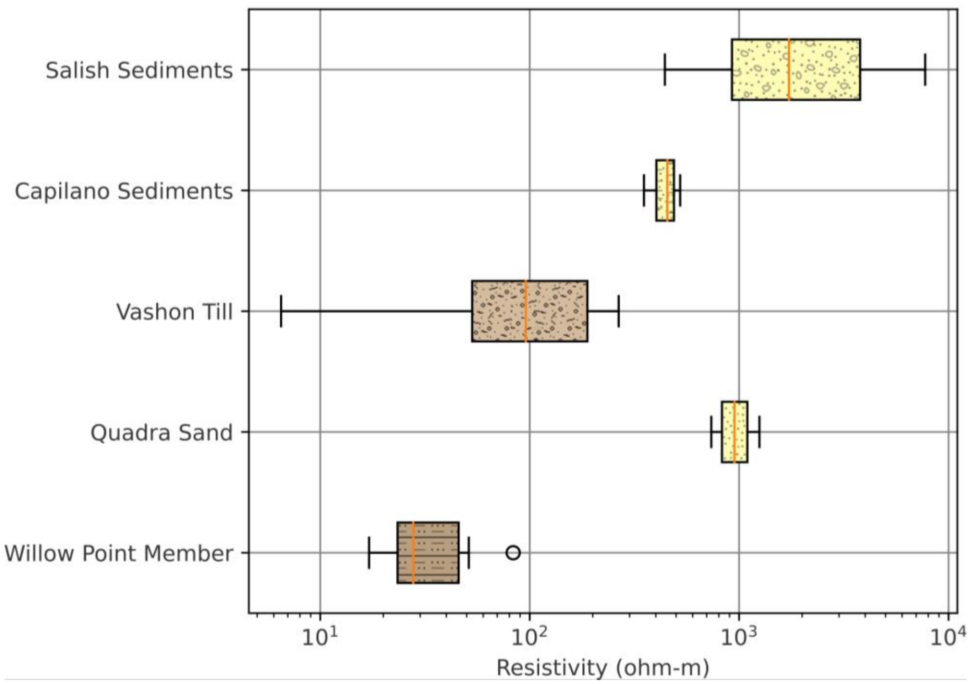

Figure 42: Resistivity ranges determined for the dominant lithological units in this study represented in a semi-log box-and-whisker plot. The boxed resistivity values for each unit extend from the first quartile to the third quartile and the whiskers represent the interquartile range multiplied by 1.5. Outliers outside the whiskers are marked by an open circle. Orange lines mark the median resistivity value for each unit.

The Capilano Sediments have a relatively small range in resistivity, but this may be due to the limited number of sites that had a significant thickness of this unit. Most sites surveyed were in areas mapped to have less than 1.5 metres of Capilano Sediments (marine veneer deposits; Fyles, 1960); most of the resistivity values in these areas are likely affected by human surface activities and/or by extreme dryness at the time of the survey. The only site that had a thick unit of Capilano Sediments (deltaic deposits) was the Macartney location. This sounding was unfortunately marked by high error and negative resistivity values. The upper portion of the sounding correlated reasonably well with the well lithology, but there are only three values to define a range of resistivity values for the Capilano Sediments.

The Vashon Till has a relatively small resistivity range from 6 to ~250 ohm-m, with half of the values falling between 50 and 200 ohm-m. The Vashon Till was encountered at a variety of different sites, and the resistivity range likely reflects the nature of the varied composition of till (e.g., variable clay content), and possibly water content.

The Quadra Sand has a small resistivity range centred around 1,000 ohm-m. This is partly due to the uniformity of the grain size attributed to Quadra Sand, and the limited number of soundings done through Quadra Sand (2: Cochrane and Bowser). The Quadra Sand is also deeper and often saturated so it is less affected by variations in saturation that would impact the resistivity values.

A notable result in Figure 42 is the gap in resistivity values between the Vashon Till and the Willow Point shale bedrock (less permeable; higher clay content) and the Quadra Sand and the Salish Sediments (more permeable). The strength of the resistivity surveying is in its ability to distinguish boundaries between contrasting layers. With the help of stratigraphy and an idea of the thickness of these units, it should be possible to differentiate between water-bearing layers such as gravel and sand and less permeable layers such as till and bedrock without the control wells. This is an encouraging result for using resistivity to fill in patchy well data and assist with aquifer mapping and characterization.

The purpose of this project was to test the viability of electrical resistivity techniques to find important boundaries between lithological units, using control wells for ground truthing. In short, the study has verified the usefulness of using VES data to infill sparse well control data, especially in the mapping of bedrock elevation. However, the analysis may be limited where control wells are shallow, do not penetrate bedrock, or where there is significant subsurface heterogeneity due to faulting, complex geologic history or other factors.

The next step is to move from the proof of concept to obtaining more field data away from the well control locations. This will increase the density and areal distribution of the data, meaning that more meaningful aquifer maps can be generated.

6. RECOMMENDATIONS

Recommendations cover two broad areas of investigations: 1) continued use of surface geophysics to characterize hydrogeological units and depth to the underlying bedrock, 2) further explore characterization of the most important aquifers in the BWS area (refer to tabulated list of regional aquifers in Appendix B).

6.1 Continued use of Surface and Downhole Geophysics

- Conduct additional 1D and select 2D resistivity surveys, especially inland west of the Island Highway where subsurface data are sparse and in areas likely to host a significant thickness of the Capilano, Salish and Vashon or Quadra sand. The 1D sounding could be repeated near the Macartney site, where a significant thickness of Capilano sediments is mapped but the 2021 survey had large errors; an alternative centre point further NW or SE along the E&N railway could be used. Aquifers in this area that could be further evaluated to understand vertical and lateral extent and interrelationships between layered Quaternary deposits include AQ414 (Rosewall Creek fan), AQ417 (Cumberland to Puntledge River), AQ419 (Wilfred Creek), AQ661 (Spider Lake), AQ662 (Big-Little Qualicum River), in addition to unmapped aquifers along the coast from Fanny Bay to Union Bay. Soundings should be done near known wells but also at locations where wells do not exist. The purpose of this work would be to obtain additional resistivity data for the various surficial and bedrock units and also to map the bedrock surface within the BWS area.

- The SPID/Fanny Bay 2D profile should be repeated in an effort to determine if there is any temporal variability in the interface between fresh water and sea water. Additional surveys could be completed south of Fanny Bay, in Aquifer 415 (Tsable River delta), which has known tidal influence, to develop representative resistivity values for formations containing brackish or saline water within the transition zone between sea water and fresh water. A 2D profile should also be conducted along the SE shore of Fanny Bay for the same reason.
- Subsurface information could be used to develop hydrogeologic cross-sections through mapped aquifers and areas with unmapped aquifers to identify the spatial extents of developed and undeveloped aquifer units.
- The use of geophysical methods to evaluate aquifer vulnerability (e.g., to identify the extent and thickness, or absence, of confining materials with higher clay or silt content) or to examine surface water-groundwater hydraulic connectivity and interrelationships (e.g., identifying unsaturated zone thicknesses and presence of low permeability, clay-rich units adjacent to streams) could be further examined within representative areas.
- Review the GSC 2D seismic reflection data acquired in 2011 in close proximity to the Cochrane (WTN 107880) and Bowser (WTN 37367) control wells (Benoit et al., 2015) for an improved understanding of subsurface structure.
- Review the downhole geophysical logs acquired in the Cochrane control well (WTN 107880) (Crow et al., 2014), to better understand the geophysical properties of subsurface lithologies.
- In addition to the previously mentioned seismic reflection data, other geophysical methods that might be considered in the future are ground-penetrating radar which is good for dry surfaces and shallow targets or seismic reflection, which would need an energy source for generation of the seismic signal, and would be more expensive than using resistivity, though more accurate.

6.2 Further Characterization of Regional Aquifers and Information Sharing

Additional hydrogeological assessments should be considered to complement the geophysical surveys. Given the effort and cost, it may be more feasible to target aquifers in the BWS area that are the most heavily developed, including within the deltaic/alluvial fan aquifers at Wilfred Creek (AQ419) and Rosewall Creeks (AQ414). To gain better understanding of the hydrogeology of local aquifers, consider the following:

- Conduct a field survey in Aquifers 419 and 414 to verify well locations, purpose and amount of water use, and to measure current (point in time) groundwater elevations. These data could be used to map contours of groundwater elevation and to infer horizontal direction of groundwater flow in these aquifers. Future geophysical work could be planned in areas of interest where the additional data are gathered.
- Additional surveys could target areas identified as having moderately high or high vulnerability to sea water intrusion within recently completed sea water intrusion risk mapping (Sivak and Wei, 2021). Survey results could be used to identify strategic water supply wells to monitor geochemical indicators of sea water intrusion (chloride, electrical conductivity and Total Dissolved Solids) and to evaluate potential sea water intrusion impacts from groundwater development in these coastal aquifers.
- Seek opportunities to collaborate with the Province to identify locations for monitoring of groundwater conditions (level, temperature) within a community-led monitoring network or as a part of the Provincial monitoring networks (e.g., hydrometric, groundwater, or climate monitoring). Installation of dedicated multi-level observation wells could provide additional

subsurface data in targeted zones and enable collection of data to assist with understanding of vertical gradients between layered aquifer systems, surface-groundwater interactions and long-term environmental trends.

- Utilize new well construction data and geophysical survey results to update and enhance aquifer mapping in the BWS area, including extending the boundaries of developed unconsolidated aquifers and bedrock aquifers in Nanaimo Group (type 5a) aquifers.
- Present report and results to groups working and interested in this area, e.g., K'omoks First Nation, and Comox Valley Regional District, and Provincial government agencies.

REFERENCES

Abbey, D.G., 2000. The applicability and scale dependence of aquifer testing methods: an integrated geophysical and hydrogeological characterization of two fractured systems. MSc thesis, Simon Fraser University, Burnaby, BC, Canada, 319p.

Advanced Geosciences, Inc., 2009. Instruction Manual for EarthImager 2D, Version 2.4.0. Austin, Texas, 139p.

Advanced Geosciences, Inc., 2014. Instruction Manual for EarthImager 1D, Version 2.0.5. Austin, Texas, 36p.

Allen, D. M., Liteanu, E., Bishop, T.W., and Mackie, D.C., 2003. Determining the hydraulic properties of fractured bedrock aquifers of the Gulf Islands, B.C. Final Report submitted to Ministry of Water, Land and Air Protection, March 2003, 107 pp.

Bednarski, J. M., 2015. Surficial Geology and Pleistocene stratigraphy from Deep Bay to Nanoose Harbour, Vancouver Island, British Columbia. Geological Survey of Canada, Open File 7681, 1 zip file, doi:10.4095/295609.

Benoit, N., Paradis, D., Bednarski, J.M., Hamblin, T., Russell, H.A.J. 2015. Three dimensional hydrostratigraphic model of the Nanoose - Deep Bay area, Nanaimo Lowland, British Columbia. Commission géologique du Canada, Dossier public 7796, 2015, 30p., https://doi.org/10.4095/296302

Burger, H.R., Sheehan, A.F., and Jones, C.H. 2006. Introduction to applied geophysics: exploring the shallow subsurface, W.W. Norton & Co., New York, 554p.

Beaufort Water Stewards (BWS). 2020. Beaufort Watershed Stewards Web Site. https://beaufortwater.org/

Cathyl-Bickford, C.G. 1992. Geology and energy resource potential of the Tsable River and Denman Island (92F/10, 11). British Columbia Geological Survey Geological Fieldwork 1991, Paper 1992-1, p. 419-426.

Cathyl-Bickford, C. G. and Hoffman, G. L. 1998. Geology of the Tsable River area, Comox Coalfield, British Columbia. British Columbia Ministry of Energy and Mines, Geological Survey Branch Open File 1998-07, Sheet 6 and 7 of 8.

Crow, H.L. 2016. 2.7 Borehole Geophysics; in Russell, H.A.J., and Benoit, N., (compilers); Nanoose Bay - Deep Bay Area, Nanaimo Lowland Groundwater Study Atlas, Regional District of Nanaimo, British Columbia; Geological Survey of Canada, Open File 7877.

Crow, H.L., Knight, R.D., Russell, H.A.J., Pugin, A.J-M., and Cartwright, T.J. 2014. Downhole geophysical data from five boreholes in the Nanaimo Lowlands, British Columbia; Geological Survey of Canada, Open File 7567, 1 zip file, doi:10.4095/294925.

Cui, Y., Miller, D., Schiarizza, P., and Diakow, L.J. 2017. British Columbia digital geology. British Columbia Ministry of Energy, Mines and Petroleum Resources, British Columbia Geological Survey Open File 2017-8, 9p.

Foster, S.B. 2014. Characterizing groundwater - surface water interactions within a mountain to ocean watershed, Lake Cowichan, British Columbia. MSc thesis, Simon Fraser University, 207p.

Fyles, J.G. 1960. Surface Geology of Courtenay, Comox, Nelson, Nanaimo and Newcastle Districts, Vancouver Island, British Columbia, Ottawa: Geological Survey of Canada.

Fyles, J.G. 1963a. Surficial geology of the Horne Lake and Parksville map-areas, Vancouver Island, British Columbia. Memoir 318. Geological Survey of Canada: Ottawa, ON.

Fyles, J.G. 1963b. Surficial Geology of Horne Lake Vancouver Island, British Columbia (Map). Ottawa: Geological Survey of Canada.

Griffiths, D.J. 2017. Introduction to Electrodynamics (4th edition). Cambridge: Cambridge University Press, doi:10.1017/9781108333511.

Guthrie, R.H. 2005. Geomorphology of Vancouver Island: Extended legends to nine thematic maps. (Digital surficial geology map layers). Research Report No. RR02, Nanaimo, B.C.: Ministry of Environment.

Hamblin, A.P. 2015. Detailed measured sections, bedrock aquifer/aquitard facies and potential bedrock aquifer systems of the Upper Cretaceous Nanaimo Group, Nanaimo Lowland, eastern Vancouver Island, British Columbia, Canada. Geological Survey of Canada Open File 7849, 1 .zip file, doi:10.4095/296979.

Lake, M.I. 1978. A report of a resistivity survey of the South Pilling area of North West Lancashire. Unpublished report completed as part of the requirement for a M.Sc. in Applied Geophysics at the University of Birmingham, U.K. for the session 1977- 1978.

Mackie, D. M. 2002. An integrated structural and hydrogeologic investigation of the fracture system in the upper Cretaceous Nanaimo Group, Southern Gulf Islands, British Columbia. MSc Thesis, Simon Fraser University, Burnaby, BC, Canada, 358p.

Massey, N.W.D., Desjardins, P.J. and Grunsky, E.C. 1994. Geological Compilation Vancouver Island, British Columbia, (92B,C,E,F,G,K,L; 102I); B.C. Ministry of Energy, Mines and Petroleum Resources, Open File 1994-6.

Moncur, M.C. 1974. Groundwater investigations on Mayne Island - Report No. 3: Groundwater exploration on Mayne Island. Water Investigations Branch, B.C. Water Resources Service, File 0239013, 177p.

Palacky, G.J. 1988. Resistivity characteristics of geologic targets, in: Neitzel, E.B. (ed.), Investigations in Geophysics, Vol. 3: Electromagnetic methods in applied geophysics, Society of Exploration Geophysicists, p. 53-129.

Province of B.C., 2022a. Ground Water Wells and Aquifers Database (GWELLS). Province of B.C.: Victoria, B.C. https://apps.nrs.gov.bc.ca/gwells.

Province of B.C., 2022b. BC Data Catalogue Map Layers (Freshwater Atlas, Water Rights, Groundwater Wells, Aquifer Intrinsic Vulnerability, Aquifer Vulnerability to Saltwater Intrusion). Victoria, B.C.

Surrette, M., Allen, D.M., and Journeay, M. 2008. Regional evaluation of hydraulic properties in variably fractured rock using a hydrostructural domain approach. *Hydrogeology Journal*, v. 16, p. 11-30.

Sivak, T. and Wei, M. 2021. GIS Modelling of Sea Water Intrusion Risk along British Columbia's Coast. Water Science Series WSS2021-06, Province of British Columbia, Victoria.

Zohdy, A.A.R., Eaton, G.P., and Mabey, D.R. 1974. Chapter D1: Application of surface geophysics to ground-water investigations. Techniques of Water-Resources Investigations of the United States Geological Survey, p. 1-116.

APPENDIX A. CONTROL WELL DATA

Table A1: Control well information. Unless otherwise stated, data are from B.C. Ministry of Environment water well database, accessible at: https://apps.nrs.gov.bc.ca/gwells/, last accessed August 2021.

WTN #	Name	Offset (m)[1]	Latitude (°N)	Longitude (°W)	Ground elevation (mASL)[1]	Finished well depth (mbgl)	Mapped surface geology	Water depth[2] (btoc)
77113	Fanny Bay Hall	130 m NW	49.48961	124.8128	9.1	16.2	16: Salish Sediments: shore, deltaic and fluvial deposits, including gravel, sand, silt, clay, and peat. (Fyles, 1963)	6 m (20 ft)
95528	SPID/ Fanny Bay	25 m SW	49.49222	124.80205	0.9	15.5	16: Salish Sediments: shore, deltaic and fluvial deposits, including gravel, sand, silt, clay, and peat. (Fyles, 1963)	0.6 m (2 ft)
37367	Bowser	10 m N	49.4489	124.715	75.9	25.3	12c/5: 12c is Capilano Sediments: marine veneer complex, including gravel, sand, silt, clay, and stony loam (typically less than 1.5 m thick). 5 is Quadra sand: sand, minor gravel. (Fyles, 1963)	9 m (30 ft)
87591	Yake Road	50m W	49.504123	124.82976	15.8	73.1	5d/3. 5d: Capilano Sediments: marine veneer complex, including gravel, sand, silt, clay, and stony loam (typically less than 1.5 m thick). 5d is underlain by 3: Vashon Drift: ground moraine deposits, including till, and lenses of gravel, sand, and silt. (Fyles, 1960)	Dry hole
107880	Cochrane Road	10 m S	49.39481	124.66601	110.9	81.1	12c/7. 12c: Capilano Sediments: marine veneer complex, including gravel, sand, silt, clay, and stony loam (typically less than 1.5 m thick). 12c is underlain by 7: Vashon Drift: ground moraine deposits, including till, and lenses of gravel, sand, and silt. (Fyles, 1963)	40 m (130 ft)
120708	Mac artney Drive	170 m W	49.47829	124.80359	14.0	73.1	13a: Capilano Sediments: deltaic deposits, including gravel and sand, commonly underlain by silt and clay. (Fyles, 1963)	N/A

[1] Calculated via Google Earth.

[2] Water depth (below top of casing) at time of drilling.

WTN #	Name	Offset (m)[1]	Latitude (°N)	Longitude (°W)	Ground elevation (mASL)[1]	Finished well depth (mbgl)	Mapped surface geology	Water depth[2] (btoc)
26165	Buckley Bay	250 m SW	49.524255	124.84954	16.2	78.6	5d/3. Capilano Sediments: marine veneer complex, including gravel, sand, silt, clay, and stony loam (typically less than 1.5 m thick). 5d is underlain by 3: Vashon Drift: ground moraine deposits, including till, and lenses of gravel, sand, and silt. (Fyles, 1960)	N/A
83158	Union Bay ENV	260 m E	49.58389	124.89306	37.5	98.1	5a,5b or 5d/3 (on boundary): Capilano Sediments. 5a is marine/glaciomarine deposits including silt, clay, and stony clay; 5b is marine/glaciomarine deposits including sand, pebbly sand, sandy gravel. 5d is marine veneer complex, including gravel, sand, silt, clay, and stony loam (typically less than 1.5 m thick). 3: Vashon Drift: ground moraine deposits, including till, and lenses of gravel, sand, and silt. (Fyles, 1960)	48 m (158 ft)
85165	Union Bay Kens	170 m E	49.585847	124.89182	26.2	29.9	6a: Capilano Sediments: deltaic deposits, including gravel and sand, commonly underlain by silt and clay. (Fyles, 1960)	6.5 m (21 ft)
103795	Royston	140 m WSW	49.63809	124.92365	6.1	17.4	8: Salish Sediments: shore, deltaic and fluvial deposits, including gravel, sand, silt, clay, and peat. (Fyles, 1960)	4.2 m (14 ft)

APPENDIX B. AQUIFER SUMMARY TABLE

Table B1: Aquifers in the Beaufort study area. Data from BC Data Catalogue (water layers), Province of B.C. (2022b); Fyles (1963a).

Aquifer	**Location**	**Aquifer Material[3] and Subtype[4]**	**Lithostrati-graphic Unit**	**Area (km^2)**	**Provincial Observation Well(s)**	**Description**
217	Qualicum	UNC 4b	Primarily Quadra Sand (& younger Salish Sediments in French Creek estuary)	42.0	295, 303, 321, 434	Partially confined, unconsolidated aquifer that underlies much of the Qualicum Beach municipal area. Hydraulically connected to French Creek and Beach Creek where the river has incised through confining sediments into the Quadra sand. AQ217 footprint includes areas of high groundwater demand (by volume) and dependence for municipal and industrial water supply including hatcheries and golf courses. Locally vulnerable to sea water intrusion near the coast in areas of lower elevation and higher well density. Also includes deltaic deposits in the French Creek estuary.
414	Alluvial fan at the mouth of Rosewall Creek	UNC 2	Salish Sediments	1.5		Highly productive unconfined, unconsolidated delta at the mouth of Rosewall Creek. AQ414 is a source groundwater primarily for industrial use (hatcheries, water bottling) in addition to domestic use on unserviced rural residential properties. AQ414 is a low elevation delta that extends into the sea and therefore has a moderately high to high vulnerability to sea water intrusion.
415	Tsable River delta deposit	UNC 2	Salish Sediments	0.8	371	Deltaic aquifer at the mouth of Tsable River, south of Bulkley Bay. Borders Tsable River and may extend spatially to the north and south of the delta, and upstream to the southwest within fluvial deposits bordering the river. AQ415 is likely hydraulically connected to the river and to coastal waters. The hydrograph of provincial OW371, sited in AQ415, exhibits tidal influence. Low level of aquifer development, used for domestic drinking water and potentially agricultural irrigation.

[3] Aquifer material categories: UNC=Unconsolidated (sand and gravel), BED=Fractured bedrock
[4] For an introduction and descriptions of aquifer types, see Wei et al (2009).

Aquifer	Location	Aquifer Material and Subtype	Lithostrati-graphic Unit	Area (km^2)	Provincial Observation Well(s)	Description
416	Thames Creek to Mapleguard Point	UNC 4b	Quadra Sand	13.7	310	**Bowser Survey Area.** Highly productive confined glaciofluvial aquifer that extends along the lower elevation coastal benchland from Thames Creek to Deep Bay at Mapleguard Point. AQ416 has a moderate to high vulnerability to seawater intrusion and may be hydraulically connected to the sea in areas proximal to coast. Source of water for local water supplier (waterworks), commercial, irrigation, and private domestic use. Thames Creek is interpreted to be a groundwater divide that separates AQ416 from AQ665 to the southeast.
417	North of Cumberland to Puntledge River	UNC 4a	Vashon Drift or Quadra Sand	37.4		Partially confined aquifer located in the area east of Comox Lake, underlying Cumberland, and bordering south side of Puntledge River, west of Courtenay. Potentially hydraulically connected to Perseverance Creek and Morrison Creek, and Puntledge River. Understanding of aquifer thickness and extent is limited in some areas due to lack of subsurface information where few wells are present. Unconsolidated glacial deposits may be thicker within the central part of the aquifer, associated with outwash deposits from glacial melt in the Comox Lake valley (Vashon) or earlier periods (Quadra sand). The major water source for municipal supplies in this area is Comox Lake, and the level of groundwater development in AQ417 is low, used for local water services, agricultural purposes (irrigation, livestock watering), commercial-industrial purposes (parks, campgrounds, public facilities) and domestic residential water supply outside of municipal service areas.
419	Wilfred Creek delta south of Fanny Bay	UNC 2	Salish Sediments (overlying Capilano)	4.3		**Fanny Bay and Macartney Survey Areas.** Small, highly productive, unconfined, unconsolidated aquifer that borders the lower reaches of Wilfred Creek, at Ships Point Peninsula, southeast of Fanny Bay. AQ419 is a coastal deltaic alluvial fan with high vulnerability to sea water intrusion. It is likely hydraulically connected to Wilfred Creek, and potentially hydraulically connected to Cowie Creek and Waterloo Creek which border the northwestern and southeastern edges of the aquifer, respectively. Groundwater is used for industrial purposes (hatchery, water bottling, public facilities), local water services, and private domestic (rural residential) consumption.

Aquifer	Location	Aquifer Material and Subtype	Lithostrati-graphic Unit	Area (km^2)	Provincial Observation Well(s)	Description
421	Nile Creek to Thames Creek	UNC 4b	Quadra Sand	6.2		Confined, unconsolidated aquifer north of Qualicum Bay, between Nile Creek and Thames Creek. Comprised of layered water-bearing sand and gravel seams confined above and below by dense rocky clay and silt. AQ421 underlies or forms an aquifer complex with shallower AQ665. AQ421 is potentially larger or smaller in spatial extent, however there is a limited number of deeper wells to determine subsurface geology, particularly in the upgradient/west side of the aquifer. The eastern tip of the aquifer forms a small deltaic fan deposit at the Nile Creek estuary. Shallower aquifers in this area are considered to have a moderate vulnerability to sea water intrusion. This deeper aquifer is largely undeveloped but could be further explored as a potential water source.
661	Spider Lake near Horne Lake	UNC 4a	Vashon Drift	7.9		Confined, unconsolidated, moderately productive aquifer in the Horn Lake and Spider Lake valley. AQ661 is made up of mixed interglacial, and glacial outwash, kame deposits, overlain by, dense clay-silt (till) and silty lacustrine sediments. Low level of aquifer development. Groundwater is mainly utilized for domestic (rural residential) purposes, with some industrial use.
662	Between Big Qualicum & Little Qualicum River	UNC 4b	Quadra Sand	50.2	391, 426	Large partially confined, unconsolidated aquifer between Little Qualicum and area north of Big Qualicum River. Borders AQ664 (Little Qualicum River) to the south. Potentially hydraulically connected to Kinkade Creek, Annie Creek and Big Qualicum River. Moderately vulnerable to sea water intrusion, with higher vulnerability to intrusion in areas of higher well density proximal to the coast. Groundwater source for local water service, agriculture (irrigation and livestock watering) and domestic (rural residential) use.

Aquifer	Location	Aquifer Material and Subtype	Lithostrati-graphic Unit	Area (km^2)	Provincial Observation Well(s)	Description
663	Upper reaches of Whisky Creek	UNC 4a	Vashon Drift	9.8		Small, partially confined, unconsolidated shallow aquifer in the Whiskey Creek watershed, a sub-tributary to Little Qualicum River. The aquifer and groundwater table are relatively shallow, consisting of kame terrace and delta glacio-fluvial outwash deposits, with water-bearing gravel lenses. Where present, confining sediments consist of dense, sandy silt (till) or clay (glaciomarine) sediments. Aquifer is potentially hydraulically connected to Whiskey Creek, Harris Creek and Crocker Creek. Aquifer boundaries and spatial extent toward the northeast, and potential connectivity to AQ217 could be further evaluated. The aquifer has a moderate to low productivity, and groundwater is used for large and small local water services, agriculture (irrigation and livestock watering), industrial use (camps, public facilities), commercial operations, and domestic (rural residential) use outside of serviced areas.
664	Little Qualicum River valley and delta	UNC 1c	Salish Sediments	4.4		Narrow, highly productive, unconfined, unconsolidated aquifer composed of fluvial and deltaic deposits along the Little Qualicum River floodplain and estuary. Hydraulically connected to the river, and highly vulnerable to sea water intrusion at the river mouth (delta). Source of water for local water service (Qualicum Beach), camps, commercial and residential (domestic) use. Most developed along the coast.
665	Between Big Qualicum River & Thames Creek	UNC 4a (1b and 2)	Capilano Sediments	22.8		**Cochrane Survey Area.** Moderately productive, unconfined, unconsolidated aquifer that extends along the coastal benchland between Big Qualicum River and Thames Creek. Includes fluvial deposits, sub-type 1b, along moderate river drainages (Big Qualicum River, Nile Creek), and sub-type 2 deltaic deposits e.g., at the mouth of Thames Creek, Nile Creek and Qualicum River. AQ665 is moderately vulnerable to sea water intrusion, and most development is along the coast. Mainly used for domestic purposes on rural residential properties, minor commercial and industrial use (e.g., camps).

Aquifer	Location	Aquifer Material and Subtype	Lithostrati-graphic Unit	Area (km^2)	Provincial Observation Well(s)	Description
951	Puntledge to Courtenay	UNC 4a	Vashon Drift or Quadra Sand	34.2		**Royston Survey Area**. Confined, unconsolidated aquifer mapped within the Courtenay area from Puntledge River south to Royston. AQ951 consists of glacial and interglacial outwash sediments from which groundwater is obtained from laterally discontinuous gravel seams, underlying dense sandy, silt (till) and stony clay (glaciomarine) deposits. AQ951 is potentially associated with AQ417, which borders it to the west. AQ951 varies in thickness and productivity over its mapped extent, and a significant number of wells are drilled into the underlying sedimentary bedrock of AQ411. The aquifer is bounded to the north by the Puntledge River, to the east by Comox Harbour, and to the south by the Trent River. Potentially hydraulically connected to larger Puntledge and Trent Rivers, however where thicker confining sediments are present, the aquifer may be disconnected hydraulically from smaller overlying tributaries including Arden Creek, Willemar Creek, Millard Creek, Morrison Creek and Piercy Creek. The aquifer was historically developed. Currently the urban areas of Courtenay and Royston are within the Comox Valley Regional District municipal water service area with water supply provided primarily from Comox Lake, which likely reduces groundwater demand. Main groundwater use is for agricultural irrigation and processing/manufacturing, and minor domestic use outside of serviced areas. Moderate to low vulnerability to sea water intrusion, and low level of development along the coast.
411	South of Oyster River	BED 5a	Nanaimo Group	731.9		**Royston, Union Bay Survey Areas.** Largest aquifer mapped in the Beaufort study area, consisting of fractured sedimentary bedrock (Nanaimo Group conglomerate, sandstone, siltstone and shale). AQ411 is partially confined by silty, clay (till) overburden, and may be hydraulically connected to major river systems such as Trent River and Oyster River. This bedrock aquifer also underlies several smaller, unconsolidated aquifers including AQ417, AQ857, AQ951, AQ952 and additional aquifers north and northwest of the Beaufort study area. The level of aquifer development is low considering the large aquifer extent with most wells constructed closer to the coast; susceptibility to sea water intrusion is considered low to moderate. Groundwater from the aquifer is utilized for municipal and smaller local water service providers, agriculture (irrigation and livestock watering),

Aquifer	Location	Aquifer Material and Subtype	Lithostrati-graphic Unit	Area (km^2)	Provincial Observation Well(s)	Description
						industrial use (camps, public facilities, greenhouses), and commercial enterprises as well as for domestic use.

Aquifer sub-types categories (Wei, et al, 2009):

- 1b Unconfined sand and gravel fluvial deposits along medium stream system
- 1c Unconfined sand and gravel fluvial deposits along small stream system
- 2 Unconfined sand and gravel deltaic deposits
- 4a Unconfined glaciofluvial sand and gravel, glacial or pre-glacial origin
- 4b Confined sand and gravel, glacial or pre-glacial origin (glaciofluvial or glaciolacustrine)
- 5a Fractured sedimentary bedrock

APPENDIX C. BEDROCK STRATIGRAPHY

Table C1. Bedrock stratigraphy of eastern Beaufort Watershed region, Vancouver Island (modified from Cathyl-Bickford, 1992 and Cathyl-Bickford and Hoffman, 1998; igneous data from Cui et al., 2017).

Group (approx. age)	Formation (age)	Member	Description	Approx. thickness (m)
	Lambert		Mudstone and siltstone; minor sandstone and argillaceous limestone	0-115
		Norman Point	Sandstone; minor siltstone	25-40
	Denman (Campanian)	Graham	Conglomerate; minor sandstone and siltstone	65-80
		Madigan	Sandstone; minor conglomerate and siltstone	55-75
		Willow Point	Mudstone and siltstone; minor sandstone	120-150
		Baynes Sound	Sandstone and siltstone; minor conglomerate	10-60
		Royston	Shale and siltstone; minor sandstone and argillaceous limestone	50-220
Nanaimo (Upper Cretaceous)	*Trent River (Campanian)*	Tsable	Mud-matrix conglomerate; minor sandstone and pebbly siltstone	5-140
		Browns	Sandstone and siltstone; minor shale and coal	0-45
		Puntledge	Mudstone and siltstone; minor sandstone	0-130
		Cowie	Sandstone; minor siltstone	2-15
		Cougarsmith	Mudstone and siltstone; minor sandstone	8-22
		Dunsmuir	Sandstone; minor siltstone; shale, conglomerate and coal	120-190
	Comox (Santonian - Campanian)	Cumberland	Siltstone, shale and coal; minor sandstone	30-90
		Benson	Conglomerate, minor red shale and siltstone	0-220
Island Plutonic Suite (Early to Middle Jurassic)			Granodiorite	
Vancouver (Upper Triassic)	*Karmutsen*		Basalt, basaltic breccia, tuff	

APPENDIX D. ELECTRODE SPACINGS

1D Schlumberger array electrode spacings are shown in Table D1. Data were collected at these spacings at all sites except for minor changes at Fanny Bay Hall (due to a shorter spread), Bowser (two spacings omitted: AB/2 = 140 m, 110 m) and Cochrane (some changes were made because of compact ground that the electrodes could not sufficiently penetrate). AB/2 is the distance between the outer electrodes divided by two and MN/2 is the distance between the inner electrodes divided by two.

Table D1: Schlumberger array electrode spacings used in this study.

AB/2 (m)	MN/2 (m)
1	0.25
1.5	0.25
2	0.25
2.5	0.25
3	0.25
3	1
5	1
7	1
10	1
10	2.5
12	2.5
15	2.5
18	2.5
25	2.5
25	5
36	5
50	5
50	10
70	10
80	10
100	10
100	15
110	15
120	15
130	15
140	15
150	30

APPENDIX E. VES AND ERT SURVEYS AND LOCATION COORDINATES

Table E1: Positions of centre and endpoints of VES and ERT survey lines, measured using a handheld GPS.

Survey[5]	Centre latitude (°N)	Centre longitude (°W)	End 1 latitude (°N)	End 1 longitude (°W)	End 2 latitude (°N)	End 2 longitude (°W)
Fanny Bay Hall NW-SE	49.49009	124.813	49.49032	124.8137	49.48982	124.8124
Fanny Bay Hall SW-NE	49.49009	124.813	49.49042	124.8127	49.48971	124.8134
Fanny Bay Hall SW-NE 2D	49.49010	124.81299	49.49041	124.8127	49.48980	124.8133
SPID Fanny Bay SW-NE	49.49213	124.8019	49.49099	124.803	49.49329	124.8009
SPID Fanny Bay SW-NE 2D	49.4925	124.8017	49.49213	124.802	49.49281	124.8015
Yake Rd SE-NW	49.5042	124.8304	49.50294	124.8296	49.50542	124.8312
Bowser SW-NE	49.44904	124.7155	49.44837	124.7172	49.44964	124.7136
Cochrane SE-NW	49.39473	124.6663	49.39401	124.6645	49.39523	124.6682
Macartney SE-NW	49.47773	124.8059	49.47648	124.8051	49.47895	124.8067
Buckley Bay SE-NW	49.52577	124.8523	49.52685	124.8535	49.52464	124.8511
Union Bay SE-NW	49.58502	124.8899	49.58374	124.8895	49.58638	124.8902
Royston W-E	49.63738	124.9255	49.63742	124.9276	49.6373	124.9234

[5] 1D sounding except where specified otherwise.

APPENDIX F. MACARTNEY DRIVE 1D DATA

Noisy data from Macartney Drive 1D sounding. Table F1 includes all data points collected - note that there are some negative apparent resistivity data points (cannot be modelled in EarthImager) and that many data points have large error values, based on the difference between two subsequent measurements at identical spacings. Figure F1 shows the non-negative data points plotted on a log-log graph.

Table F1: Data collected during the Macartney Drive 1D sounding.

AB/2 (m)	MN/2 (m)	Current I (mA)	Potential difference over current dV/I (ohm)	Apparent Resistivity (ohm-m)	Error (%) (based on 2 measurements)
1	0.25	2	3393.3	19988.00	0
1.5	0.25	2	1447.4	19894.00	0
2	0.25	5	701.07	17344.00	0.1
2.5	0.25	2	326.32	12686.00	0
3	0.25	2	163.23	9166.50	0.1
3	1	2	1010.04	12697.00	0
5	1	2	78.508	2959.70	0.1
7	1	2	17.49	1318.70	0
10	1	1	4.9299	766.65	0.5
10	2.5	1	11.478	676.11	0.2
12	2.5	2	5.7621	498.72	0
15	2.5	2	3.6965	508.07	0.1
18	2.5	5	1.3052	260.58	0
25	2.5	2	0.76331	296.75	0.5
25	5	2	2.7638	520.96	0.1
36	5	2	0.95188	380.08	0.6
50	5	10	0.074856	58.20	15
50	10	10	0.1813	68.35	1.4
70	10	10	0.035906	27.07	0.1
80	10	10	0.084947	84.06	2.9
100	10	10	0.36568	568.67	85.6
100	15	10	-2.4426	-2500.30	55
100	15	10	-0.71704	-733.99	79.4
110	15	10	-3.4238	-4257.70	52.2
120	15	10	0.33032	490.34	389.5
130	15	10	3.3125	5784.30	39.8
140	15	20	0.32708	663.63	94.8
150	15	20	-1.1773	-2746.10	53.8
150	30	20	-0.30855	-348.96	46
140	30	20	0.11012	107.82	67.9
130	30	10	1.1662	976.98	20.4
120	30	10	0.565	399.38	93
110	30	10	-0.8106	-475.36	86.7

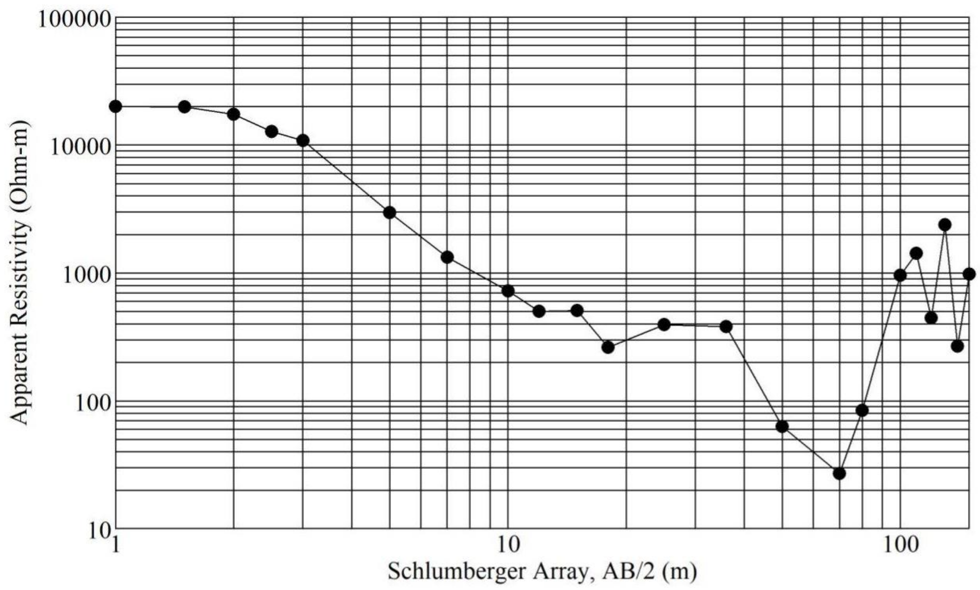

Figure F1: VES data (apparent resistivity versus electrode spacing AB/2) collected at the Macartney Drive site. Negative values are excluded. See Table F1 for full dataset.